

**DISSERTATION**

**OVINE PULMONARY ADENOCARCINOMA AS AN ANIMAL MODEL FOR  
HUMAN LUNG ADENOCARCINOMA**

Submitted by

Susan Hudachek

Cell and Molecular Biology Graduate Program

In partial fulfillment of the requirements

For the Degree of Doctor of Philosophy

Colorado State University

Fort Collins, Colorado

Spring 2008

UMI Number: 3321283

### INFORMATION TO USERS

The quality of this reproduction is dependent upon the quality of the copy submitted. Broken or indistinct print, colored or poor quality illustrations and photographs, print bleed-through, substandard margins, and improper alignment can adversely affect reproduction.

In the unlikely event that the author did not send a complete manuscript and there are missing pages, these will be noted. Also, if unauthorized copyright material had to be removed, a note will indicate the deletion.

**UMI**<sup>®</sup>

---

UMI Microform 3321283

Copyright 2008 by ProQuest LLC.

All rights reserved. This microform edition is protected against unauthorized copying under Title 17, United States Code.

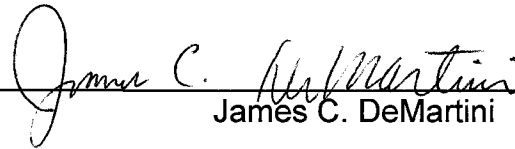
ProQuest LLC  
789 E. Eisenhower Parkway  
PO Box 1346  
Ann Arbor, MI 48106-1346

COLORADO STATE UNIVERSITY

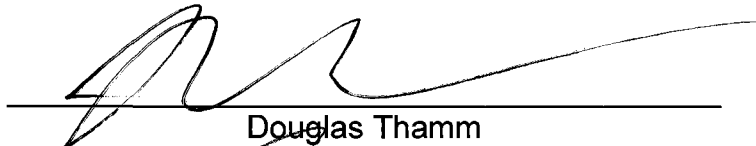
November 16, 2007

WE HEREBY RECOMMEND THAT THE DISSERTATION PREPARED UNDER OUR SUPERVISION BY SUSAN HUDACHEK ENTITLED OVINE PULMONARY ADENOCARCINOMA AS AN ANIMAL MODEL FOR HUMAN LUNG ADENOCARCINOMA BE ACCEPTED AS FULFILLING IN PART REQUIREMENTS FOR THE DEGREE OF DOCTOR OF PHILOSOPHY.

Committee on Graduate Work

  
James C. DeMartini

  
Susan Kraft

  
Douglas Thamm

  
Robert Ulrich

  
**Advisor: William S. Dernell**

  
**Department Head: Norman P. Curthoys**

## **ABSTRACT OF DISSERTATION**

### **OVINE PULMONARY ADENOCARCINOMA AS AN ANIMAL MODEL FOR HUMAN LUNG ADENOCARCINOMA**

Appropriate animal models of disease allow defined and controlled investigations that can ultimately be applied to the management of human disease. Based on symptomatic, histopathologic, and possible molecular signaling similarities, we hypothesized that sheep experimentally affected by OPA are a relevant animal model for the study of human lung adenocarcinoma and, in particular, for the evaluation of lung cancer therapeutics. The value of this model is dependent upon its predictability, reproducibility, amenability, and validity. The former two features have been previously reported; OPA induction in sheep is both predictable and reproducible following JSRV inoculation of neonatal lambs. The overall objective of this body of work was to assess the amenability of this animal model for therapeutic research and to assess the validity of OPA-affected sheep as an animal model for human lung adenocarcinoma in terms of genetic similarities.

We determined that this animal model is amenable for therapeutic studies because, using CT, OPA can be detected early, before the onset of clinical signs, and cancer development can be monitored noninvasively. However, not only did we observe OPA disease progression during this study, but surprisingly, we also witnessed spontaneous regression of OPA. In fact, the latter was the more common outcome seen in our research after JSRV inoculation of neonatal lambs. We propose that the immune system, particularly CD3<sup>+</sup> T-cells, is an important

mediator of the spontaneous regression of JSRV-induced OPA seen in our work. Regardless of the cause, the mere occurrence of spontaneous regression of cancer in OPA-affected sheep severely restricts the use of this animal model for therapeutic research.

In addition to assessing the amenability of OPA-affected sheep for therapeutic research, we also found that OPA tumors do not harbor genetic mutations in the TK domain of the EGFR, KRAS codons 12 and 13, or the DNA-binding domain of P53 and therefore, are not genetically similar to human lung adenocarcinomas that contain these mutations. Based on these genetic disparities, OPA-affected sheep are not an ideal animal model for human lung adenocarcinoma. Overall, the genetic profile combined with the disease development data provided further characterization of OPA and facilitated an assessment of the utility and relevance of this animal model for human lung cancer studies.

Susan Hudachek  
Cell and Molecular Biology Graduate Program  
Colorado State University  
Fort Collins, CO 80523  
Spring 2008

## TABLE OF CONTENTS

TITLE PAGE.....	i
SIGNATURE PAGE.....	ii
ABSTRACT.....	iii
TABLE OF CONTENTS .....	v
LIST OF TABLES .....	vi
LIST OF FIGURES .....	viii
CHAPTER I: INTRODUCTION.....	1
CHAPTER II: RADIOGRAPHIC IMAGING OF OVINE PULMONARY ADENOCARCINOMA DEVELOPMENT.....	36
CHAPTER III: HISTOPATHOLOGY OF OVINE PULMONARY ADENOCARCINOMA AND IMMUNE RESPONSE TO JAAGSIEKTE SHEEP RETROVIRUS.....	86
CHAPTER IV: GENETIC PROFILING OF OVINE PULMONARY ADENOCARCINOMA.....	116
CHAPTER V: DISCUSSION.....	146
REFERENCES.....	175

## LIST OF TABLES

### *CHAPTER II:*

Table 2.1: Characteristics of sheep used as viral inoculum sources .....	60
Table 2.2: CT scan and euthanasia schedule for sheep inoculated with virus.....	61
Table 2.3: Lung disease characteristics evaluated via CT.....	62
Table 2.4: JSRV copy numbers in inocula .....	63
Table 2.5: Summary of CT disease presentation and development.....	64
Table 2.6: JSRV copy numbers in virus-inoculated sheep.....	65
Table 2.7: Presence of nodules via CT and JSRV copy numbers in virus-inoculated sheep.....	66
Table 2.8: Lung nodule characteristics evaluated via CT in relation to nodular disease development groups.....	67-68
Table 2.9: DLP characteristics evaluated via CT .....	69
Table 2.10: DLP characteristics evaluated via CT in relation to nodular disease development groups .....	70
Table 2.11: Total radiation dose from CT scanning .....	71

### *CHAPTER III:*

Table 3.1: Radiographic development and histologic features of lung disease in relation to nodular disease development .....	103
Table 3.2: Histologic features of lung disease in archival OPA sections.....	104
Table 3.3: Correlation of radiographic development of nodular disease and immunostaining of JSRV envelope and CD3.....	105
Table 3.4: Correlation of radiographic development of nodular disease and JSRV envelope antibody titers .....	106
Table 3.5: OvLV AGID serology results .....	107

*CHAPTER IV:*

Table 4.1: Characteristics of sheep infected with JSRV and analyzed for mutations.....	129
Table 4.2: Primer sets and annealing temperatures used for PCR amplification.....	130
Table 4.3: Summary of heterozygous single base substitutions found in exons 18-21 of ovine EGFR.....	131

## LIST OF FIGURES

### CHAPTER II:

Figure 2.1: RT activity in inocula.....	72
Figure 2.2: JSRV PCR amplification products from inocula.....	73
Figure 2.3: CT scan series for sheep 04RS4 (nodular disease progressor).....	74
Figure 2.4: 3D volume rendering for sheep 04RS4 (nodular disease progressor).....	75
Figure 2.5: Gross lungs from sheep 04RS4 (nodular disease progressor) and 04RS6 (nodular disease partial regressor).....	76
Figure 2.6: CT scan series for sheep 04RS6 (nodular disease partial regressor).....	77
Figure 2.7: 3D volume rendering for sheep 04RS6 (nodular disease partial regressor).....	78
Figure 2.8: CT scan series for sheep 04RS3 (nodular disease complete regressor).....	79
Figure 2.9: 3D volume rendering for sheep 04RS3 (nodular disease complete regressor).....	80
Figure 2.10: CT scan series for sheep 04RS8.....	81
Figure 2.11: 3D volume rendering for sheep 04RS8.....	82
Figure 2.12: CT scan features seen during disease development.....	83
Figure 2.13: Sheep weights over time, grouped by inoculum source .....	84
Figure 2.14: Sheep weights over time, grouped by nodular disease development groups.....	85

### CHAPTER III:

Figure 3.1: H&E staining of sheep lung tumor tissue.....	108
Figure 3.2: H&E staining and JSRV envelope immunostaining of ARJenv (+) lung tumor tissue.....	109

Figure 3.3: JSRV envelope immunostaining of sheep lung tumor tissue.....	110
Figure 3.4: H&E staining of follicular hyperplasia and bronchus associated lymphoid tissue hyperplasia .....	111
Figure 3.5: H&E staining of lung parenchyma lymphocyte infiltration and intratumor lymphocyte infiltration.....	112
Figure 3.6: CD3 immunostaining of sheep lung tumor tissue .....	113
Figure 3.7: CD3 immunostaining image analysis.....	114
Figure 3.8: Graphical representation of the percent of tissue surface area that stained positive for CD3 .....	115

*CHAPTER IV:*

Figure 4.1: JSRV DNA copy numbers from sheep and mouse lung tissue.....	132
Figure 4.2: EGFR exon 18 alignment of nucleotide sequences.....	133
Figure 4.3: Chromatograms of heterozygous single base substitutions in ovine EGFR .....	134
Figure 4.4: EGFR exons 18-21 alignment of amino acid sequences.....	135
Figure 4.5: EGFR exon 19 alignment of nucleotide sequences.....	136
Figure 4.6: EGFR exon 20 alignment of nucleotide sequences.....	137
Figure 4.7: EGFR exon 21 alignment of nucleotide sequences.....	138
Figure 4.8: KRAS exon 1 alignment of nucleotide sequences.....	139
Figure 4.9: KRAS exon 1 alignment of amino acid sequences.....	140
Figure 4.10: P53 exon 5 alignment of nucleotide sequences .....	141
Figure 4.11: P53 exon 6 alignment of nucleotide sequences .....	142
Figure 4.12: P53 exon 7 alignment of nucleotide sequences .....	143
Figure 4.13: P53 exon 8 alignment of nucleotide sequences .....	144

Figure 4.14: P53 exons 5-8 alignment of amino acid sequences.....145

## CHAPTER I

### INTRODUCTION

#### *Lung cancer statistics*

Lung cancer is the most common malignancy in humans worldwide in terms of both incidence and mortality (Parkin et al. 2001). In the United States alone, an estimated 213,380 new cases are expected in 2007, accounting for 15% of all new cancer diagnoses (American Cancer Society 2007). Fortunately, the incidence is declining significantly in men, from a high of 102.1 per 100,000 in 1984 to 79.8 per 100,000 in 2000 and, in the 1990s, the increasing trend previously noted among women leveled off with an incidence of 52.8 per 100,000 (Ginsberg et al. 2007). These long-term trends in age-adjusted incidence among both sexes are consistent with the historic pattern of tobacco use, which reflects a 30-year lag time between increasing prevalence of smoking in women and development of lung cancer as compared with men (Ginsberg et al. 2007).

Regarding deaths, an estimated 160,390 are expected in 2007, accounting for 29% of all cancer mortalities (American Cancer Society 2007). The 5-year relative survival rate for all types of lung cancer combined is only 16% and has improved just slightly in the last few years (American Cancer Society 2007). This dismal outcome can be partly attributed to the late stage of disease at diagnosis. For cases detected when the disease is still localized, the 5-year relative survival rate is 49%; however, only 16% of lung cancers are caught at this early state (American Cancer Society 2007). Unfortunately, most lung cancers do not cause any symptoms until the disease is in an advanced stage, thus making early diagnosis difficult. Additionally, screening programs aimed at early detection have shown limited effectiveness in improving survival (Humphrey et al. 2004).

### *Lung cancer imaging*

For the evaluation of lung cancer, structural and functional imaging have become incredibly valuable tools, with roles in detection, diagnosis, staging, and therapeutic response assessment. The main advantages of imaging over other biomarkers (eg, bronchoscopy, fluid analysis, and tissue sampling) include the direct visualization of disease processes, the ability to quantitate changes over time, and the non-invasive nature of the tests (Rudin and Weissleder 2003). The modalities used to evaluate lung cancer include chest radiography (CXR), computed tomography (CT), magnetic resonance imaging (MRI), and nuclear imaging techniques [eg, positron emission tomography (PET)]. For visualization, CXR, CT, and MRI exploit the interaction of various forms of energy with tissues

while PET requires the administration of a radioactive glucose analog. Currently, CT is the imaging modality of choice for the morphological assessment of the pulmonary parenchyma, including the study of lung tumors and the detection of lymph node and extrathoracic metastases (Schaefer-Prokop and Prokop 2002). Although CXR may be preferential due to its availability, low cost, and low radiation dose, CT is vastly superior in terms of sensitivity and detection of small nodules (1-5mm). Also, data from a single CT imaging procedure can be viewed in multiple planes, allowing multiplanar reconstruction (MPR) and three-dimensional (3D) volume rendering. As for MRI, despite continuous improvements in examination technique and image quality, this modality has not yet become established as a routine procedure for the detection of lung tumors due to the high susceptibility of MRI to motion artifacts (respiratory and cardiac), the intrinsic low proton density of the lung parenchyma, and the further decrease of signal by strong susceptibility to artifacts due to the multiple air-soft tissue interfaces within the lung (Schaefer-Prokop and Prokop 2002). For visualization of pulmonary perfusion and ventilation, nuclear medicine techniques are widely used, despite major limitations in spatial and temporal resolution. Improved resolution can be achieved with PET, but the potential of broad clinical use appears restricted, as the technical requirements are particularly demanding (Schuster 1998).

Major developments in thoracic CT imaging include high-resolution CT (HRCT) and spiral CT. HRCT is defined as thin-section CT (1-2mm slice width), optimized by using a high spatial resolution algorithm, and currently has the best

sensitivity and specificity of any imaging method for the assessment of focal and diffuse lung diseases (Muller 2002). Spiral CT, in which the X-ray beam follows a helical path, allows for multiplanar and 3D display of structures and visualization of pulmonary and systemic vessels. While these imaging advances have allowed for more accurate diagnosis of lung cancer, it is often challenging to differentiate malignancies from benign abnormalities, as many morphological features overlap considerably.

### *Lung cancer types and treatment*

The outcome of a lung cancer patient depends on the stage and type of the malignancy. Lung cancers are divided into two major types based on histological classification: small cell lung carcinoma (SCLC) and non-small cell lung carcinoma (NSCLC). SCLC exhibits a more aggressive biological behavior, characterized by a rapid doubling time, high growth fraction, and early development of widespread metastases (Kane and Bunn 1998). Fortunately, SCLC is highly sensitive to chemotherapy and radiotherapy (Simon et al. 2001). NSCLC includes all grades of adenocarcinomas, squamous cell carcinomas, and large cell carcinomas and accounts for about 85% to 90% of lung cancers (American Cancer Society). Adenocarcinomas alone account for about 40% of lung cancers (American Cancer Society) and have become the most common type of lung neoplasm in the US (Wingo et al. 1999). On average, NSCLC grows more slowly and metastasizes locally and regionally before widespread dissemination (Kane and Bunn 1998). NSCLC is generally less sensitive to

chemotherapy than SCLC and curative intent surgical resection is the treatment of first choice (Sekido et al. 1998). For patients who cannot be treated surgically or with targeted radiation therapy, chemotherapy is the optimal treatment.

Cisplatin-based combinations have been proven superior to best supportive care in advanced, incurable disease, making platinum-based doublet chemotherapy the standard of care for patients with advanced NSCLC (Wozniak et al. 1998; Gatzemeier et al. 2000; Sandler et al. 2000). Unfortunately, it appears that a chemotherapy efficacy plateau has been reached (Belani 2000), as little progress towards improving the effectiveness of chemotherapy for patients with advanced NSCLC has been made in the last 20 years (Breathnach et al. 2001; Kelly et al. 2001; Schiller et al. 2002).

As a result of molecular advances, cancer treatment has recently revolutionized from chemotherapy, a non-specific cell poison, to targeted drug therapy. The major categories of novel therapeutics for the treatment of lung cancer include signal-transduction or cell-cycle inhibitors [eg, farnesyl transferase inhibitors, protein kinase C-alpha (PKC $\alpha$ ) inhibitors, cyclin-dependent kinase (Cdk) inhibitors], apoptosis inducers [eg, Bcl-2 inhibitors, cyclooxygenase-2 (Cox-2) inhibitors, lipoxygenase (Lox) inhibitors], angiogenesis inhibitors [eg, endostatin, angiostatin, anti-vascular endothelial growth factor (Vegf) antibodies, matrix metalloproteinase (MMP) inhibitors], gene therapy (eg, P53 gene replacement), vaccines (eg, GVAX, MUC1, BEC2, Mage-3), and receptor-targeted therapy.

## *EGFR*

Due to their important role in cancer pathogenesis, receptor tyrosine kinases (RTKs) and their ligands are popular targets for therapeutic intervention (Gschwind et al. 2004). The most advanced clinical applications for the treatment of lung cancer target the epidermal growth factor (ErbB) receptors. One approach uses monoclonal antibodies (eg, cetuximab or Erbitux, trastuzumab or Herceptin) that bind to the extracellular domain of the receptor, preventing ligand binding and subsequent receptor activation. The other promising compounds that target the ErbB receptors are the quinazoline small-molecule reversible tyrosine kinase inhibitors (TKIs) gefitinib (Iressa; AstraZeneca) and erlotinib (Tarceva; OSI Pharmaceuticals, Genentech). These TKIs compete with adenosine triphosphate (ATP) for binding to the intracellular catalytic domain of the receptor, thus preventing autophosphorylation and activation of downstream signaling (Arteaga 2001). Gefitinib and erlotinib have shown some success in advanced NSCLC patients who are no longer responding to chemotherapy. Two multi-centre Phase II trials, IDEAL1 and 2 (Iressa Dose Evaluation in Advanced Lung Cancer), evaluated the efficacy of gefitinib in advanced NSCLC patients who received  $\leq 2$  (IDEAL1) or  $\geq 2$  (IDEAL2) previous chemotherapy regimens (Fukuoka et al. 2003; Kris et al. 2003). The response rates in IDEAL1 and IDEAL2 were 18.7% and 10.5%, respectively. A randomized placebo-controlled trial of erlotinib in patients with advanced NSCLC following failure of first-line or second-line chemotherapy showed an overall response of 9% (Shepherd et al. 2004). However, response rates to these TKIs have shown significant variability,

with the greatest degree of benefit in patients with adenocarcinomas versus other histologies, for never-smokers versus ever-smokers, for patients of East Asian ethnicity versus other ethnicities, and for females versus males (Fukuoka et al. 2003; Kris et al. 2003; Perez-Soler et al. 2004). Interestingly, this subpopulation of responders frequently has mutations within the tyrosine kinase (TK) domain of the epidermal growth factor receptor (EGFR) gene that correlate with increased sensitivity of these cancers to TKIs (Lynch et al. 2004; Paez et al. 2004). Overall, the incidence of EGFR mutations in NSCLC among clinical responders to gefitinib or erlotinib is 77%, compared with 7% in NSCLC cases that are refractory to gefitinib or erlotinib (Huang et al. 2004; Lynch et al. 2004; Paez et al. 2004; Pao et al. 2004; Bell et al. 2005; Chou et al. 2005; Cortes-Funes et al. 2005; Han et al. 2005; Kim et al. 2005; Kondo et al. 2005; Mitsudomi et al. 2005; Mu et al. 2005; Rosell et al. 2005; Takano et al. 2005; Taron et al. 2005; Tomizawa et al. 2005; Zhang et al. 2005; Niho et al. 2006; Tokumo et al. 2006; Sharma et al. 2007). Recently, EGFR TK domain mutations have been correlated with overexpression of this receptor in lung cancer (Suzuki et al. 2005). However, analyses of both preclinical xenograft models (Sirotnak et al. 2000) and specimens from gefitinib-sensitive and gefitinib-refractory tumors have shown no correlation between Egfr expression levels and sensitivity to gefitinib (Cappuzzo et al. 2003; Parra et al. 2004). Furthermore, the phosphorylation (activation) status of Egfr has also been shown to have no predictive value for gefitinib response (Han et al. 2005).

Although Egfr is frequently overexpressed (43%-89%) in NSCLC (Hirsch et al. 2003), particularly in the bronchioloalveolar carcinoma (BAC) histologic subtype (80%) (Hirsch et al. 2003), the prognostic significance of Egfr overexpression remains controversial. This ambiguity is partly due to the lack of a consistent method for evaluating gene copy number and levels of Egfr (Scagliotti et al. 2004). Several studies have shown Egfr overexpression to be associated with shortened survival (Volm et al. 1998; Cox et al. 2000; Ohsaki et al. 2000; Selvaggi et al. 2004) whereas other studies have shown no prognostic association (Pfeiffer et al. 1996; Pastorino et al. 1997; Rusch et al. 1997; Fontanini et al. 1998; Greatens et al. 1998; D'Amico et al. 1999). Further support for the latter stance comes from an extensive, investigative review, including more than 200 studies, in which Nicholson et al. found that Egfr expression was of little prognostic significance in NSCLC (Nicholson et al. 2001). A further meta-analysis involving 2185 patients from 11 studies largely confirmed that Egfr expression was not a statistically significant prognostic factor for survival in NSCLC (Meert et al. 2002). In contrast, the presence of EGFR TK domain mutations does correlate with better progression-free survival and overall survival in patients receiving gefitinib for NSCLC (Chou et al. 2005).

To date, reports of mutations involving the TK domain of the EGFR gene have been limited to NSCLC. These mutations target functionally important structures of the TK domain that are in close proximity to the ATP-binding cleft of the receptor (Lynch et al. 2004). Combined data from published reports (Kosaka et al. 2004; Lynch et al. 2004; Paez et al. 2004; Pao et al. 2004; Tokumo et al.

2005) indicate that the mutations consist of three very different types: multinucleotide in-frame deletions that eliminate four highly conserved amino acids (LREA) encoded by exon 19, duplications/insertions involving a small region in exon 20, and missense mutations in exons 18, 19, and 21, especially a single point mutation, L858R, in exon 21. The LREA deletion, exon 20 duplications/insertions, and L858R missense point mutation constitute ~95% of the mutations identified to date (Gazdar et al. 2004). Rare missense mutations in exon 18, as well as in other exons, constitute the remainder. The mutations appear to result in similar structural changes, causing a shift of the protein axis and consequent narrowing of the ATP-binding cleft (Gazdar et al. 2004; Lynch et al. 2004; Paez et al. 2004). It is postulated that this repositioning stabilizes the interaction with both ATP and its competitive inhibitor gefitinib (Lynch et al. 2004), thereby increasing both kinase activity and TK-inhibitor sensitivity (Gazdar et al. 2004; Lynch et al. 2004; Paez et al. 2004). Thus far, hundreds of primary lung cancers have been analyzed for the EGFR TK domain mutations (Lynch et al. 2004; Paez et al. 2004; Pao et al. 2004; Shigematsu et al. 2005) and, collectively, 149 mutations were detected in 759 tumor specimens (19.6%) (Pao and Miller 2005). These mutations are present only in the tumor and, to date, no germline mutations in the EGFR have been described (Janne et al. 2005).

Under normal physiological conditions, activation of the ErbB receptors is controlled by the spatial and temporal expression of their ligands, which are members of the epidermal growth factor (EGF) family of growth factors (Riese and Stern 1998; Yarden and Sliwkowski 2001). Six ligands are well

characterized: EGF (Gregory 1975), transforming growth factor- $\alpha$  (De Larco et al. 1980), amphiregulin (Shoyab et al. 1988), heparin-binding EGF-like growth factor (Higashiyama et al. 1991), betacellulin (Shing et al. 1993) and epiregulin (Toyoda et al. 1995). Ligand binding to ErbB receptors induces the formation of receptor homo- and heterodimers and activation of the intrinsic kinase domain, resulting in phosphorylation on specific tyrosine residues within the cytoplasmic tail.

Phosphorylation creates binding sites for several proteins containing a Src-homology 2 (SH2)-domain or a phosphotyrosine-binding (PTB)-domain (Prenzel et al. 2000; Sedlacek 2000; Bogdan and Klambt 2001; Yarden and Sliwkowski 2001). These proteins function in signal transduction and subsequent downstream pathways include cell survival via phosphatidylinositol-3 kinase (PI3K)/Akt and signal transducer and activator of transcription (STAT) and cell proliferation via Ras/Raf/MEK/extracellular signal-regulated kinase (Erk) (Yarden and Sliwkowski 2001; Jorissen et al. 2003). EGFR kinase domain mutants appear to selectively activate PI3K/Akt and STAT signaling pathways, promoting cell survival, but have no effect on Ras/Raf/MEK/Erk signaling (Sordella et al. 2004; Tracy et al. 2004).

### *Ras*

The Ras pathway plays a critical role in cell proliferation and is frequently activated in cancer cells by somatic mutations (Downward 2003). Mutated RAS oncogenes are encountered in about 30% of all human neoplasms, including lung cancer (Adjei 2001). Roughly 15-20% of NSCLCs and, particularly, 30-50%

of adenocarcinomas contain activating mutations in the RAS family member, KRAS (Rodenhuis et al. 1988). The majority of these mutations occur in codons 12 and 13 in exon 1 (Rodenhuis et al. 1988; Pao et al. 2005) and may be associated with an unfavorable outcome (Rodenhuis and Slebos 1990). The mutations are predominantly G to T transversions that result in the substitution of a single amino acid at these critical positions in the encoded protein, termed Kras or p21 (Barbacid 1987; Rodenhuis and Slebos 1990). Studies have suggested that these point mutations may be a direct result of one or more carcinogenic ingredients of tobacco smoke (Rodenhuis et al. 1987; Rodenhuis et al. 1988).

Ras cycles between the GDP-bound inactive form and the GTP-bound active form. GTP-bound Ras initiates cell proliferation through several downstream effectors, including Raf/MEK/Erk, PI3K, and RaIGDS. Normally, these Ras signaling cascades are only transiently activated because Ras has low intrinsic guanine triphosphatase (GTPase) activity that gradually quenches its own signaling function by hydrolyzing the bound GTP to GDP, thus inactivating the protein and controlling cell growth. Ras acquires transforming potential as a result of critical amino acid substitutions, all of which abolish GTPase activating protein (GAP)-induced GTP hydrolysis, leading to constitutive activation of Ras and thus, continuous stimulation of cellular proliferation.

Because of the high percentage of human tumors harboring oncogenic Ras mutants, interrupting the Ras-signaling pathway has been a main focus of new drug development efforts. The major approaches taken include: 1) the inhibition of Ras protein expression through ribozymes, antisense

oligonucleotides, or RNAs; 2) the prevention of membrane localization of Ras; and 3) the inhibition of downstream effectors of Ras function (Adjei 2001).

Interestingly, recent studies have demonstrated that KRAS and EGFR mutations are mutually exclusive in lung adenocarcinomas (Kosaka et al. 2004). Like mutations in the EGFR gene, KRAS mutations also occur in distinct populations; whereas EGFR mutations are more common in tumors from never-smokers, KRAS mutations frequently occur in individuals with a history of substantial cigarette use (Ahrendt et al. 2001; Pao et al. 2004). Also in contrast to mutations in EGFR, KRAS mutations are associated with a lack of sensitivity to the TKIs, gefitinib and erlotinib (Pao et al. 2005).

### *P53*

EGFR and KRAS are proto-oncogenes, normally responsible for promoting regulated cell growth. Mutations in these genes can activate their oncogenic potential, resulting in uncontrolled cell growth and cancer progression. Conversely, tumor suppressor genes normally function to inhibit progress through the cell cycle and/or promote apoptosis. Mutations in these genes often lead to inactivation, also resulting in uncontrolled cell growth and cancer progression. A tumor suppressor gene frequently mutated in many cancers, including about 50% of human lung tumors, is P53 (Hollstein et al. 1991; Greenblatt et al. 1994; Brambilla and Brambilla 1997). Mutations in the P53 gene occur in approximately 70% of SCLCs and 50% of NSCLCs, (Takahashi et al. 1989; Bodner et al. 1992; Mao 2001), including 33% of lung adenocarcinomas

(Greenblatt et al. 1994). The majority of these mutations are found in the highly conserved core domain of the gene within exons 5-8 (Hollstein et al. 1991), most frequently in codons 157, 158, 179, 245, 248, 249 and 273 (Denissenko et al. 1996; Denissenko et al. 1997; Hernandez-Boussard and Hainaut 1998; Hainaut and Pfeifer 2001). The spectrum of P53 mutations in lung cancer is different from that in other cancers; specifically, lung tumors are characterized by an excess of G to T transversions (Hollstein et al. 1991; Greenblatt et al. 1994; Hainaut and Hollstein 2000; Hainaut and Pfeifer 2001), presumably induced by polycyclic aromatic hydrocarbons (PAHs) from cigarette smoke (Hainaut and Hollstein 2000). Interestingly, most of the G to T transversion hotspots in lung cancers occur at guanines that are part of the dinucleotide sequence 5'-CpG-3' (CpG) (Yoon et al. 2001). CpG dinucleotides are sequences targeted by deoxyribonucleic acid (DNA) methyltransferases in mammalian cells, which methylate the cytosine ring at position 5 (Pfeifer et al. 1985; Bestor 1988). Mutational hot spots at methylated CpG sequences in the P53 gene may be a consequence of preferential carcinogen binding at these sites (Denissenko et al. 1997; Chen et al. 1998). Thus, similar to KRAS but unlike EGFR, P53 mutations are correlated with carcinogens in tobacco smoke and, consequently, are more common in lung malignancies of smokers than never-smokers (Husgafvel-Pursiainen et al. 2000).

The p53 protein binds to double-stranded DNA and has three main physiological functions: cell cycle regulation, stabilization of the genome, and induction of apoptosis (Ferreira et al. 1999). Wild-type p53 induces the

expression of p21<sup>WAF1/CIP1</sup> (Chang et al. 1995) which inhibits cyclin-dependent kinases (cdks) and cyclin-induced phosphorylation of the retinoblastoma (Rb) protein, resulting in inhibition of the cell cycle at the G<sub>1</sub> entrance point, thus providing an opportunity for either DNA repair or apoptosis (Steinman et al. 1994). p53 also functions directly in DNA repair by inducing the gene GADD45 (Kastan et al. 1992) and triggers apoptosis in irreversibly damaged cells through induction of the BAX gene (Miyashita et al. 1994). Mutations in the p53 protein result in altered DNA binding and reduced transactivation of p53-dependent genes (Unger et al. 1992). Also, these mutations often result in the production of a p53 protein with increased stability. This leads to the presence of positive immunohistochemical staining of mutant cells, in contrast to cells containing wild-type p53, which generally do not stain due to the relatively short half-life of the wild-type protein (Iggo et al. 1990).

Clinical trials utilizing P53 gene therapy offer an innovative approach for lung cancer therapy (Roth et al. 1996). Advances in biotechnology have made it possible to deliver the P53 gene into lung cancer cells by viral vectors (Fujiwara et al. 1993; Zhang et al. 1994) or liposomes (Ramesh et al. 2001) and have demonstrated an antitumor effect, including a bystander effect induced by wild-type P53 gene transfer to adjacent tumor cells (Nishizaki et al. 1999).

#### *Animal models of lung cancer*

Due to the aggressive biological nature and considerable heterogeneity of lung cancer as compared to other cancers, the study of this disease in humans is

difficult (Liu and Johnston 2002). Thus, the development and use of experimental models is necessary to investigate the complexities of lung cancer, including carcinogenesis, proliferation, invasion, angiogenesis, metastasis, prevention, and therapy. Currently, several types of animal models are widely used for experimental lung cancer research. These models can be generally divided into two groups: spontaneous or induced tumors and transplanted tumors. The former group consists of transgenic animals and models induced by some extrinsic chemical or carcinogen. The latter group includes the allograft and heterograft models.

In general, the spontaneous or chemically induced tumor models most closely mimic the clinical situation (Liu and Johnston 2002). These model systems are typically used for studies of carcinogenesis and cancer prevention (Curt 1994). As for spontaneous lung cancer, humans are one of only a few species susceptible to development (Liu and Johnston 2002). On the other hand, chemical or carcinogen induced lung tumors have been described in a variety of species, including dogs, cats, ferrets, hamsters, rats and mice. Several studies have shown that lung tumors developed in rats and mice are quite similar in histology and molecular characteristics to human lung cancer (Hoffman 1999; Howard et al. 1999; Balmain and Harris 2000; Malkinson 2001). Unfortunately, these tumors are usually measurable only late in their course, their metastatic pattern is not uniform, and their response to therapy is generally poor (Liu and Johnston 2002).

The allograft and heterograft models require malignant cells or tissue to be directly inoculated into the host animal. Thus, effects of early events, such as initiation and carcinogenesis, are not well suited for study (Zhao et al. 2000). Areas that are amenable for investigation in these models include tumor growth, invasion, and metastasis, as tumor development uniformly follows inoculation with predictable growth and metastatic pattern. Testing of new therapeutic approaches and screening strategies are also particularly well suited for these models.

Recent genetic advances have added to our understanding of the molecular mechanisms of human and mouse lung carcinogenesis. In fact, comparisons of gene expression changes in human and mouse lung cancers have revealed some parallels; in an oligonucleotide array analysis study, 39 genes with similar expression changes were identified, including the oncogene-related BCL7B, the cell cycle regulator CDK4, and the proapoptotic endophilin B1 (Bonner et al. 2004). Also, mutations comparable to those found in human lung cancers have been identified in mouse lung tumors; KRAS mutations occur in greater than 80% of spontaneous lung tumors from aging A/J mice and virtually all carcinogen-treated A/J mice (Belinsky et al. 1992; Horio et al. 1996; Wakamatsu et al. 2007), and mouse lung tumors induced by benzo(a)pyrene treatment exhibit a high proportion of KRAS codon 12 G to T transversions (You et al. 1992; Massey et al. 1995; Sills et al. 1999). Conversely, in spontaneous and chemically induced mouse lung tumors, P53 is not commonly mutated; when a mutation does occur, it is a late event (Wakamatsu et al. 2007). As for the

relatively newer EGFR mutations in lung cancer, transgenic mice have just recently been developed that express an exon 19 deletion mutant or the L858R mutant in type II pneumocytes and expression of either EGFR mutant leads to the development of lung adenocarcinomas (Politi et al. 2006). Thus, mouse models can provide valuable insight into human lung carcinogenesis on a molecular level; however, the disparities, including metabolic, anatomic, and cellular differences, between mouse and human lungs should not be overlooked.

Limitations of rodent models include dissimilarities in terms of lung architecture and physiology as well as problems of scale inherent with all small animal models (Emerson et al. 2003). For example, the total lung capacity of a mouse is about 1ml compared to 10ml for a rat and 6,000ml for a human (Irvin and Bates 2003). As for large animal models, there is a substantial body of evidence that shows close structural, histological, and functional similarities between the ovine and human lung (Begin et al. 1981; Mariassy et al. 1994; Harris 1997; Pemberton et al. 2000; Bischof et al. 2003). These anatomical and physiological similarities suggest that appropriate experimental studies in sheep are of direct relevance to human respiratory disease (Magno 1990; Charan and Carvalho 1992; Bakhai et al. 2002; Bischof et al. 2003). In fact, sheep are commonly used as animal models to study cystic fibrosis (Harris 1997), emphysema (Ingenito et al. 2001) and asthma (Bischof et al. 2003). Several advantages of sheep over smaller animal models include (1) capacity for substantial, multiple, and repeated samples, (2) capability to harbor a sizeable tumor burden, (3) ease of surgical procedures, (4) commonality of imaging

techniques and treatment options with humans, and (5) longevity, allowing long-term experimentation. Also, in terms of genetics, sheep represent a more natural outbred population than inbred laboratory animals. In addition, sheep have not undergone artificial immunologic manipulation, as is the case for severe combined immune deficiency (SCID) mice and athymic nude mice and rats.

#### *Ovine pulmonary adenocarcinoma*

Furthermore, ovine pulmonary adenocarcinoma (OPA) induced by jaagsiekte sheep retrovirus (JSRV) shares both symptomatic and histopathologic characteristics with human BAC (De las Heras et al. 2000; Palmarini and Fan 2001; Fan et al. 2003; Mornex et al. 2003; Sharp and DeMartini 2003; Christiani et al. 2006). Symptomatically, OPA presents with the same clinical signs as BAC in humans: progressive dyspnea, abundant bronchorrhea, cough, anorexia and cachexia (Mornex et al. 2003). Histopathologically, in both BAC and OPA, the tumor originates from differentiated alveolar type II cells and non-ciliated bronchiolar epithelial (Clara) cells (Nisbet et al. 1971; Perk et al. 1971; Sharp 1987; Platt et al. 2002). Also, in both cancers, the neoplastic tissues are preferentially localized at the periphery of the lungs (Palmarini and Fan 2001) and the lesions tend to be multifocal (Palmarini and Fan 2001), presumably due to either intrapulmonary metastasis (Manning et al. 1984) or a multiclonal origin (Barsky et al. 1994). Traditionally, OPA has been classified as a BAC (Bonne 1939; Nobel and Perk 1978; Perk and Hod 1982). However, in the 1999 World Health Organization (WHO) classification of lung tumors, the BAC criteria

underwent a major change, requiring that all BACs demonstrate pure lepidic (bronchioloalveolar) growth without invasion of the stroma, blood vessels, or pleura (Travis et al. 1999). Accordingly, OPA is now classified as a mixed-subtype adenocarcinoma, as these ovine tumors have both bronchioloalveolar and invasive (acinar and papillary) growth patterns (Mornex et al. 2003).

OPA was first recognized in South Africa in the 19<sup>th</sup> century as a cause of respiratory distress in sheep when they were herded (Dykes and M'Fadyean 1888). Since then, this infectious disease has been identified on all continents (Leroux et al. 2007). The incidence of clinical disease in an affected flock is generally around 2-5%, although in some countries, such as Britain, it can be as high as 30% (Sharp and DeMartini 2003). In contrast, OPA is infrequently diagnosed in the USA or Canada, where only 11 and 43 cases have been reported, respectively (Stevenson et al. 1980; Cutlip and Young 1982; Rosadio et al. 1988; Sharp and DeMartini 2003). Most clinical cases of OPA occur in sheep between two and four years of age; diseased animals develop symptoms of progressive respiratory distress that worsen with increasing size of the lesions and resulting loss of alveolar function (Sharp and DeMartini 2003). Animals inflicted with OPA usually die within a few weeks of the onset of clinical signs and, in an affected flock, this disease can be responsible for more than 50% of the mortalities (Sharp and Angus 1990).

A viral etiology for OPA was suspected beginning in the late 1940s. At that time, OPA was experimentally reproduced by inoculating lambs with a cell-free glycerin solution into which OPA-affected sheep had exhaled (Dungal 1946). The

causative agent of OPA is now known to be jaagsiekte sheep retrovirus (JSRV), the term jaagsiekte coined from the Afrikaans “driving” (jaag) and “sickness” (ziekte), reflecting the tendency of diseased sheep to lag behind the flock during herding (Tustin 1969). Occasionally, this virus has also been postulated to be the etiological agent of human BAC (Stinson et al. 1972; Geddes 1987; Morabia and Wynder 1992; Peterschmitt et al. 1994; Nuorva et al. 1995). For instance, the multiclinality of at least some multifocal cases of BAC might suggest an environmental carcinogen or an infectious agent (Barsky et al. 1994). Also, antibodies against the JSRV major capsid protein were found to react with about 30% (39 of 129) of human BACs and 26% (17 of 65) of human pulmonary adenocarcinoma samples (De las Heras et al. 2000). However, attempts to identify such viruses by polymerase chain reaction (PCR) have been unsuccessful thus far (Yousem et al. 2001; Hiatt and Highsmith 2002; Morozov et al. 2004).

Naturally, OPA is an infectious disease transmitted between animals by close contact, mainly through aerosolized particles (Leroux et al. 2007). For experimental induction, initial transmission studies involved several routes of inoculation or aerosol exposure, using tumor cells or crude tumor extracts, and even contact-exposure to OPA-affected sheep (Dungal 1946; Wandera 1968; Sharp and DeMartini 2003). Since those and other early studies, it has been demonstrated that OPA can be induced within a much shorter time frame by intratracheal inoculation of newborn lambs with JSRV extracted from lung fluid or tumor (Sharp et al. 1983; DeMartini et al. 1987; Sharp and DeMartini 2003). In

these studies, histologically confirmed OPA was induced successfully in 70-100% of inoculated animals, with most lambs developing clinical signs within 3-6 weeks of inoculation (Sharp et al. 1983; DeMartini et al. 1987; Sharp and DeMartini 2003). In a recent study, OPA was induced in a high proportion of lambs that had been inoculated intratracheally with infectious lung fluid at 1, 3, and 6 months of age (Salvatori et al. 2004). However, the incubation periods were longer in these three age groups than in one week-old lambs that were used as controls, suggesting an age-dependent susceptibility to OPA, possibly determined by the availability of JSRV target cells in the ovine lung (Salvatori et al. 2004) as well as by the immaturity of the neonatal immune response to viral infections (Rosadio et al. 1988).

#### *Jaagsiekte sheep retrovirus*

JSRV is classified as a betaretrovirus (Hunter et al. 2000) and has the canonical *gag*, *pro*, *pol*, *env* genome arrangement flanked by a long terminal repeat (LTR) on each end, as well as an additional open reading frame, *orfX*. The tropism of a retrovirus is primarily determined by the envelope gene and the long terminal repeat (LTR). The envelope gene encodes the viral glycoprotein that interacts with cell surface receptor(s) and facilitates viral entry (Weiss and Taylor 1995). For JSRV, the cellular receptor has been cloned and identified as hyaluronidase-2 (Hyal2) (Rai et al. 2001), a glycosylphosphatidylinositol-linked cell surface protein that is expressed in many cell types (Lepperdinger et al. 1998; Strobl et al. 1998). Accordingly, JSRV can infect a variety of cells, but

primarily targets differentiated epithelial cells of the lungs (Palmarini et al. 1995; Platt et al. 2002). Also, using sensitive PCR assays, JSRV DNA and RNA transcripts have been detected in lymphoreticular organs, including spleen, thymus, and bone marrow, peripheral blood mononuclear cells (PBMCs), and in lymphoid cells, including adherent cell (macrophage/monocyte) populations, CD4<sup>+</sup> T cells, CD8<sup>+</sup> T cells, and B lymphocytes, isolated from the mediastinal lymph nodes of both natural and experimental OPA cases (Palmarini et al. 1996b; Holland et al. 1999; Garcia-Goti et al. 2000; Gonzalez et al. 2001; Salvatori et al. 2004). Notably, there is no evidence of viral transformation in any of these cell types (Palmarini et al. 1996b; Holland et al. 1999). Instead, in OPA-affected sheep, JSRV expression and subsequent transformation are restricted to alveolar type II cells/type II pneumocytes in the alveoli and Clara cells in the bronchioli (Palmarini et al. 1995; Platt et al. 2002). This restriction is due to the preferential activation of the JSRV LTR in these cells, as viral expression is driven more efficiently in cells that express transcription factors that interact with the viral promoter and enhancer elements contained in the LTR (Palmarini et al. 2000a). JSRV appears to be unique among retroviruses in inducing transformation of the differentiated epithelial cells of the lungs (Rosenberg and Jolicoeur 1997); thus, JSRV-induced tumors occur exclusively in the sheep lung. In addition, metastases to both thoracic and extrathoracic tissues have been observed (Nobel et al. 1969; Hunter and Munro 1983; Snyder et al. 1983; Verwoerd et al. 1985; Palmarini and Fan 2001).

### *Host immune response to JSRV*

The disseminated JSRV infection of the lymphoreticular system may indicate viral interference with the immune system of the host. Interestingly, JSRV dissemination was found to be an early event following experimental infection of young lambs; JSRV proviral DNA was detected in lymphoid cells as early as 7 days post inoculation, when no histological signs of OPA were present (Holland et al. 1999). Thus, infection of lymphoid cells precedes neoplastic transformation and may be advantageous to the virus either by directly facilitating the infection and subsequent transformation of epithelial cells or by indirectly inducing an immunosuppressive state in the host (Holland et al. 1999). In fact, natural cases of OPA have been shown to have marked peripheral CD4<sup>+</sup> lymphocytopenia and neutrophilia, although similar phenotypic changes were not seen in experimentally-infected animals (Holland et al. 1999; Summers et al. 2002). Moreover, reduced responses of PBMCs to the mitogen concanavalin A were demonstrated; as early as 8 weeks post inoculation, the response of JSRV-inoculated lambs was only 33% that of uninfected control lambs, and, for natural cases, the response was only 58% that of age-matched, unaffected controls (Summers et al. 2002). Conversely, in the same study, no significant differences were shown for the lymphoproliferative responses to stimulation with either phytohaemagglutinin or pokeweed mitogen. Overall, it appears that there is some evidence to indicate that OPA-affected sheep are immunocompromised.

In further support of this notion, no JSRV-specific humoral response has been detected in sera or lung fluid of affected sheep by Western blotting or

enzyme-linked immunosorbent assay (ELISA), despite a highly productive infection in the lungs (Sharp and Herring 1983; Ortin et al. 1998; Summers et al. 2002; Sharp and DeMartini 2003). However, a recent study has shown that inoculation of sheep with recombinant JSRV-capsid protein in adjuvant (complete Freund's adjuvant or incomplete Freud's adjuvant) can successfully induce a JSRV-specific humoral response (Summers et al. 2005). Thus, the ovine immune system appears to be capable of recognizing and responding to the JSRV-capsid antigen (Summers et al. 2005). In all mentioned studies, it is important to note that only JSRV-capsid antigens, from natural sources (lung fluid or nasal exudate) or protein recombination, have been used for the detection of circulating antibodies. Thus far, there has been no investigation of antibodies against the envelope protein, the oncogenic component of JSRV.

Details regarding the local immune response within the lungs of OPA-affected sheep remain vague. Evaluation of bronchioloalveolar lavage samples from natural and experimental OPA cases showed a 24-fold increase in total leukocytes and alveolar macrophages, a 185-fold increase in polymorphonuclear cells, and an 11-fold increase in lymphocytes compared to controls (Rosadio and Sharp 2000). In the lung parenchyma, diffuse interalveolar septal thickening by lymphocytes, macrophages, plasma cells, and neutrophils has been reported; additionally, a similar inflammatory response, as well as lymphoid proliferation, has been consistently documented around both affected and non-affected bronchioles (Payne and Verwoerd 1984; Rosadio et al. 1988; De Las Heras et al. 1995; Garcia-Goti et al. 2000; De las Heras et al. 2003). However, it has been

postulated that these influxes may be due to concurrent infections, such as ovine lentivirus (OvLV) or mycoplasma, commonly present in OPA cases (Cutlip and Young 1982; Demartini et al. 1988; Verwoerd 1990). A recent study that experimentally infected specific pathogen-free lambs with JSRV found no influx of dendritic cells, B-cells, CD4<sup>+</sup> T-cells, CD8<sup>+</sup> T-cells, or  $\gamma\delta$  T-cells in the neoplastic nodules or in their periphery (Summers et al. 2005). Alternatively, this study found that the local immune response during OPA development is mediated predominantly by infiltrating macrophages that secrete high levels of interferon-gamma (IFN- $\gamma$ ) (Summers et al. 2005).

The inadequate immune response seen in OPA cases has been proposed to be a consequence of transcriptionally active endogenous JSRV (enJSRV) sequences expressed during fetal ontogeny; therefore, enJSRV is recognized as self by the host immune system, thus resulting in central tolerance to the nearly homologous (90-98% at the amino acid level) exogenous JSRV (exJSRV) (Bai et al. 1996; Palmarini et al. 1996; Bai et al. 1999; Rosati et al. 2000; Palmarini et al. 2000b; Spencer et al. 2003; Palmarini et al. 2004). In addition to the female reproductive tract, enJSRV RNA has also been detected in a variety of tissues, including lungs, kidneys, thymus, bone marrow, spleen, mediastinal lymph nodes, and leukocytes (Palmarini et al. 1996b). The notion of an endogenous retrovirus acting as an immunosuppressant is not without precedence; the expression of the envelope protein encoded by a human endogenous retrovirus belonging to the HERV-H family has immunosuppressive properties and enables tumor cells to escape immune rejection and proliferate (Mangeny et al. 2001).

The absence of an immune response against JSRV in infected sheep could provide a permissive environment for the development of neoplasms in the lung (Ortin et al. 1998). Interestingly, it has been shown that the JSRV envelope can transduce not only sheep cells but also human, monkey, bovine, dog, and rabbit cells *in vitro*; yet, there is an absence of evidence of infection with JSRV *in vivo*, possibly due to the development of a strong immune response leading to virus clearance (Rai et al. 2000). In a study using immunodeficient mice, lung adenocarcinomas were induced by a replication-defective adeno-associated virus type 6 (AAV6) vector that expressed the JSRV envelope protein (ARJenv); the consequent mouse tumors were similar, both in location and histology, to OPA (Wootton et al. 2005; Wootton et al. 2006). However, in the same study, immunocompetent mice mounted a strong serum antibody response against the JSRV envelope and tumor development was almost entirely blocked, indicating that JSRV envelope tumorigenesis can be controlled by the normal immune system of these mice (Wootton et al. 2005).

#### *JSRV-induced transformation*

One of the most intriguing questions regarding the biology of JSRV concerns the mechanism of virus-induced cell transformation. With regard to oncogenesis, retroviruses can be divided into two classes: acutely transforming retroviruses and nonacutely transforming retroviruses (Fan 1992; Rosenberg and Jolicoeur 1997). Acutely transforming retroviruses have incorporated a cellular proto-oncogene into their genome, often altering its structure (deletions, point

mutations, etc.) and expression in the process. Nonacutely transforming retroviruses lack internal oncogenes and initiate transformation by insertional activation of a cellular proto-oncogene, causing its ectopic activation by regulatory sequences in the LTR. Thus far, it is unclear if JSRV carries a viral oncogene or induces tumors by insertional activation. Examination of the JSRV genome reveals no apparent oncogene, although an alternative open reading frame (i.e., orfX) had been suspected but was later excluded (Maeda et al. 2001; Liu et al. 2003). The rapid induction of JSRV, in as little as 10 days in neonatal lambs (Verwoerd et al. 1980; Sharp et al. 1983), compounded with the multifocality of OPA tumors strongly indicate the existence of an acutely transforming oncogene and argue against a mechanism involving insertional mutagenesis (Liu et al. 2003). Further supporting this, a study analyzing 28 exJSRV integration sites in lung tumors from 4 natural OPA cases found a multiclonal pattern of integration sites (Philbey et al. 2006). In a more extensive study involving 70 exJSRV integration sites from 23 cases of OPA (19 natural and 4 experimentally-induced), integration sites were found on 20 of the 28 sheep chromosomes (Cousens et al. 2004), suggesting a random distribution. Interestingly, 4 integration sites from 4 different tumors mapped to chromosome 16, including 2 sites that mapped to within 2.5kb of each other, inside an uncharacterized predicted gene and less than 200kb from the mitogen-activated protein kinase-encoding gene MAP3K1 (Cousens et al. 2004). Significantly, this distance is within the range previously reported for enhancer activation of cellular oncogenes by retrovirus LTRs (Lazo et al. 1990). In the JS7 cell line, derived

from a natural case of OPA, a single copy of the JSRV provirus is integrated in the promoter region of the surfactant protein A gene, but no rearrangements were detected in this gene in eight tumors from natural cases of OPA; hence, the significance of this integration site is unknown (DeMartini et al. 2001). Overall, for JSRV-induced transformation, the evidence points away from insertional mutagenesis and, thus, towards a viral oncogene.

Although the mechanism of oncogenesis is unknown, the JSRV envelope has been found to transform cells in culture (Maeda et al. 2001; Palmarini et al. 2001; Rai et al. 2001; Allen et al. 2002; Chow et al. 2003; Danilkovitch-Miagkova et al. 2003; Zavala et al. 2003; Liu and Miller 2005; Maeda et al. 2005) and to induce lung adenocarcinomas in sheep (Caporale et al. 2006) and immunocompromised mice (Wootton et al. 2005). Thus, both *in vitro* and *in vivo*, the JSRV envelope has been shown to function as an oncoprotein and to be the viral component that is both necessary and sufficient to induce transformation. This concept of a retroviral envelope functioning as an oncoprotein has precedents in other transforming retroviruses. For example, the envelope glycoprotein, gp55, of the Friend spleen focus-forming virus (SFFV) induces erythroblast proliferation *in vitro* and leukemia *in vivo* (Wolff and Ruscetti 1988; Aizawa et al. 1990). Also, the envelope protein of avian hemangiosarcoma virus (ASV) has been shown to directly transform NIH-3T3 cells (Alian et al. 2000), and studies indicate that the mouse mammary tumor virus (MMTV) envelope protein participates in mammary epithelial cell transformation both *in vitro* and *in vivo* (Katz et al. 2005; Ross et al. 2006).

Regarding retroviral envelope proteins, their primary function is to interact with cell surface receptor(s) and facilitate virus entry (Weiss and Tailor 1995). As for the JSRV envelope protein, it is composed of two subunits: the surface (SU) subunit mediates receptor binding and the transmembrane (TM) subunit is involved in virus-cell fusion (York et al. 1992). The role of the SU subunit in JSRV envelope-induced transformation appears to be dependent on the target cell type (Liu and Miller 2007). For transformation of BEAS-2B human bronchial epithelial cells, the SU subunit and its interaction with the cellular receptor for JSRV, Hyal2 (Rai et al. 2001), seem to be critical (Danilkovitch-Miagkova et al. 2003). In NIH-3T3 and 208F rodent fibroblasts, the role of the SU subunit is less apparent, with two studies finding no effect (Chow et al. 2003; Liu et al. 2003) and one study showing that large deletions or small insertions in the SU subunit could abolish transformation of these cell types (Hofacre and Fan 2004).

Deletion experiments show that the TM subunit of the JSRV envelope protein is the primary determinant for cell transformation (Chow et al. 2003; Hofacre and Fan 2004; Hull and Fan 2006; Leroux et al. 2007). In particular, the 44 amino acid cytoplasmic tail within the TM region has been reported to be essential for transformation in multiple cell lines, including NIH-3T3 mouse fibroblasts (Palmarini et al. 2001), 208F rat fibroblasts (Liu et al. 2003), DF-1 chicken fibroblasts (Allen et al. 2002), and MDCK canine kidney epithelial cells (Liu and Miller 2005). This domain contains a YXXM (Y: tyrosine, X: any amino acid, M: methionine) peptide motif, which, if phosphorylated on the tyrosine at amino acid position 590 (Y590), could bind the SH2 domain of the p85 subunit of

PI3K (Songyang et al. 1993; Palmarini et al. 2001). Experiments have demonstrated that mutations of Y590 [Y590F (phenylalanine) or Y590D (aspartic acid)] and methionine at amino acid position 593 [M593T (threonine)] were sufficient to inhibit transformation in NIH-3T3 fibroblasts (Palmarini et al. 2001). Another study revealed that, in NIH-3T3, 208F, and RK3E rodent cells, mutation of this residue [Y590F, Y590D, or Y590A (alanine)] also abolished transformation (Hull and Fan 2006). In contrast, other work has shown that Y590 mutants had transforming capabilities in NIH-3T3 and 208F cells (Liu et al. 2003), MDCK cells (Liu and Miller 2005), and DF-1 cells (Allen et al. 2002; Zavala et al. 2003), but with reduced efficiency in most cases. Additionally, these studies also found that mutation of M593 did not have a significant effect on cell transformation (Allen et al. 2002; Liu et al. 2003). Recently, though, *in vivo* work has shown that a complete integrated provirus clone, JSRV(21), with the cytoplasmic tail mutation Y590D, did not cause disease nor detectable infection in sheep, indicating that the YXXM motif is absolutely required for virus replication and possibly transformation in the natural host of JSRV (Cousens et al. 2007).

Although its responsibility in JSRV envelope-induced transformation is unclear, the general consensus is that, *in vitro*, the YXXM motif does not directly activate PI3K in transformed cells (Liu and Miller 2007). Supporting evidence includes the variable role of this motif in transformation between cell types and the absence of detection of Y590 phosphorylation or interaction between the JSRV envelope and PI3K/p85 (Liu et al. 2003; Liu and Miller 2005). Furthermore, it has also been reported that mutations of this motif do not abolish activation (via

phosphorylation) of the downstream signaling molecule Akt (Liu et al. 2003; Zavala et al. 2003; Liu and Miller 2005), which can be activated by both PI3K-dependent and PI3K-independent pathways. Regarding PI3K-dependent Akt activation, it has been demonstrated that the PI3K-specific inhibitor LY294002 drastically reduces Akt phosphorylation and inhibits transformation by the JSRV envelope in NIH-3T3 cells (Maeda et al. 2001; Alberti et al. 2002; Liu et al. 2003; Maeda et al. 2003; Zavala et al. 2003; Liu and Miller 2005). Furthermore, LY294002 was able to reverse the neoplastic phenotype of JSRV envelope-transformed 208F cells (Liu et al. 2003). Conversely, in favor of a PI3K-independent pathway, Akt activation has been observed in JSRV envelope-transformed NIH-3T3 cells deficient for the p85 subunit of PI3K, and, in the same study, LY294002 failed to inhibit transformation of these cells or to reverse the transformed phenotypes (Maeda et al. 2003).

Regardless of the involvement of PI3K, it does appear the Akt is activated in several, though not all, JSRV envelope-transformed cell lines (Palmarini et al. 2001; Allen et al. 2002; Liu et al. 2003; Zavala et al. 2003; Liu and Miller 2005). In addition, phosphorylated Akt was detected in a cell line (JS-8) derived from the lung tumor of a sheep with naturally occurring OPA (Alberti et al. 2002). *In vivo*, one study found no evidence of Akt phosphorylation in lung tumor sections from natural OPA cases (Zavala et al. 2003), while another group observed Akt activation in 37% of OPA tumors sampled at a late stage of disease (Suau et al. 2006).

JSRV envelope-mediated transformation has also been associated with the Ras-MEK-MAPK pathway although, as with Akt, the significance of this signaling cascade seems to vary with cell type (Leroux et al. 2007). Activation (via phosphorylation) of the MAPK family member Erk1/2 was not detected in 208F or NIH-3T3 cells transformed by JSRV envelope (Liu et al. 2003; Maeda et al. 2005). Conversely, in JSRV-transformed BEAS-2B cells, Erk1/2 was found to be constitutively phosphorylated (Danilkovitch-Miagkova et al. 2003). Interestingly, an H/N-Ras inhibitor (FTI-277) and MEK inhibitors (PD98059 and U0126) have been shown to strongly inhibit JSRV envelope-induced transformation of NIH-3T3 cells; in RK3E cells, the MEK inhibitors also abrogated transformation, but the H/N-Ras inhibitor only partially inhibited transformation (Maeda et al. 2005). In both natural and experimentally-induced OPA cases, several proteins in the Ras-MEK-MAPK pathway were found to be activated (via phosphorylation), including Raf-1, MEK1/2, and Erk1/2, as well as downstream transcription factors 90Rsk, Elk-1, and c-Myc (Maeda et al. 2005; De Las Heras et al. 2006). Also, in unpublished work, Maeda and Fan have recently shown that two OPA-derived tumor cell lines, JS7 and JS8, have constitutively activated Erk1/2 (Maeda et al. 2005). On the whole, the above data strongly indicates that signaling through Ras-MEK-Erk1/2 is indeed likely to be important in JSRV-induced oncogenesis. The involvement of this pathway in OPA has precedent in a study that found significant expression levels of the Ras family member Kras in OPA lesions as well as Kras migrational differences between OPA samples and normal ovine lung on Western blot analyses, suggesting the presence of a

mutated species of the Kras protein in OPA (Meyers et al. 1989). Further implicating Ras involvement is the YXNX motif in the JSRV TM cytoplasmic tail, which is a putative binding site for the growth factor receptor binding protein 2 (Grb-2), an adapter molecule that provides a critical link between cell surface growth factor receptors and the Ras signaling pathway (Palmarini et al. 2001). However, mutation of the asparagine at residue 592 (N592T) did not abolish transformation of NIH-3T3 cells, thus indicating that binding of Grb-2 was not essential for JSRV envelope-induced transformation (Palmarini et al. 2001).

Another postulated mechanism involves envelope-induced Hyal2 degradation and subsequent activation of the RON receptor tyrosine kinase, which is normally suppressed by Hyal2 (Danilkovitch-Miagkova et al. 2003). However, this pathway appears to only be specific for JSRV envelope transformation of BEAS-2B cells (Liu and Miller 2007).

### *Objectives*

Appropriate animal models of disease allow defined and controlled investigations that can ultimately be applied to the management of human disease. Based on symptomatic, histopathologic, and possible molecular signaling similarities, we hypothesized that sheep experimentally affected by OPA are a relevant animal model for the study of human lung adenocarcinoma and the size of this model makes it particularly suitable for the evaluation of intrapulmonary lung cancer therapeutics. The value of this model is dependent upon its predictability, reproducibility, amenability, and validity. The former two

features have been previously reported; OPA induction in sheep is both predictable and reproducible following JSRV inoculation of neonatal lambs. The overall objective of this body of work was to assess the amenability of this animal model for therapeutic research and to assess the validity of OPA-affected sheep as an animal model for human lung adenocarcinoma in terms of genetic similarities.

To be amenable for therapeutic research, we must be able to detect disease early, before the cancer reaches an advanced stage. Currently, there is not a method for diagnosis of OPA before the onset of clinical signs, which are manifested when the lung lesions are relatively advanced. At this end-state, treatment strategies would likely be futile. In addition to early detection, we must also be able to monitor the development of cancer. To be amenable for therapeutic research, we must be able to follow disease development in order to assess therapeutic response after the hypothetical administration of treatment. For our work, we used CT technology as a noninvasive imaging modality to monitor the development of OPA after inoculation of neonatal lambs with JSRV.

To be a valid animal model for human lung adenocarcinoma, OPA should harbor genetic alterations similar to those found in the human disease. Thus, we evaluated OPA tumors for mutations commonly found in human lung adenocarcinomas, including activating mutations in the EGFR and KRAS genes and inactivating mutations in the P53 tumor suppressor gene. This genetic profile combined with the disease development data provided further characterization of

OPA and facilitated an assessment of the utility and relevance of this animal model for human lung cancer studies.

## **CHAPTER II**

### **RADIOGRAPHIC IMAGING OF OVINE PULMONARY ADENOCARCINOMA DEVELOPMENT**

#### **INTRODUCTION**

The aim of this body of work was to determine if sheep affected by OPA can be used as a relevant animal model for the study of human lung carcinogenesis and, in particular, for the evaluation of lung cancer therapeutics. The value of this model is dependent upon its predictability, reproducibility, amenability, and validity. The former two features have been previously reported: for newborn lambs inoculated intratracheally with JSRV isolated from lung fluid or tumor tissue, the OPA induction rate is 70-100%, with most lambs developing clinical signs of disease within 3 to 6 weeks of inoculation (Sharp et al. 1983; DeMartini et al. 1987; Sharp and DeMartini 2003; Salvatori et al. 2004). In the most recent study, JSRV infection was induced in 100% of lambs aged 1 week to 6 months at the time of inoculation and a high proportion of these animals

developed OPA-associated clinical signs (62-90%) and lesions (87-100%) (Salvatori et al. 2004). Thus, OPA induction in sheep is both predictable and reproducible following JSRV inoculation of neonatal lambs. However, if this model is to be useful for therapeutic intervention studies, we must be able to detect disease early, before the cancer reaches an advanced stage and treatment strategies would likely be futile. Currently, diagnosis of OPA is possible only when clinical signs or lesions at necropsy are observed (De las Heras et al. 2003) and the presence of JSRV is confirmed in lung fluid or tumors by immunoblotting (Sharp and Herring 1983), ELISA (Palmarini et al. 1995) or PCR (Bai et al. 1996; Palmarini et al. 1996). It is more difficult to identify infected animals during the pre-clinical period due to the lack of detectable JSRV proteins outside the tumor (Palmarini et al. 1995) and the absence of circulating JSRV-specific antibodies (Sharp and Herring 1983; Ortin et al. 1998). A blood test was recently developed that used PCR to detect JSRV; however, this test was unreliable for detection of disease in affected sheep that did not exhibit clinical signs of OPA (De Las Heras et al. 2005). Consequently, a dependable method is lacking for the noninvasive detection of OPA prior to the onset of clinical signs.

In addition to early detection, we must also be able to monitor the development of OPA. To be amenable for therapeutic research, we must be able to follow disease development in order to assess therapeutic response after the hypothetical administration of treatment. For the evaluation of lung cancer, structural and functional imaging have become incredibly valuable tools, with roles in detection, diagnosis, staging, and therapeutic response assessment.

Currently, CT is the imaging modality of choice for the *in vivo* morphological appraisal of the pulmonary parenchyma, including the study of lung tumors and the detection of lymph node and extrathoracic metastases (Schaefer-Prokop and Prokop 2002). The main advantages of imaging over other biomarkers (eg, bronchoscopy, fluid analysis, and tissue sampling) include the direct visualization of disease processes, the ability to quantitate changes over time, and the non-invasive nature of the tests (Rudin and Weissleder 2003).

The goal of the subsequent study was to utilize CT as a noninvasive imaging modality to detect OPA earlier than possible with clinical observations and follow the development of disease over time. Our aim was to detect the absence or presence of lung parenchymal abnormalities, and further characterize the identified abnormalities in terms of presentation, location, and appearance. For OPA induction, we used neonatal lambs, as an age-dependent susceptibility to JSRV-induced tumorigenesis has been suggested and indicates that disease induction is most rapid and efficient in newborn lambs (Salvatori et al. 2004). CT images were acquired prior to JSRV inoculation, and post inoculation on a monthly basis through one month (one animal), four months (two animals), five months (three animals), and six months (six animals). Post mortem, sheep lungs were examined grossly and sampled for subsequent analyses, including histopathological evaluation and genetic profiling.

## **MATERIALS AND METHODS**

### *Preparation of jaagsiekte sheep retrovirus (JSRV) inocula*

Inocula were prepared as described previously (DeMartini et al. 1987) from lung tissue that had been stored at -70°C for 8 to 16 years. Briefly, five gram portions of lung tumor tissue from each of three OPA cases [one experimental (91RS13) and two natural cases (98RS3, 99RS27)] were homogenized in 20mLs of TNE buffer [0.01M Tris-HCl, 0.1M NaCl, and 0.001M EDTA (pH 7.4)], clarified by centrifugation at 2,000 x g for 20 minutes at 4°C, 10,000 x g for 30 minutes at 4°C, and pelleted by ultracentrifugation at 100,000 x g for 60 minutes at 4°C. Pellets from each sample were resuspended in 5mLs of TNE buffer and subsequently used as inocula. All three inocula tested positive for ovine lentivirus (OvLV) via polymerase chain reaction (PCR) (analyzed by Veterinary Diagnostic Laboratories, Colorado State University). In an attempt to neutralize the OvLV, the inoculum from 99RS27 was incubated with OvLV antiserum (300µL/mL inoculum) for 30 minutes at 37°C. All three inocula tested negative for mycoplasma (analyzed by Veterinary Diagnostic Laboratories, Colorado State University).

### *Jaagsiekte sheep retrovirus (JSRV) inoculation*

Twelve colostrum-fed neonatal female lambs were obtained from a local flock, allegedly free of OvLV infection (Josh Livestock, Greeley, CO). All lambs received Naxcel® [indicated for the treatment of ovine bacterial pneumonia associated with *Mannheimia (Pasteurella) haemolytica* and *Pasteurella multocida*, (Pfizer)] and combined diphtheria and tetanus (CD-T) vaccination

[provides three-way protection against enterotoxemia caused by *Clostridium perfringens* types C and D and tetanus (lockjaw) caused by *Clostridium tetani*]. At approximately one week of age, lambs were administered inoculum (that had been stored at -70°C after preparation) from varied sources (Table 2.1). For inoculation, the lamb was restrained, an 18-gauge needle was inserted into the distal trachea between two tracheal rings, and 5mLs of the respective inoculum was injected. With inhalation, the inoculum was aspirated into the airways. Animals were monitored daily for clinical signs of respiratory disease suggestive of OPA. Lambs were euthanized humanely at predetermined time points, (one animal at one month, two animals at four months, three animals at five months, and six animals at six months) (Table 2.2). At necropsy, gross examination of the lungs was performed to identify any lesions suggestive of OPA. Neoplastic-like areas and/or tissue from all lobes were taken for microscopic examination and further analysis. For microscopy, tissue samples were fixed in 10% neutral-buffered formalin, processed routinely, sectioned at 5µm, and stained with haematoxylin and eosin (H&E). Other tissue samples obtained at the time of sacrifice were rapidly frozen in liquid nitrogen and stored at -80°C. Serum samples were obtained at each CT scan time point, rapidly frozen in liquid nitrogen, and stored at -80°C. All experimental procedures were approved by Colorado State University's Animal Care and Use Committee.

#### *Computed tomography (CT) imaging*

Disease progression was monitored by acquiring serial sheep thorax images via spiral CT using a modified Picker PQ CT scanner. Scan factors were 130.0kV, 150mA, 1.5 pitch, 512 x 512, field of view 25cm using a transverse imaging plane, and reconstructed as 5.0mm contiguous slices. Scanning was performed both before and after intravascular contrast material [Hypaque 76 (370mg/mL iodine), GE/Amersham] administration (1 cubic centimeter per pound), with the exception of the pre-inoculation scans (no contrast material). For all scans, sheep were anesthetized with morphine and isoflurane and subsequently situated in the supine position. Images were acquired prior to inoculation, and post inoculation on a monthly basis through one month (one animal), four months (two animals), five months (three animals), and six months (six animals) (Table 2.2).

Using a lung window width and level, CT scans were evaluated by board-certified veterinary radiologist Susan Kraft. Disease characteristics, including location, presentation, appearance, extent, internal features, and nodule margin characteristics, were recorded (Table 2.3).

Disease location: The location of disease was arbitrarily considered to be central if the disease was located within the inner two-thirds of the lung and peripheral if the disease was located within the outer one-third of the lung. Dorsal and ventral disease location was also noted. Additionally, disease location was described by lobe [right cranial lobe (RCrL), right middle lobe (RML), right caudal lobe (RCdL), right accessory lobe (RAL), left cranial lobe (LCrL), or left caudal lobe (LCdL)].

Disease presentation: The presentation of disease was described as a solitary nodule, multiple nodules, or diffuse lung pattern. A pulmonary nodule was defined as a discrete focal opacity less than 3cm in maximum diameter (Austin et al. 1996). An area of opacity larger than 3cm was described as a diffuse lung pattern.

Disease appearance: Disease attenuation was described as ground glass opacity (GGO), solid, or mixed (GGO/solid). GGO was defined as hazy increased attenuation of the lung without obscuration of underlying vessels (Austin et al. 1996). Solid attenuation was defined as a homogenous increase in pulmonary parenchymal attenuation with obscuration of underlying vessels. Mixed (GGO/solid) consisted of heterogeneous attenuation with both GGO and solid components.

Extent of disease: Extent of disease, whether diffuse or nodular, was expressed according to lobar or sublobar locations or general occurrence. Nodule(s) were described in terms of size (millimeters) and number (1, 1-10, 10-20, 20-30, >30).

Internal features of disease: An air bronchogram was described as the appearance of an air-filled bronchus surrounded by airless lung parenchyma (Tuddenham 1984). A cystic air space was described as a well-defined, circumscribed air-containing lesion, surrounded by a wall of variable thickness (Austin et al. 1996). CT angiogram sign was described as enhanced branching pulmonary vessels in a low-attenuating consolidation of the lung parenchyma (Im et al. 1990). In addition, for nodules, a halo sign was described as GGO

surrounding the circumference of a nodule or mass (Austin et al. 1996) and pseudocavitation was described as lucency within a nodule that does not represent a cavity (Tuddenham 1984).

Nodule margin characteristics: Nodule margins were considered ill defined if the perimeter was hazy or indistinct. If the nodule was sharply and distinctly separated from surrounding lung parenchyma, the margins were considered well defined. Well defined margins were described as smooth or irregular. Nodule margins were considered smooth if the margin was round and distinctly separated from surrounding lung parenchyma. Nodule margins were considered irregular if the margin was erratic and/or indistinct. Nodules with irregular margins were further examined for spiculations and pleural tags. Spiculations were defined as fine linear strands extending from the nodule margin into lung parenchyma without contacting the pleural surface (Kawaguchi et al. 2005). A pleural tag was defined as a linear area of high attenuation that was surrounded by aerated lung, originated from the margin of the nodule, and extended peripherally to contact the pleural surface (Kawaguchi et al. 2005).

#### *Nodular disease development*

Nodular disease progression was defined as a temporary or permanent increase in the size and/or number of nodules over time. Nodular disease partial regression was defined as a temporary or permanent decrease in the size and/or number of nodules over time. Nodular disease complete regression was defined as a temporary or permanent total disappearance of nodules over time.

### *Three-dimensional (3D) volume reconstruction*

CT slices were reconstructed with 3D analytical volume software (Barco Voxar 3D, Ampronix Imaging Technology). To estimate volumes of normal lung, settings used were 3D: Color Volume (Classic), Preset: Lung (Solid).

### *Radiation dose*

Radiation dose to the lungs from CT scanning was calculated using CT Dose Version 1.0.1 freeware (Department of Biomedical Engineering, University of Aarhus, Denmark and National Board of Health, National Institute of Radiation Hygiene, Denmark).

### *Lentiviral reverse transcriptase (RT) activity in inocula*

Inocula were tested for lentiviral reverse transcriptase activity using a Lenti RT Activity Kit (Cavidi Tech) in accordance with the manufacturer's instructions. Briefly, inocula were incubated with immobilized template (poly-rA), primer (oligo-dT), and dNTP substrate bromo-deoxyuridine-triphosphate (BrdUTP). Incorporated BrdUTP was quantitatively detected using an anti-BrdUTP antibody conjugated to alkaline phosphatase (AP) and para-nitrophenyl phosphate as the substrate for colorimetric detection at 405 nm after 1 hour incubation.

### *Real-time polymerase chain reaction (PCR)*

DNA was extracted from inocula using a DNeasy Tissue Kit (Qiagen, Cat. No. 69504). The exJSRV TM domain was amplified in a one-step PCR using the MultiBlock PCR System (MBS) (Thermo Electron Corporation). Each 50 $\mu$ L PCR reaction contained 45 $\mu$ L Platinum<sup>®</sup> PCR SuperMix (22U/ml complexed recombinant *Taq* DNA polymerase with Platinum<sup>®</sup> *Taq* Antibody, 22mM Tris-HCl (pH 8.4), 55mM KCl, 1.65mM MgCl<sub>2</sub>, 220 $\mu$ M dGTP, 220 $\mu$ M dATP, 220 $\mu$ M dTTP, 220 $\mu$ M dCTP, and stabilizers) (Invitrogen, Cat. No. 11306-016), 200nM (final concentration) forward primer, 200nM (final concentration) reverse primer, and 500ng template DNA.

The following primers, based on GenBank accession number AF105220 and specific for the TM region of exJSRV, were used:

exJSRV env (forward) (TA7F-B): 5'-TTGGTGTAGGAATACTTGTGTT-3'

exJSRV env (reverse) (TA8R): 5'-TATTTCTATATTTTCATATGCAGCA-3'

PCR cycling parameters were: one template denaturation/enzyme activation cycle at 94°C for 2 minutes, 35 cycles of denaturation at 94°C for 30 seconds, annealing at 53°C for 30 seconds and extension at 72°C for 30 seconds, followed by one final extension cycle at 72°C for 10 minutes.

PCR amplification products were then run on a TBE ReadyAgarose™ Mini Gel, 3% plus ethidium bromide (BioRad, Cat. No. 161-3006) and imaged on a Typhoon 9410 Variable Mode Imager (Amersham Biosciences).

*Quantitative real-time polymerase chain reaction (qPCR)*

DNA was extracted from lung tissue (tumor tissue, if available) using a DNeasy Tissue Kit (Qiagen, Cat. No. 69504).

Integrated exJSRV copy number was detected using a fluorogenic probe in combination with real-time PCR. Each 25 $\mu$ L PCR reaction contained 12.5 $\mu$ L Platinum<sup>®</sup> Quantitative PCR Supermix-UGD with ROX (60U/ml Platinum<sup>®</sup> *Taq* DNA polymerase, 40mM Tris-HCl (pH 8.4), 6mM MgCl<sub>2</sub>, 400 $\mu$ M dGTP, 400 $\mu$ M dATP, 400 $\mu$ M dCTP, 800 $\mu$ M dUTP, 40U/ml uracil DNA glycosylase (UDG), 1 $\mu$ M ROX Reference Dye, and stabilizers) (Invitrogen, Cat. No. 11743-100), 200nM (final concentration) forward primer, 200nM (final concentration) reverse primer, 100nM (final concentration) fluorogenic probe, and 250ng template DNA.

The following primers, based on GenBank accession number AF105220 and specific for the TM region of exJSRV, were used:

exJSRV env (forward) (TA7F-B): 5'-TTGGTGTAGGAATACTTGTGTT-3'

exJSRV env (reverse) (TA8R): 5'-TATTTCTATATTTTCATATGCAGCA-3'

The following probe, based on GenBank accession number AF105220 and specific for the TM region of exJSRV, was used for the qPCRs: 5'-FAM-CTCGTTCGTGGCATGGTTCG-TAMRA-3' (TAProbe-1), where 6-carboxyfluorescein (FAM) serves as the reporter fluorochrome and tetramethyl-6-carboxyrhodamine (TAMRA) serves as the quencher.

qPCR cycling parameters were: one UDG incubation cycle at 50°C for 2 minutes, one template denaturation/enzyme activation cycle at 95°C for 2 minutes, 45 cycles of denaturation at 95°C for 15 seconds and annealing at 55°C for 45 seconds (this step was enabled for data collection). Reactions were done

in triplicate. A full length JSRV envelope provirus clone (pBlue-JSRV) was serially diluted and used as a standard. Previous work has shown that qPCR is able to detect one copy of this standard (Nuno Carreiro, DeMartini laboratory, unpublished work). DNA from an ovine skin fibroblast (OSF) cell line, which contains enJSRV sequences, was used as a viral specificity control and as a negative control for exJSRV.

### *Statistical analysis*

Two-tailed unpaired Student's *t* test (normal distributions and equal variances), two-tailed unpaired Student's *t* test with Welch's correction (normal distributions and unequal variances), and one-way analysis of variance (ANOVA) with Bonferroni's multiple comparison post test were used for statistical analysis. Differences were significant when  $P < 0.05$ . Statistical analysis was done using GraphPad Prism software program (version 4.03, San Diego, CA).

## **RESULTS**

### *Reverse transcriptase (RT) activity and viral DNA in inocula*

Three batches of JSRV inocula were prepared using lung tumor homogenate from three sheep with confirmed OPA. Two sheep, 98RS3 and 99RS27, were natural cases of OPA and the other, 91RS13, was an experimentally-induced OPA case. To verify viable, infectious retrovirus in the inoculum preparations, we measured the activity of RT, an RNA-dependent DNA

polymerase that retroviruses employ to transcribe their RNA genome into complementary DNA, which can then be integrated into the host cell's DNA. For experimentally-induced OPA, it has been reported that the amount of JSRV RT activity in the inoculum is inversely proportional to the time required to induce lung tumors (Verwoerd et al. 1985). The inoculum prepared from 91RS13 had the greatest RT activity, followed by 99RS27 and lastly, 98RS3 (Figure 2.1). However, via PCR, JSRV DNA was only detected in the inocula prepared from 91RS13 and 98RS3; no JSRV DNA was found in the inoculum from 99RS27 (Figure 2.2). Further analysis was performed using qPCR with a fluorogenic probe and JSRV copy number per 250ng of DNA isolated from each inoculum was determined: 91RS13 inoculum DNA contained over 850 JSRV copies and 98RS3 inoculum DNA contained more than four times that amount, with over 3750 JSRV copies. Conversely, there were no JSRV copies detected in any of the six replicates of 99RS27 inoculum DNA qPCRs (Table 2.4). Thus, although all inocula had RT activity, only two of the three inocula contained JSRV DNA. To explain this discrepancy, we looked for an alternative source of RT activity in the inoculum preparations and found that all three tested positive via PCR for OvLV, another member of the retrovirus family that commonly coexists with JSRV in OPA-affected sheep. Consequently, the RT activity in the inoculum preparations cannot be solely attributed to JSRV. In summary, the inocula prepared from 91RS13 and 98RS3 contained both JSRV and OvLV whereas the inoculum from 99RS27 contained only OvLV.

### *Disease development via computed tomography (CT)*

To noninvasively monitor disease development, sheep were CT scanned prior to inoculation and at pre-determined time points through six months post inoculation. Sheep were also euthanized during the study, based on pre-determined time points as well as CT results. Concisely, pulmonary abnormalities were visible on CT scans in all twelve sheep (100%) and were predominated by two distinctive disease presentations: nodules and a diffuse lung pattern (DLP) (Table 2.5). In total, nodules were seen in eight of twelve sheep (67%) and a DLP was evident in all twelve sheep (100%). These two disease presentations occurred both individually and concurrently, and, when found together, nodules were seen both within the DLP and/or independent of the DLP.

In terms of inoculum groups, all four sheep (100%) inoculated with JSRV from 98RS3 tumor homogenate developed visible nodules during the study. In one sheep (04RS1), nodules were seen as early as two weeks post inoculation. At one month post inoculation, nodules were detected in an additional two sheep (04RS2 and 04RS3) and, at two months post inoculation, nodules were radiographically evident in all four sheep. Of the four sheep inoculated with 91RS13 inoculum, one (04RS8) was euthanized at one month post inoculation due to positive serology results for OvLV antibodies. At this time, CT scanning revealed a DLP in this sheep; however, no nodules were apparent radiographically, grossly, or histologically. Of the other three sheep in this group, all had visible nodules at some point during the study. In two sheep (04RS6 and 04RS7), nodules were first detected at one month post inoculation and in the

other sheep (04RS5), nodules were initially found at two months post inoculation. Of the four sheep receiving the presumed JSRV-negative inoculum from 99RS27, only one (04RS10) developed a solitary nodule visible on CT scan at 1 month.

Surprisingly, not all sheep with radiographically visible nodules during the course of the study had progressive disease. In fact, only two (04RS4 and 04RS5) of eight animals exhibited progressive nodular disease, as evidenced by increasingly more and/or larger nodules over time (Figures 2.3, 2.4, and 2.5A). The CT scans from the other six sheep showed nodules that apparently regressed over time, either partially (04RS1, 04RS2, and 04RS6) (Figures 2.5B, 2.6, and 2.7) or completely (04RS3, 04RS7, and 04RS10) (Figures 2.8 and 2.9). In the latter case, there was neither radiographic nor gross indication of nodules at the end point of the study (euthanasia); additionally, no evidence of OPA was found histopathologically. Based on nodular disease development, sheep were divided into four groups for subsequent analyses: no nodules (n = 4: 04RS8, 04RS9, 04RS11, and 04RS12), progressors (n = 2: 04RS4 and 04RS5), partial regressors (n = 3: 04RS2, 04RS3, and 04RS6), and complete regressors (n = 3: 04RS3, 04RS7, and 04RS10).

### *JSRV DNA*

As for JSRV, in eleven of the twelve sheep, we were able to detect and quantitate JSRV DNA copy numbers, which varied greatly between individuals and ranged from 2.97 to 9270.12 copies (Table 2.6). Regarding inoculum groups,

JSRV DNA copy numbers also differed considerably between sheep in the same group as well as between groups. When copy numbers were averaged for each group, the sheep receiving the inoculum with the least amount of RT activity (98RS3) had the highest number of JSRV copies. This result would conflict with the notion that the RT activity in the inoculum directly corresponds with JSRV infectivity if, in fact, JSRV was the only retrovirus in the inoculum preparation. However, as mentioned previously, all three inocula also tested positive for another retrovirus, OvLV, and thus, the RT activity measurement in the inocula is indicative of the collective reverse transcription of both retroviruses. As for the group that received the presumed JSRV-negative inoculum (99RS27), JSRV DNA was detected in three of four sheep at the time of euthanasia, although in significantly less quantities relative to the JSRV-positive inocula groups. The presence of viral DNA in the JSRV-negative inoculum group could likely be a result of aerosol transmission of the virus from JSRV-infected flockmates, as all animals in this study were housed together in close quarters.

In terms of nodular disease development groups, the mean JSRV copy number was significantly different ( $p < 0.05$ ) between all groups with the exception of the partial regressors compared with the complete regressors (Table 2.7). In comparison to the sheep with no nodules, the progressors had ~350 times more JSRV DNA, the partial regressors had ~30 times more JSRV DNA, and the complete regressors had ~5 times more JSRV DNA. Thus, in this study, JSRV copy number at euthanasia was found to be related to nodule disease development; of the sheep with radiographically visible nodules during the study,

those with the most JSRV DNA demonstrated progressive nodular disease while those with the least amount of JSRV DNA showed complete regression of visible nodule(s).

#### *CT characteristics of nodules*

To determine if the nodule characteristics present on CT scans varied between nodular disease development groups, we compared presentation, lung involvement, location, appearance, and extent of nodular disease between progressors, partial regressors, and complete regressors over time (Table 2.8). Regarding initial nodule detection, all regressors (6/6) had visible nodules as early as one month post inoculation whereas, for both progressors, nodules were not detected until two months post inoculation. By this time, two (04RS7 and 04RS10) of the six regressors no longer had perceptible nodules and, thus, complete regression had occurred, as these two sheep remained nodule-free throughout the remaining four months of the study. For the other complete regressor (04RS3), nodules continued to be discernable through three months post inoculation but were no longer visible on the six month post inoculation CT scan. For the partial regressors, all three sheep continued to have detectable nodules through the remainder of the study; however, at varying time points, a decrease in nodule number and/or size was observed.

In terms of presentation, a solitary nodule was detected in only two sheep and this occurred early in the study (two weeks and one month post inoculation). One of these sheep (04RS10) went on to become a complete regressor while the

other (04RS1) developed multiple nodules that partially regressed. The other six sheep presented with multiple nodules at some point during the study, indicating that JSRV predominantly induces multinodular/multifocal disease. In the progressors, this disease always involved both lungs whereas, in the partial regressors, both unilateral and bilateral nodules were seen. Interestingly, in two of the three complete regressors, the nodular disease was unilateral. Taken together, these results suggest that the more extensive the nodular disease, in terms of multiple nodules versus a solitary nodule and bilateral versus unilateral lung involvement, the more likely it is that the nodular disease will progress as opposed to regress.

As for nodule location, there appears to be no clear relationship between central, peripheral, dorsal, or ventral locale and disease development or time. In all sheep, nodules were more frequent in the peripheral and ventral parts of the lung and less frequent centrally and dorsally. In terms of lung lobes, again there is no obvious correlation between a particular lobe and disease development or time; overall, the data indicate that the right and left caudal lung lobes are the most often affected.

Concerning the appearance of the nodules, attenuation, size, and number were assessed. Nodule attenuation was not evidently different between disease development groups or over time, with the majority of sheep having an assortment of nodules with opacities varying from GGO to mixed (GGO/solid) to solid. Size did not vary significantly between nodules with different opacities, between nodular disease development groups, or over time. In fact, the largest

nodule (13mm) had a mixed appearance and was found in a partial regressor at three months post inoculation. Nodule numbers were often greater than 30 and this was not found to be specific to a particular nodule opacity, group, or time. Even two of the three complete regressors had >30 nodules at some point during the study. Thus, nodule attenuation, size, and number were not found to be good predictors of nodular disease progression or regression.

#### *CT characteristics of diffuse lung pattern (DLP)*

In addition to nodules, another disease presentation, a DLP, was detected via CT during this study (Table 2.9). Actually, a DLP was seen more frequently than nodular disease and was observed in all twelve sheep on the majority of the post inoculation CT scans. In as few as two weeks post inoculation, 83% of sheep presented with a DLP, and, one month post inoculation, 100% of sheep had a DLP (Figures 2.10 and 2.11). This resolved in 25% of the sheep by two months post inoculation but reoccurred and was then consistently found in all sheep at all time points including and after four months post inoculation. This disease presentation was significantly more apparent bilaterally than unilaterally ( $p < 0.001$ ). In terms of detailed location, a DLP was seen in the central, peripheral, and ventral portions of the lungs, as well as dorsally, although significantly less often ( $p < 0.001$ ). Lung lobe involvement was not preferential, as a DLP was commonly detected in all lobes. Regarding attenuation, we did notice a pattern over time. At two weeks post inoculation, GGO predominated in all groups; at one month post inoculation, the GGO progressed to a DLP with

mixed attenuation and then reverted back to primarily GGO until four months post inoculation, after which a mixed appearance prevailed, with the solid component becoming more prominent over time.

To determine if the DLP characteristics present on CT scans varied between nodular disease development groups, we compared lung involvement, location, and appearance of DLP disease between progressors, partial regressors, and complete regressors over time (Table 2.10). As mentioned previously, all sheep developed a DLP, so this disease presentation was not unique to a particular group. Also, the colocalization of a DLP and nodules was seen in all groups, was not time specific, and, accordingly, was not determined to be indicative of either the eventual progression or regression of nodular disease. As for unilateral versus bilateral lung involvement, no trends among groups or time were evident; as for precise location, results similar to nodular disease were found, with a DLP present primarily in the central, peripheral, and ventral parts of the lungs and, less often, dorsally. Particular lung lobes did not appear to be preferentially affected. In terms of appearance, group differences were not appreciable. In brief, a DLP was seen in all sheep involved in this study; this disease presentation generally appeared around two weeks post inoculation, partially resolved, and then was observed consistently on the successive CT scans. These DLPs were not specific to a particular part of the lungs. The appearance of the DLPs progressed from mild GGO to a mixed attenuation, with the predominant component being solid. Overall, we found no obvious association between a DLP and nodule presence, progression, or regression.

### *Features of disease*

Several internal features of disease were often observed during this study. These included angiogram signs, cystic air spaces, and air bronchograms (Figure 2.12); all were seen within DLPs and were not specific to a particular nodular disease development group or time post inoculation.

As for nodules, internal features were difficult to discern, primarily because the majority of nodules were small and, thus, the CT resolution was not adequate to detect this level of detail. On the other hand, nodule margin characteristics were more perceptible, but again, due to size, were difficult to precisely evaluate. Nonetheless, a spectrum of obvious margin attributes, including ill defined, well defined, smooth, and irregular perimeters as well as the presence of spiculations, were seen throughout the study and were not found to be specific to a distinct group or time post inoculation.

### *Clinical signs of JSRV*

Sheep were monitored closely for clinical signs of OPA, including audible breathing, moist rales, progressive dyspnea, abundant bronchorrhea, nasal discharge, and cachexia. Very mild audible breathing was observed in all sheep during the study and was not specific to nodular disease development group but did progress, though not substantially, over time. No other clinical signs were evident, even as far out as six months post inoculation. Regarding both inoculum and nodule disease development groups, weights did not vary significantly over

time (Figures 2.13 and 2.14). At euthanasia, the “wheelbarrow test”, where the hindquarters of the animal are lifted above the head to check for lung exudate flow out the nose and mouth, was performed on all sheep; no fluid was observed. Overall, only very mild clinical signs of respiratory distress were apparent in the sheep involved in this study.

#### *Radiation dose from CT scanning*

Six of the eight sheep that developed lung nodules visible on CT during this study demonstrated either partial or complete regression of these nodules over time, in the absence of any intentional therapeutic intervention. However, when reflecting on this study, we acknowledged that these sheep were CT scanned frequently and wondered if the radiation dose received while monitoring disease development could account for an inadvertent, therapeutic dose of radiation. Thus, we calculated the radiation dose each sheep received and, on average, this amounted to approximately 0.005 Gy per CT scan. Cumulatively, this resulted in total radiation doses ranging from 0.0237 to 0.0766 Gy, depending on the number of times the sheep was scanned (Table 2.11). In terms of nodular disease development groups, there was not a statistically significant difference in total radiation dose. To put these values into perspective, the 2003 recommendation from the American Society for Clinical Oncology (ASCO) for unresectable stage III lung cancer is chemotherapy in association with definitive thoracic irradiation; this radiotherapy should be no less than the biologic equivalent of 60 Gy in 1.8- to 2.0-Gy fractions (Pfister et al. 2004). According to

the International System for Staging Lung Cancer, the disease seen in our sheep would be classified as stage IIIB when multiple lesions were detected in one lobe (T4N0M0) and stage IV when multiple lobes were involved (T4N0M1) (Kawaguchi et al. 2005), which was the vast majority of cases. ASCO's suggestion for stage IV is solely chemotherapy, as radiotherapy has been found to have no beneficial effect on disease at this advanced stage. Thus, the recommended therapeutic radiation dose in humans is more than 1000 times higher than the average dose received by our sheep, making it very unlikely that the nodular regression was a consequence of radiation from the CT scanning.

## **CONCLUSIONS**

In this study, we monitored disease development in the lungs of sheep inoculated with JSRV and OvLV. One of our goals was to detect disease earlier than is possible with simple observation of clinical signs. Other than mild audible breathing, our animals did not develop any symptoms characteristic of OPA or OPP; however, using CT, we were able to detect diffuse lung disease and discrete nodules as early as two weeks post inoculation. Overall, during the course of the study, a DLP was apparent in all twelve sheep and nodules were evident in eight of twelve sheep. Surprisingly, not all animals with visible nodules had progressive disease. In fact, only two of eight showed increasingly more and/or larger nodules over time, whereas the other six demonstrated either partial or complete regression of nodular disease. This nodular disease development was found to be associated with JSRV DNA copy number in the

lung tissue (tumor tissue, if available) at euthanasia; sheep with the most JSRV DNA had progressive disease while sheep with the least amount of JSRV DNA had complete regression of visible nodules. Nodular disease development also correlated with presentation; the more extensive the disease, in terms of multiple nodules versus a solitary nodule and bilateral versus unilateral lung involvement, the more likely it was that the nodular disease progressed as opposed to regressed. However, nodule number, size, and attenuation were not found to be good predictors of nodular disease progression or regression. Also, we noticed no obvious connection between a DLP and nodule presence or development. In summary, by utilizing CT as a noninvasive imaging modality, we were able to detect disease early and monitor the development of OPA and OPP after inoculation of neonatal lambs with JSRV and OvLV.

Table 2.1: Characteristics of sheep used as JSRV inoculum sources. JSRV was isolated from the lung tumor tissue of three sheep with confirmed OPA and subsequently used to inoculate twelve lambs (four lambs per inoculum).

<i>Inoculum Source Sheep</i>	<i>Sex</i>	<i>JSRV Source</i>	<i>Date of Euthanasia</i>	<i>Age at Euthanasia</i>	<i>Recipient Lamb</i>
<b>98RS3</b>	Female	Natural case from a farm in southern Wyoming	11/26/1998	4+ years	04RS1 04RS2 04RS3 04RS4
<b>91RS13</b>	Male	Experimental case; inoculated with lung homogenate from 85RS7	6/13/1991	2 months	04RS5 04RS6 04RS7 04RS8
<b>99RS27</b>	Female	Natural case from a farm in southern Wyoming	9/23/1999	4+ years	04RS9 04RS10 04RS11 04RS12

Table 2.2: CT scan and euthanasia schedule for sheep inoculated with JSRV. Row shading indicates groups of sheep (n=4 per group) based on inoculum source.

Sheep	Inoculum Source	Pre	Post-JSRV Inoculation								
			2 Weeks	1 Month	2 Months	3 Months	4 Months	5 Months	6 Months		
04RS8	91RS13	CT	CT	euthanasia							
04RS1	98RS3	CT	CT	CT		euthanasia					
04RS2	98RS3	CT	CT	CT	CT		euthanasia				
04RS5	91RS13	CT	CT	CT	CT		euthanasia				
04RS7	91RS13	CT	CT	CT	CT		euthanasia				
04RS3	98RS3	CT	CT	CT	CT		euthanasia				
04RS6	91RS13	CT	CT	CT	CT		euthanasia				

Table 2.3: Lung disease characteristics evaluated via CT.

<i>Disease Presentation</i>	<i>Lung Involvement</i>	<i>Disease Location</i>	<i>Lobe</i>	<i>Disease Appearance</i>	<i>Extent of Disease</i>	<i>Internal Features of Disease</i>	<i>Margin Characteristics</i>
solitary nodule	unilateral bilateral	central peripheral dorsal ventral	RCrL RML RCdL RAL LCrL LCdL	ground glass opacity solid mixed	millimeters  millimeters <10>20>30>	air bronchogram angiogram sign cystic air space halo sign pseudocavitation	ill defined well defined smooth irregular spiculations pleural tags
multiple nodules							
diffuse lung pattern	unilateral bilateral	central peripheral dorsal ventral	RCrL RML RCdL RAL LCrL LCdL	ground glass opacity solid mixed	lobar sublobar	air bronchogram angiogram sign cystic air space	

Table 2.4: JSRV copy numbers per 250ng of DNA isolated from the three inocula used for OPA induction. Copy numbers are the mean of three replicates  $\pm$  standard error. For 99RS27, a total of six replicates were run.

<i><b>Inoculum Source Sheep</b></i>	<i><b>JSRV Copy Number</b></i>	<i><b>Recipient Sheep</b></i>
<b>98RS3</b>	3768.51 $\pm$ 278.94	04RS1 04RS2 04RS3 04RS4
<b>91RS13</b>	864.42 $\pm$ 55.71	04RS5 04RS6 04RS7 04RS8
<b>99RS27</b>	undetectable	04RS9 04RS10 04RS11 04RS12

Table 2.5: Summary of radiographic disease presentation and nodule progression/regression in inoculated sheep. All sheep developed a diffuse lung pattern during the study whereas nodules were detected in only eight of twelve sheep. These nodules progressed over time in two sheep; in the other six sheep, nodule regression, either partial or complete, over time was observed.

Inoculum Source Sheep	Sheep	Pre	Post Inoculation									
			2 Weeks	1 Month	2 Months	3 Months	4 Months	5 Months	6 Months			
98RS3	04RS1	NA	DwN	P	DwN, N	RP	P	DwN				
	04RS2	NA	NA		DwN	P		DwN, N	RP			RP DwN
	04RS3	NA	D		DwN	P		D, N	P			RC D
	04RS4	NA	D		D			DwN, N	P		P	DwN
91RS13	04RS5	NA	D		D			N	P			P DwN
	04RS6	NA	D		DwN, N	P		DwN	P			RP DwN
	04RS7	NA	D		DwN	RC		D				RP DwN, N
	04RS8	NA	D		D							D
99RS27	04RS9	NA	D		D							D
	04RS10	NA	D		DwN	RC	NA					D
	04RS11	NA	D		D			D				D
	04RS12	NA	NA		D			D				D

Disease Presentation → NA: Normal Appearance; D: Diffuse Lung Pattern; N: Nodules; DwN: Diffuse Lung Pattern with Nodules. Nodular Change → P: Progressive Disease; RC: Regressive Disease; Complete; RP: Regressive Disease; Partial.

Table 2.6: In virus-inoculated sheep, JSRV copy numbers per 250ng of DNA isolated from lung tissue (tumor tissue, if available). JSRV copy numbers are the mean of three replicates  $\pm$  standard error.

<b><i>Inoculum Source Sheep</i></b>	<b><i>Sheep</i></b>	<b><i>JSRV Copy Number</i></b>	<b><i>Mean JSRV Copy Number</i></b>
98RS3	<b><i>04RS1</i></b>	6.85 $\pm$ 1.36	2413.99 $\pm$ 1195.78
	<b><i>04RS2</i></b>	376.05 $\pm$ 22.41	
	<b><i>04RS3</i></b>	2.97 $\pm$ 0.68	
	<b><i>04RS4</i></b>	9270.12 $\pm$ 271.38	
91RS13	<b><i>04RS5</i></b>	6080.54 $\pm$ 282.69	1997.81 $\pm$ 736.10
	<b><i>04RS6</i></b>	1615.69 $\pm$ 20.25	
	<b><i>04RS7</i></b>	240.34 $\pm$ 24.65	
	<b><i>04RS8</i></b>	54.68 $\pm$ 3.85	
99RS27	<b><i>04RS9</i></b>	17.69 $\pm$ 1.07	31.15 $\pm$ 10.94
	<b><i>04RS10</i></b>	91.50 $\pm$ 10.61	
	<b><i>04RS11</i></b>	15.42 $\pm$ 0.31	
	<b><i>04RS12</i></b>	undetectable	

Table 2.7: Presence of nodules via CT and JSRV copy numbers per 250ng of DNA isolated from lung tissue (tumor tissue, if available). JSRV copy numbers are the mean of three replicates  $\pm$  standard error. \*Between all nodular disease development groups except partial regressors and complete regressors, there was a statistically significant difference between the mean JSRV copy number ( $p < 0.05$ ). Overall, the progressors had the most JSRV DNA followed by the partial regressors, complete regressors, and lastly, the sheep with no nodules.

Sheep	Nodules during Study	Nodules at Euthanasia	JSRV Copy Number	Mean JSRV Copy Number	Nodule Development
04RS8	✓	✓	54.68 $\pm$ 3.85	21.95 $\pm$ 21.19	No nodules*
04RS9	✓	✓	17.69 $\pm$ 1.07		
04RS11	✓	✓	15.42 $\pm$ 0.31		
04RS12	✓	✓	undetectable		
04RS4	✓	✓	9270.12 $\pm$ 271.38	7675.33 $\pm$ 1798.97	Progression*
04RS5	✓	✓	6080.54 $\pm$ 282.69		
04RS1	✓	✓	6.85 $\pm$ 1.36	666.20 $\pm$ 730.32	Partial regression
04RS2	✓	✓	376.05 $\pm$ 22.41		
04RS6	✓	✓	1615.69 $\pm$ 20.25		
04RS3	✓	✓	2.97 $\pm$ 0.68	111.60 $\pm$ 106.46	Complete regression
04RS7	✓	✓	240.34 $\pm$ 24.65		
04RS10	✓	✓	91.50 $\pm$ 10.61		
04RS1, 2, 3, 6, 7, & 10				388.90 $\pm$ 136.98	Partial and complete regression*



Table 2.8 continued. Lung nodule appearance, including attenuation, size, and number, evaluated via CT.

Disease Development Nodule(s)	Post Inoculation																							
	2 weeks			1 month			2 months			3 months			4 months			5 months			6 months					
	Pro	RP	RC	Pro	RP	RC	Pro	RP	RC	Pro	RP	RC	Pro	RP	RC	Pro	RP	RC	Pro	RP	RC			
Appearance: GGO	0/2	1/3	0/3	0/2	3/3	3/3	2/2	3/3	1/3	2/2	1/1	1/1	2/2	1/1	1/1	2/2	1/1	1/1	2/2	1/1	1/1	2/2	1/1	0/3
Size	1/1			1/3	1/3	1/3	2/2	2/3	1/1	1/2	-	-	1/2	1/3		1/2	-	0	1/2	-	0	0	0	2/2
1-3mm	-	-	-	1/1	1/1	1/1	2/2	2/2	1/1	1/1	-	-	1/1	-	-	-	-	-	-	-	-	0	0	2/2
4-6mm	1/1	-	-	1/1	-	1/1	-	1/2	1/1	1/1	-	-	1/1	-	-	1/1	-	-	1/1	-	-	0	0	2/2
7-9mm	-	-	-	1/1	-	-	-	-	-	1/1	-	-	1/1	-	-	1/1	-	-	1/1	-	-	0	0	-
10+mm	-	-	-	-	-	-	-	-	-	-	-	-	-	-	-	-	-	-	-	-	-	0	0	-
Number	1/1	-	-	-	-	-	-	-	-	0	-	-	0	-	-	0	-	-	0	-	-	0	0	-
1	-	-	-	-	-	-	2/2	1/2	-	-	-	-	-	-	-	-	-	-	1/1	-	-	0	0	1/2
1<x<10	-	-	-	-	-	-	-	-	-	0	-	-	0	-	-	0	-	-	0	-	-	0	0	-
10<x<20	-	-	-	-	-	-	-	-	-	0	-	-	0	-	-	0	-	-	0	-	-	0	0	-
20<x<30	-	-	-	-	-	-	-	-	-	0	-	-	0	-	-	0	-	-	0	-	-	0	0	-
x>30	-	-	-	1/1	1/1	1/1	-	1/2	1/1	1/1	-	-	1/1	-	-	0	-	-	0	-	-	0	0	1/2
Appearance: Solid	-	-	-	2/3	2/3	2/3	2/2	1/3	1/1	-	-	-	-	-	-	1/2	-	-	-	-	-	0	0	1/2
Size	-	-	-	2/2	1/2	2/2	2/2	1/1	1/1	1/1	-	-	1/1	-	-	1/1	-	-	1/1	-	-	0	0	1/1
1-3mm	-	-	-	2/2	2/2	2/2	-	-	1/1	1/1	-	-	1/1	-	-	1/1	-	-	1/1	-	-	0	0	1/1
4-6mm	-	-	-	2/2	2/2	-	-	-	1/1	1/1	-	-	1/1	-	-	1/1	-	-	1/1	-	-	0	0	1/1
7-9mm	-	-	-	-	-	-	-	-	-	0	-	-	0	-	-	0	-	-	0	-	-	0	0	-
10+mm	-	-	-	-	-	-	-	-	-	0	-	-	0	-	-	0	-	-	0	-	-	0	0	-
Number	-	-	-	-	1/2	-	-	-	-	0	-	-	0	-	-	0	-	-	0	-	-	0	0	-
1	-	-	-	1/2	-	-	1/2	-	-	0	-	-	0	-	-	0	-	-	1/1	-	-	0	0	-
1<x<10	-	-	-	1/2	-	-	1/2	-	-	0	-	-	0	-	-	0	-	-	0	-	-	0	0	-
10<x<20	-	-	-	1/2	-	-	-	-	-	0	-	-	0	-	-	0	-	-	0	-	-	0	0	1/1
20<x<30	-	-	-	-	-	-	-	1/1	-	0	-	-	0	-	-	0	-	-	0	-	-	0	0	-
x>30	-	-	-	-	1/2	-	-	-	1/1	1/1	-	-	1/1	-	-	0	-	-	0	-	-	0	0	-
Appearance: Mixed	-	-	-	-	-	-	2/2	1/3	-	2/2	1/1	1/1	2/2	1/1	1/1	2/2	1/1	1/1	2/2	1/1	1/1	0	0	1/2
Size	-	-	-	-	-	-	2/2	1/1	-	2/2	1/1	1/1	2/2	1/1	1/1	2/2	1/1	1/1	2/2	1/1	1/1	0	0	1/1
1-3mm	-	-	-	-	-	-	2/2	1/1	-	2/2	1/1	1/1	2/2	1/1	1/1	2/2	1/1	1/1	2/2	1/1	1/1	0	0	1/1
4-6mm	-	-	-	-	-	-	1/2	1/1	-	2/2	1/1	1/1	2/2	1/1	1/1	2/2	1/1	1/1	2/2	1/1	1/1	0	0	1/1
7-9mm	-	-	-	-	-	-	1/2	1/1	-	1/2	1/1	1/1	1/2	1/1	1/1	2/2	-	-	2/2	-	-	0	0	-
10+mm	-	-	-	-	-	-	-	-	-	-	1/1	-	-	1/2	-	-	-	-	-	-	-	0	0	-
Number	-	-	-	-	-	-	-	-	-	-	1/1	-	-	1/2	-	-	-	-	-	-	-	0	0	-
1	-	-	-	-	-	-	-	-	-	-	1/1	-	-	1/2	-	-	-	-	-	-	-	0	0	-
1<x<10	-	-	-	-	-	-	-	-	-	-	1/1	-	-	1/2	-	-	-	-	-	-	-	0	0	-
10<x<20	-	-	-	-	-	-	-	-	-	-	1/1	-	-	1/2	-	-	-	-	-	-	-	0	0	-
20<x<30	-	-	-	-	-	-	-	-	-	-	1/1	-	-	1/2	-	-	-	-	-	-	-	0	0	-
x>30	-	-	-	-	-	-	2/2	-	-	2/2	1/1	1/1	2/2	1/1	1/1	2/2	1/1	1/1	2/2	1/1	1/1	0	0	1/1

Table 2.9: Diffuse lung pattern (DLP) characteristics, including lung involvement, location, and appearance, evaluated via CT. DLP is reported as the number of animals with DLP over the total number of animals that were CT scanned. DLP characteristics are reported as the number of animals with the particular characteristic over the total number of animals with DLP. Mean (%) is reported  $\pm$  standard error. For DLP location, P values are in comparison to dorsal location (\*). NS: not significant.

	Post Inoculation							P value
	2 weeks	1 month	2 months	3 months	4 months	5 months	6 months	
<b>Presentation</b>								
DLP	10/12	12/12	8/12	5/6	6/6	4/4	6/6	
<b>Lung Involvement</b>								
unilateral	4/10	3/12	4/8	2/5	0/6	0/4	2/6	26.9 $\pm$ 7.5
bilateral	6/10	9/12	4/8	3/5	6/6	4/4	4/6	73.1 $\pm$ 7.5
<b>Location</b>								
central	9/10	12/12	5/8	4/5	6/6	4/4	6/6	90.4 $\pm$ 5.4
peripheral	9/10	12/12	8/8	5/5	6/6	4/4	6/6	98.6 $\pm$ 1.4
dorsal	6/10	8/12	1/8	2/5	2/6	2/4	3/6	44.7 $\pm$ 6.8
ventral	10/10	12/12	8/8	5/5	6/6	4/4	6/6	100 $\pm$ 0.0
<b>Lobe</b>								
RCrL	7/10	12/12	5/8	3/5	6/6	4/4	5/6	82.3 $\pm$ 6.8
RML	8/10	12/12	4/8	3/5	3/6	4/4	3/6	70 $\pm$ 8.7
RCdL	8/10	12/12	5/8	4/5	2/6	4/4	4/6	74.7 $\pm$ 8.8
RAL	4/10	11/12	5/8	4/5	6/6	4/4	4/6	77.4 $\pm$ 8.4
LCrL	3/10	7/12	2/8	4/5	6/6	4/4	4/6	65.7 $\pm$ 11.5
LCdL	7/10	9/12	5/8	4/5	6/6	4/4	4/6	79.3 $\pm$ 5.7
<b>Appearance</b>								
ground glass opacity	9/10	9/12	6/8	3/5	3/6	1/4	4/6	63.1 $\pm$ 8.0
solid	0/10	8/12	4/8	1/5	4/6	2/4	3/6	43.4 $\pm$ 9.4
mixed	3/10	12/12	4/8	2/5	6/6	4/4	6/6	74.3 $\pm$ 12.3

**Table 2.10:** Diffuse lung pattern (DLP) characteristics, including lung involvement, location, and appearance, evaluated via CT. Disease development groups are divided into Pro: Progressors (n=2), RP: Regressors, Partial (n=3), and RC: Regressors, Complete (n=3). DLP is reported as the number of animals with DLP over the total number of animals that were CT scanned. Nodules are reported as number of animals with nodules over the total number of animals within the group that were CT scanned. DLP & nodules are reported as number of animals with colocalized nodules and DLP over the total number of animals with nodules within group. DLP characteristics are reported as the number of animals with the particular characteristic over the total number of animals with DLP. Mean (%) is reported  $\pm$  standard deviation.  $\emptyset$  indicates that no animals in group were CT scanned. X indicates that no nodules were present. (-) indicates that zero animals within group had the particular characteristic.

Disease Development	Post Inoculation																						
	2 weeks			1 month			2 months			3 months			4 months			5 months			6 months				
	Pro	RP	RC	Pro	RP	RC	Pro	RP	RC	Pro	RP	RC	Pro	RP	RC	Pro	RP	RC	Pro	RP	RC		
<b>Presentation</b>																							
DLP	2/2	2/3	3/3	2/2	3/3	3/3	1/2	2/3	2/3	1/2	1/1	1/1	1/1	1/1	1/1	3/3	2/2	2/2	2/2	1/1	1/1	2/2	3/3
Nodules	0/2	1/3	0/3	0/2	3/3	3/3	2/2	3/3	1/3	2/2	1/1	1/1	1/1	1/1	1/1	3/3	0/2	2/2	2/2	1/1	1/1	2/2	0/3
DLP & nodules	X	1/1	X	X	3/3	3/3	1/2	2/3	0/1	1/2	1/1	0/1	1/2	1/1	0/1	3/3	X	2/2	2/2	1/1	1/1	2/2	X
<b>Lung Involvement</b>																							
unilateral	2/2	2/2	2/3	1/2	1/3	1/1	1/2	1/2	1/2	-	-	1/1	1/1	1/1	-	1/1	-	-	-	-	-	1/2	1/3
bilateral	-	-	1/3	1/2	3/3	2/3	-	1/2	1/2	1/1	1/1	1/1	1/1	1/1	-	3/3	2/2	2/2	2/2	1/1	1/1	1/2	2/3
<b>Location</b>																							
central	1/2	2/2	3/3	2/2	3/3	3/3	1/1	1/2	1/2	1/1	1/1	1/1	1/1	1/1	1/1	3/3	2/2	2/2	2/2	1/1	1/1	2/2	3/3
peripheral	2/2	2/2	2/3	2/2	3/3	3/3	1/1	2/2	2/2	1/1	1/1	1/1	1/1	1/1	1/1	3/3	2/2	2/2	2/2	1/1	1/1	2/2	3/3
dorsal	1/2	2/2	1/3	1/2	-	3/3	-	-	-	1/1	-	-	-	-	-	1/3	-	2/2	2/2	-	-	1/2	2/3
ventral	2/2	2/2	3/3	2/2	3/3	3/3	1/1	2/2	2/2	1/1	1/1	1/1	1/1	1/1	1/1	3/3	2/2	2/2	2/2	1/1	1/1	2/2	3/3
<b>Lobe</b>																							
RCrL	1/2	2/2	2/3	2/2	3/3	3/3	1/1	2/2	-	1/1	1/1	1/1	-	-	-	3/3	2/2	2/2	2/2	1/1	1/1	2/2	3/3
RML	2/2	2/2	2/3	2/2	3/3	3/3	1/1	1/2	-	1/1	1/1	1/1	-	-	-	2/3	1/2	1/2	2/2	1/1	1/1	1/2	1/3
RCdL	2/2	1/2	2/3	2/2	3/3	3/3	1/1	1/2	-	1/1	1/1	1/1	-	-	-	1/3	-	2/2	2/2	1/1	1/1	2/2	2/3
RAL	-	1/2	1/3	1/2	3/3	3/3	-	1/2	1/2	1/1	1/1	1/1	-	-	-	3/3	2/2	2/2	2/2	1/1	1/1	2/2	2/3
LCrL	-	1/2	1/3	-	3/3	1/3	-	-	1/2	1/1	1/1	1/1	1/1	1/1	1/1	2/3	2/2	2/2	2/2	1/1	1/1	1/2	2/3
LCdL	-	2/2	2/3	1/2	3/3	2/3	-	1/2	2/2	1/1	1/1	1/1	1/1	1/1	1/1	3/3	2/2	2/2	2/2	1/1	1/1	1/2	2/3
<b>Appearance</b>																							
ground glass opacity	2/2	2/2	2/3	2/2	2/3	2/3	1/1	2/2	1/2	1/1	1/1	1/1	-	-	-	2/3	1/2	1/2	-	-	-	2/2	1/3
solid	-	-	-	1/2	3/3	2/3	-	-	2/2	-	-	-	1/1	1/1	1/1	2/3	1/2	1/2	1/2	1/1	1/1	1/2	2/3
mixed	-	-	2/3	2/2	3/3	3/3	1/1	-	-	-	1/1	-	-	1/1	-	3/3	2/2	2/2	2/2	1/1	1/1	2/2	3/3

Table 2.11: Total radiation dose from CT scanning. Mean  $\pm$  standard error.

Sheep	Total Radiation Dose (mGy)	Nodule Development	Mean Total Radiation Dose (mGy)
04RS8	23.7		
04RS9	56.3		
04RS11	74.6	No nodules	52.98 $\pm$ 10.62
04RS12	57.3		
04RS4	56		
04RS5	55.8	Progression	55.9 $\pm$ 0.10
04RS1	43.8		
04RS2	54.2		
04RS6	72.5	Partial regression	56.83 $\pm$ 8.39
04RS3	76.6		
04RS7	54.8		
04RS10	56.4	Complete regression	62.6 $\pm$ 7.02
04RS1, 2, 3, 6, 7, & 10		Partial and complete regression	59.71 $\pm$ 5.06

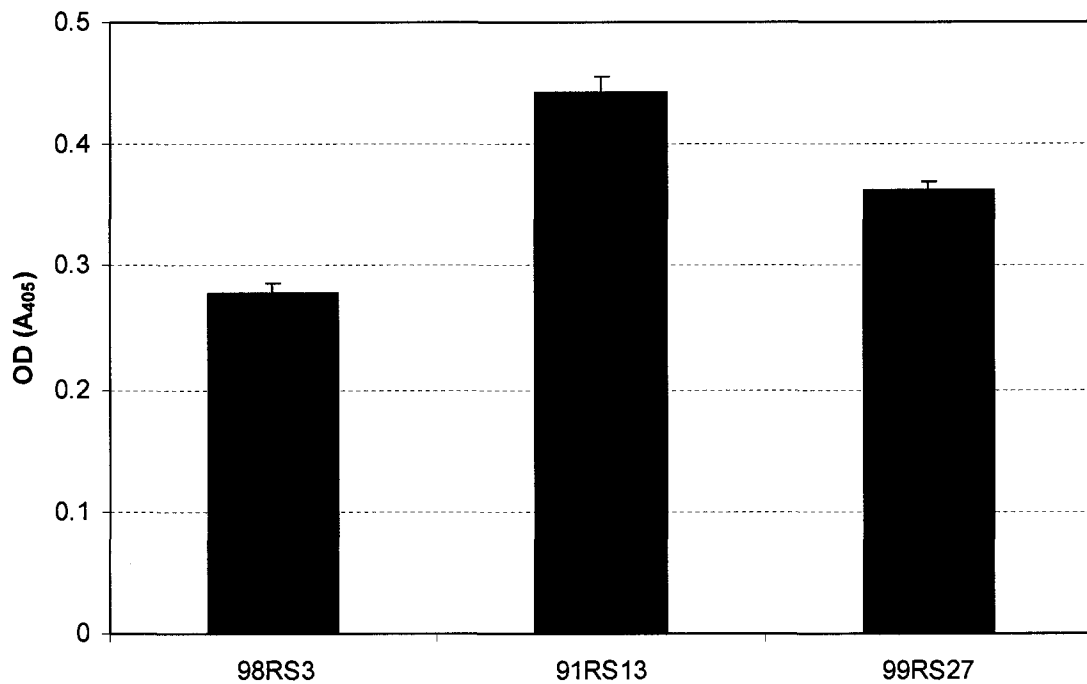


Figure 2.1: RT activity in the three inocula used for OPA induction. RT activity was detected by measuring the amount of BrdU incorporation into an immobilized RNA template. Colorimetric quantitation of BrdU incorporation was achieved by the binding of a BrdU-specific antibody conjugated with alkaline phosphatase. Columns represent the mean of two replicates  $\pm$  standard deviation.

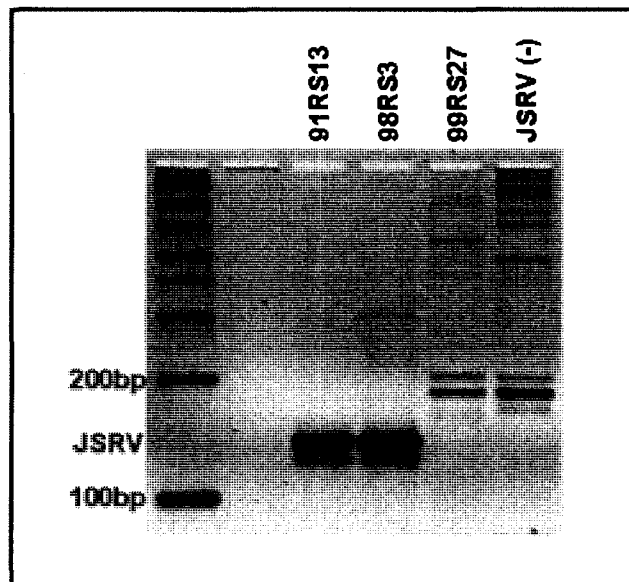


Figure 2.2: JSRV PCR amplification products (~126bp) from the three inocula used for OPA induction run on an agarose gel. The inocula prepared from 91RS13 and 98RS3 showed significant amounts of JSRV DNA whereas no JSRV DNA was apparent in the inoculum prepared from 99RS27. DNA from a JSRV negative (-) sheep was used as a negative control.

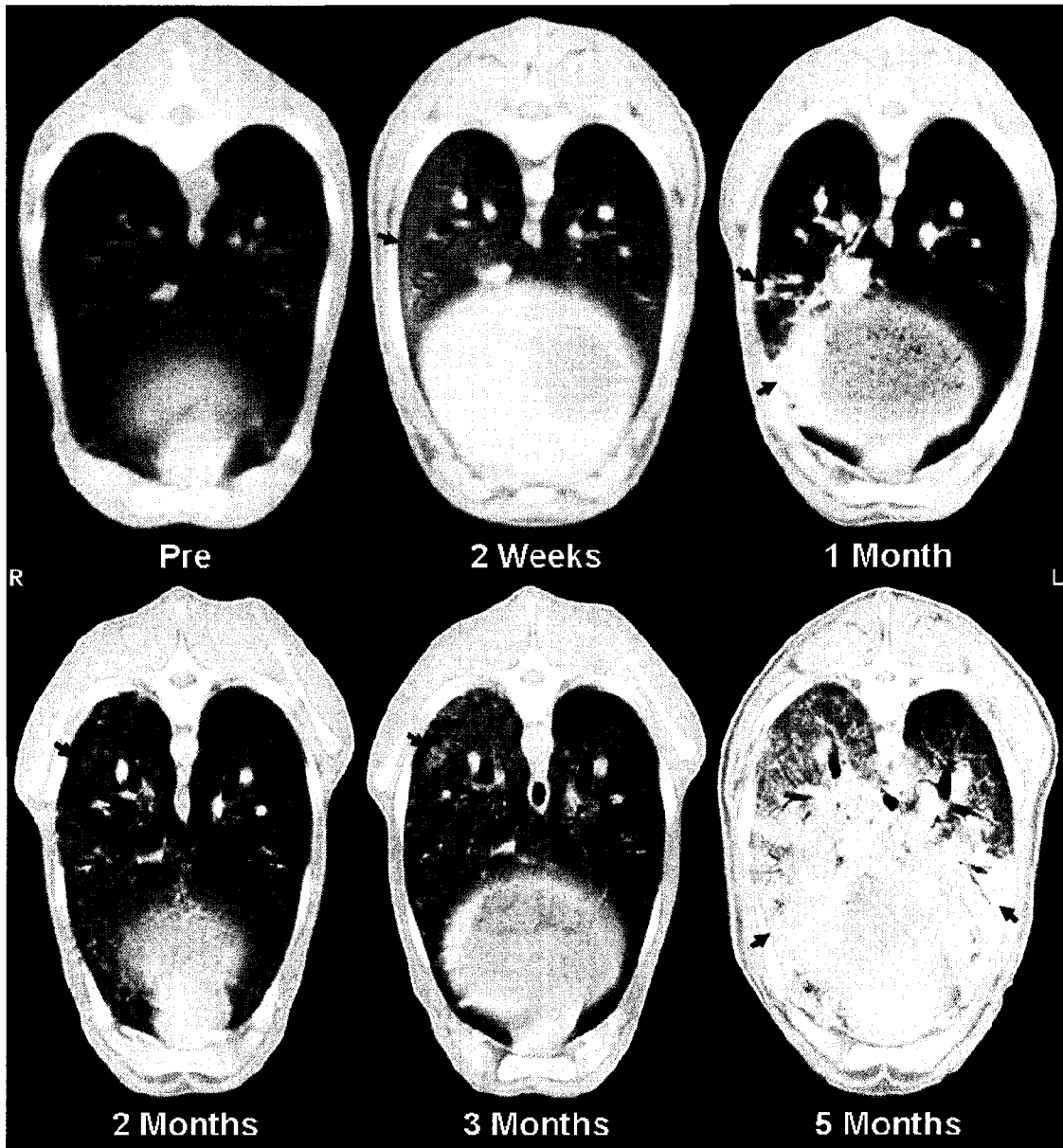


Figure 2.3: CT scan series for sheep 04RS4 showing nodular disease progression from pre-JSRV inoculation through 5 months post-JSRV inoculation. These images show disease evolution from a mild unilateral GGO DLP in the periphery of the right lung at 2 weeks post inoculation to a mixed DLP at 1 month post inoculation. Two months post inoculation, nodules are evident bilaterally and increase in size and number by 3 months post inoculation. Five months post inoculation, many of the nodules have coalesced and a solid DLP is apparent. Black arrows indicate cited features.

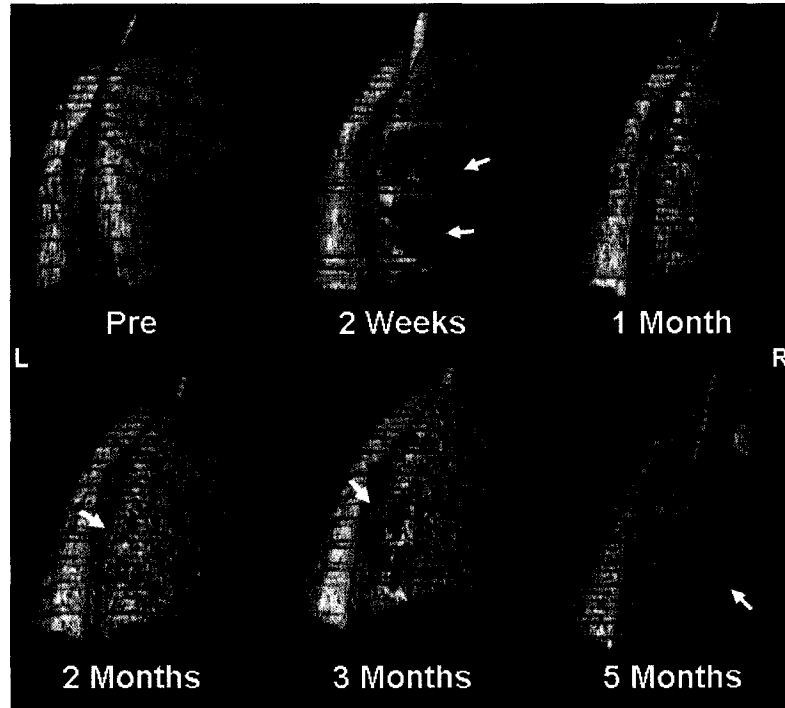


Figure 2.4: Dorsal view of 3D volume rendering for sheep 04RS4 showing nodular disease progression from pre-JSRV inoculation through 5 months post-JSRV inoculation. An algorithm based on attenuation was used for volume rendering; low-attenuation areas (healthy lung) are indicated in pink and high-attenuation areas (diseased lung) are excluded from the rendering. Two weeks post inoculation, there is disease present in the periphery of the right lung. By 1 month post inoculation, this disease has mostly resolved. At 2 months post inoculation, disease is evident in the peripheral lung and progresses by 3 months post inoculation. Five months post inoculation, severe disease is apparent, particularly in the right lung. White arrows indicate disease.

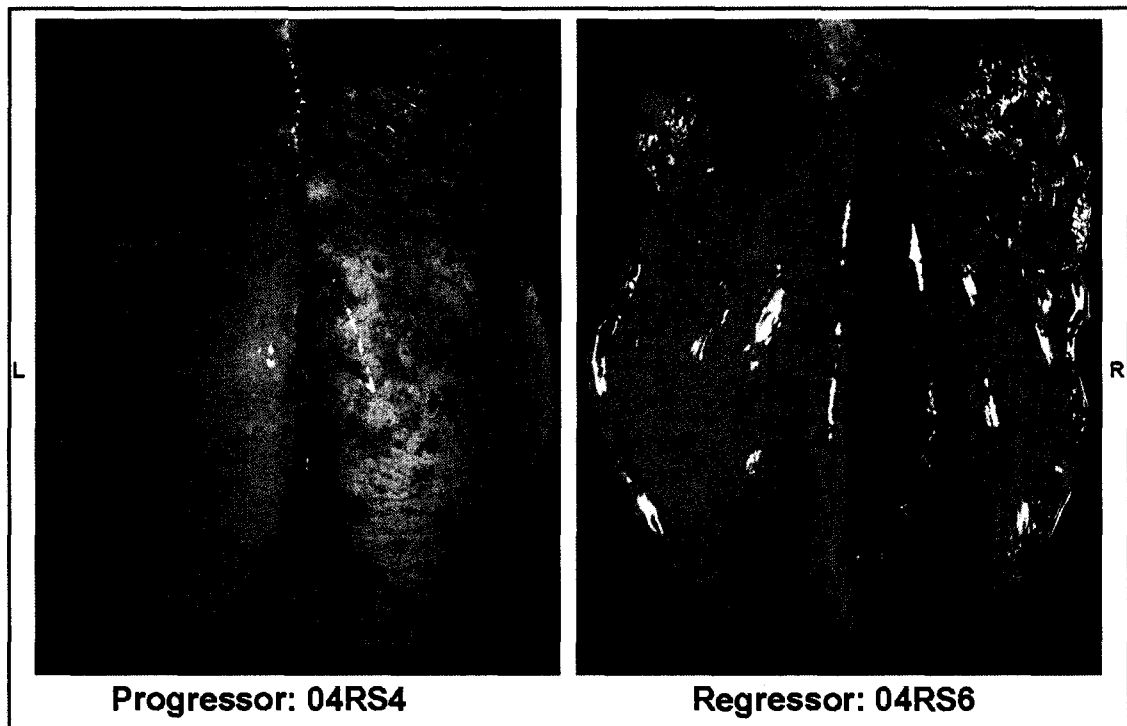


Figure 2.5: Dorsal view of gross lungs at euthanasia from sheep 04RS4 showing nodular disease progression (A) and sheep 04RS6 showing partial nodular disease regression (B). In 04RS4, numerous nodules of varying sizes are evident, particularly in the right lung. In 04RS6, considerably fewer and smaller nodules are visible, primarily in the left lung. Black arrows indicate nodules.

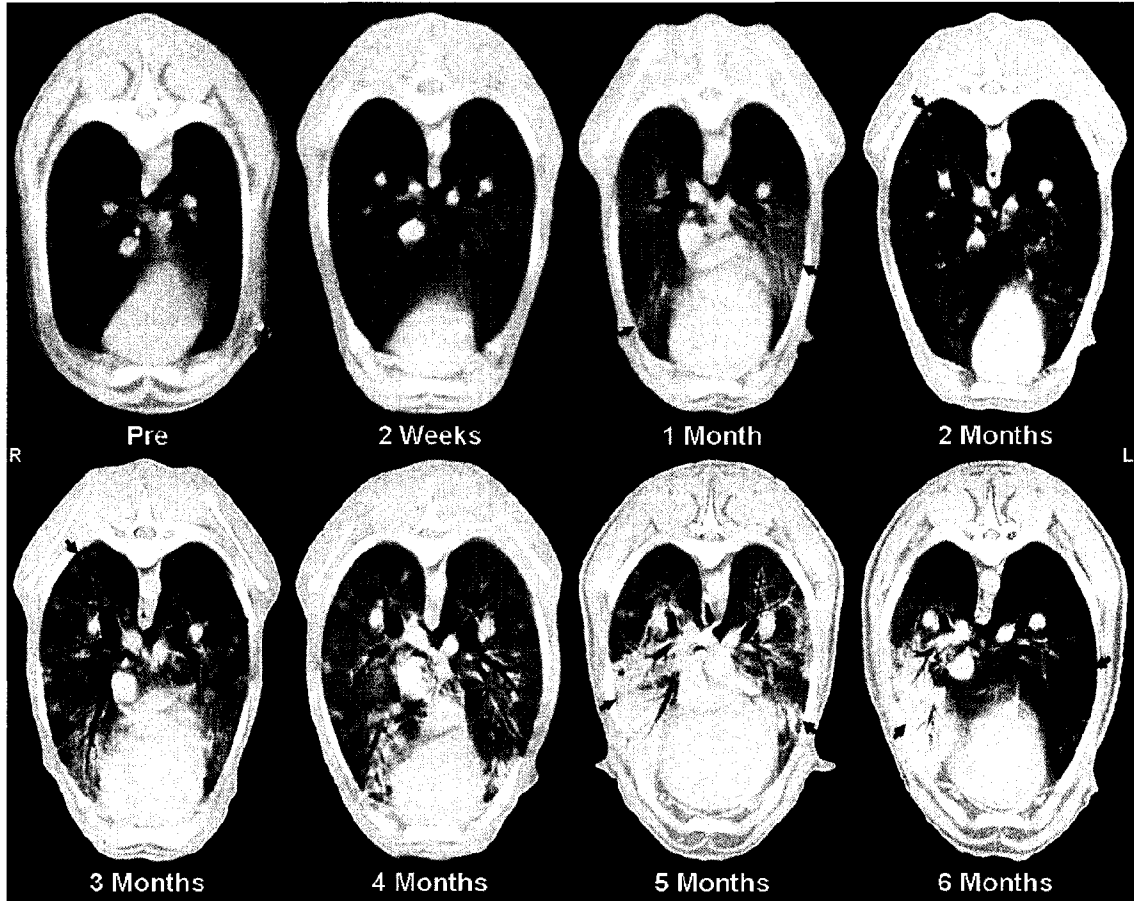


Figure 2.6: CT scan series for sheep 04RS6 showing partial nodular disease regression from pre-JSRV inoculation through 6 months post-JSRV inoculation. These images show disease evolution from an early bilateral mixed DLP at 1 month post inoculation to visible nodules by 2 months post inoculation that increase in size and number through 3 months post inoculation. By 4 months post inoculation, nodules begin to resolve. Five months post inoculation, many nodules have regressed but a mixed DLP has appeared ventrally. At 6 months post inoculation, the mixed DLP has resolved in the left lung but remains in the right lung; nodules are faint but still detectable. Black arrows indicate cited features.

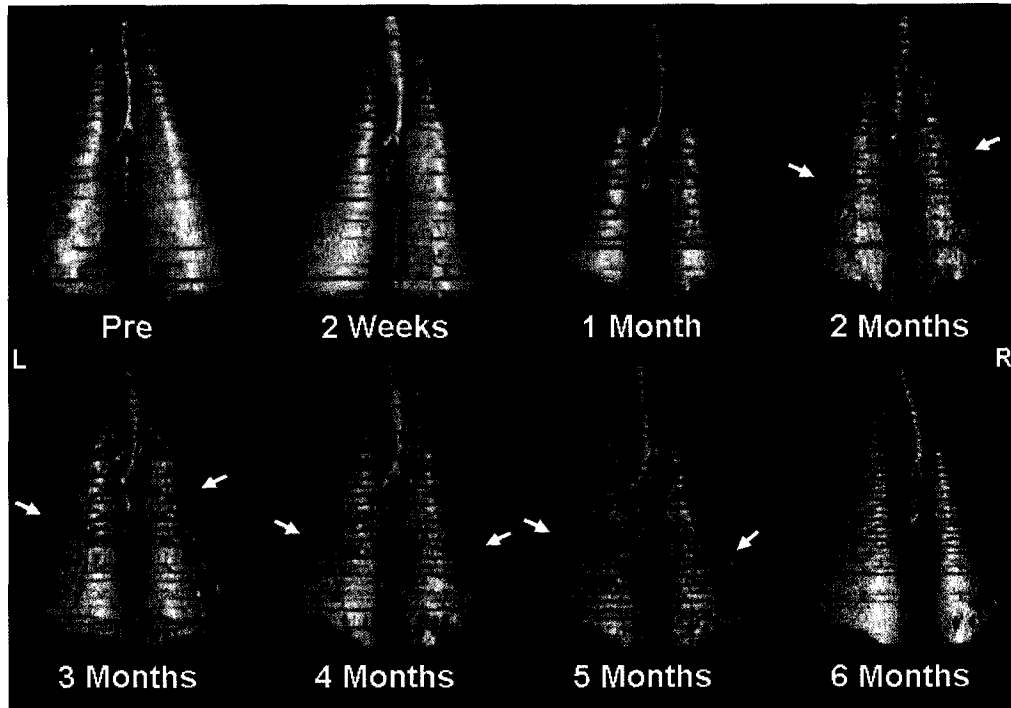


Figure 2.7: Dorsal view of 3D volume rendering for sheep 04RS6 showing partial nodular disease regression from pre-JSRV inoculation through 6 months post-JSRV inoculation. An algorithm based on attenuation was used for volume rendering; low-attenuation areas (healthy lung) are indicated in pink and high-attenuation areas (diseased lung) are excluded from the rendering. Two months post inoculation, mild bilateral peripheral disease is visible, increasing through 5 months post inoculation. By 6 months post inoculation, disease has significantly resolved. White arrows indicate disease.

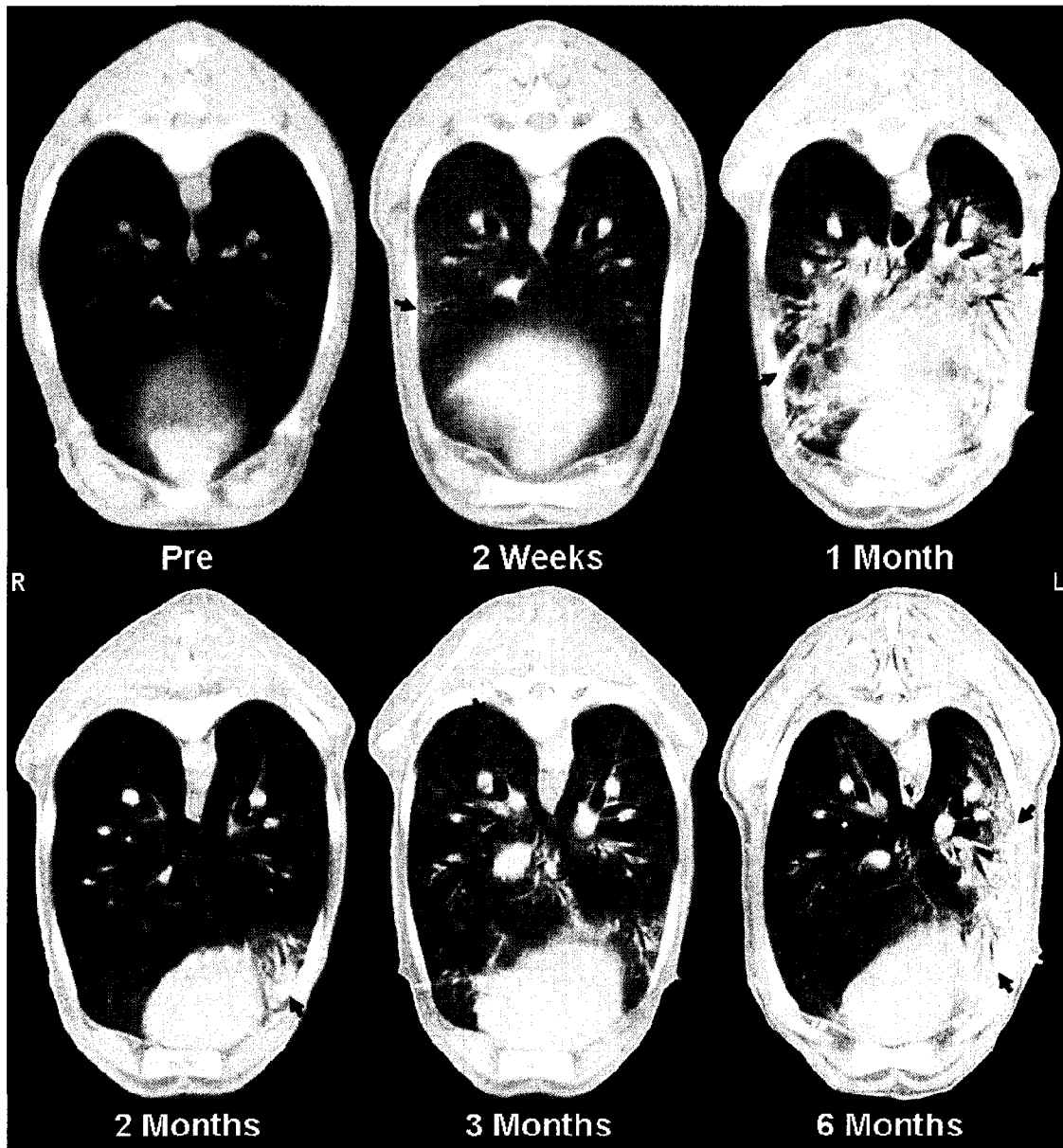


Figure 2.8: CT scan series for sheep 04RS3 showing complete nodular disease regression from pre-JSRV inoculation through 6 months post-JSRV inoculation. These images show disease evolution from a mild unilateral GGO DLP at 2 weeks post inoculation to a bilateral mixed DLP by 1 month post inoculation, which is mostly resolved by 2 months post inoculation, except in the ventral portion of the left lung. Three months post inoculation, nodules are evident but completely regress by 6 months post inoculation, when only a mixed DLP is apparent in the left lung periphery. Black arrows indicate cited features.

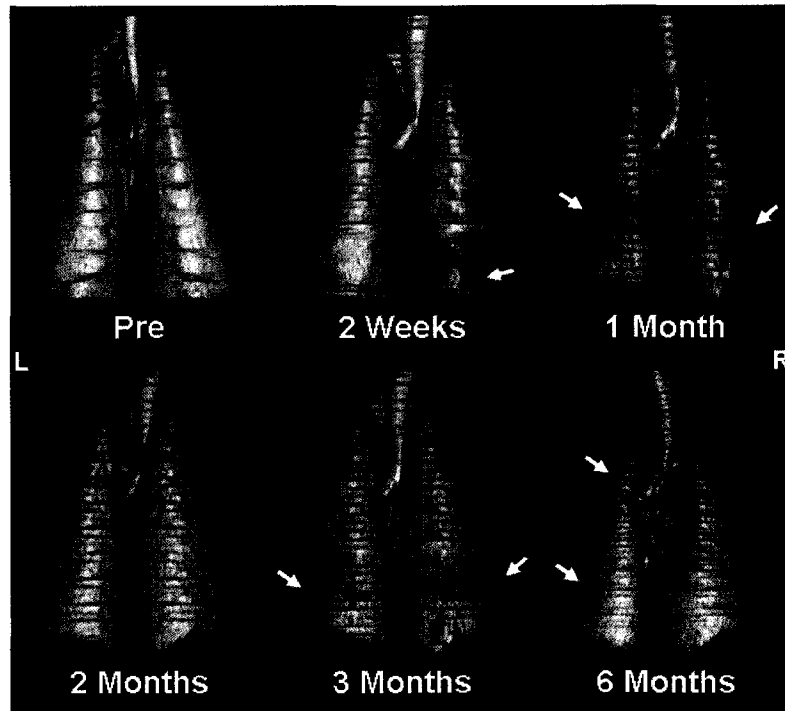


Figure 2.9: Dorsal view of 3D volume rendering for sheep 04RS3 showing complete nodular disease regression from pre-JSRV inoculation through 6 months post-JSRV inoculation. An algorithm based on attenuation was used for volume rendering; low-attenuation areas (healthy lung) are indicated in pink and high-attenuation areas (diseased lung) are excluded from the rendering. Two weeks post inoculation, there is very mild disease present in the periphery of the right lung. By 1 month post inoculation, this has progressed to a bilateral disease, which is mostly resolved by 2 months post inoculation. Three months post inoculation, disease reappears and, at 6 months post inoculation, regresses dorsally but progresses ventrally. White arrows indicate disease.

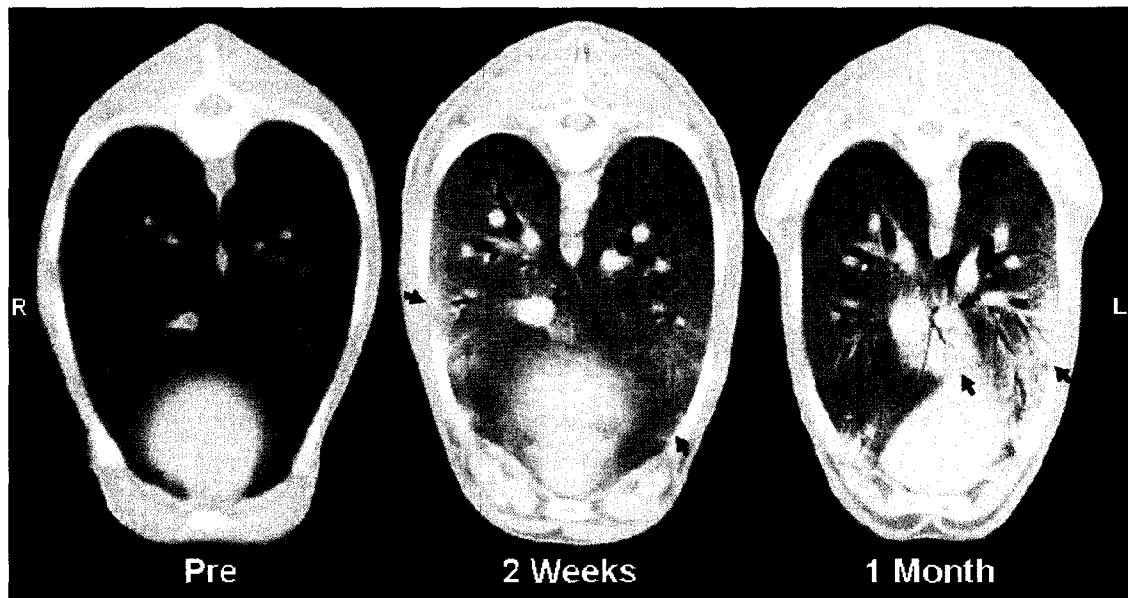


Figure 2.10: CT scan series for sheep 04RS8 showing the evolution of a mild GGO DLP from 2 weeks post inoculation to a moderate mixed DLP by 1 month post inoculation, especially severe in the right accessory lung lobe. 04RS8 was the only sheep to test positive via serology for OvLV both pre-inoculation and at 2 weeks post inoculation. Black arrows indicate cited features.

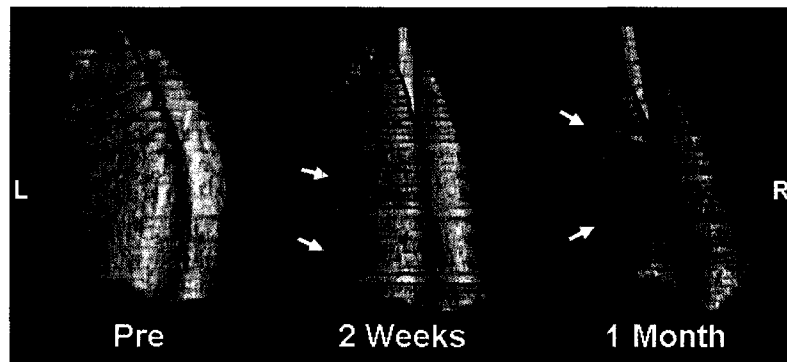


Figure 2.11: Dorsal view of 3D volume rendering for sheep 04RS8 showing the progression of disease from 2 weeks post inoculation to 1 month post inoculation. An algorithm based on attenuation was used for volume rendering; low-attenuation areas (healthy lung) are indicated in pink and high-attenuation areas (diseased lung) are excluded from the rendering. White arrows indicate disease.

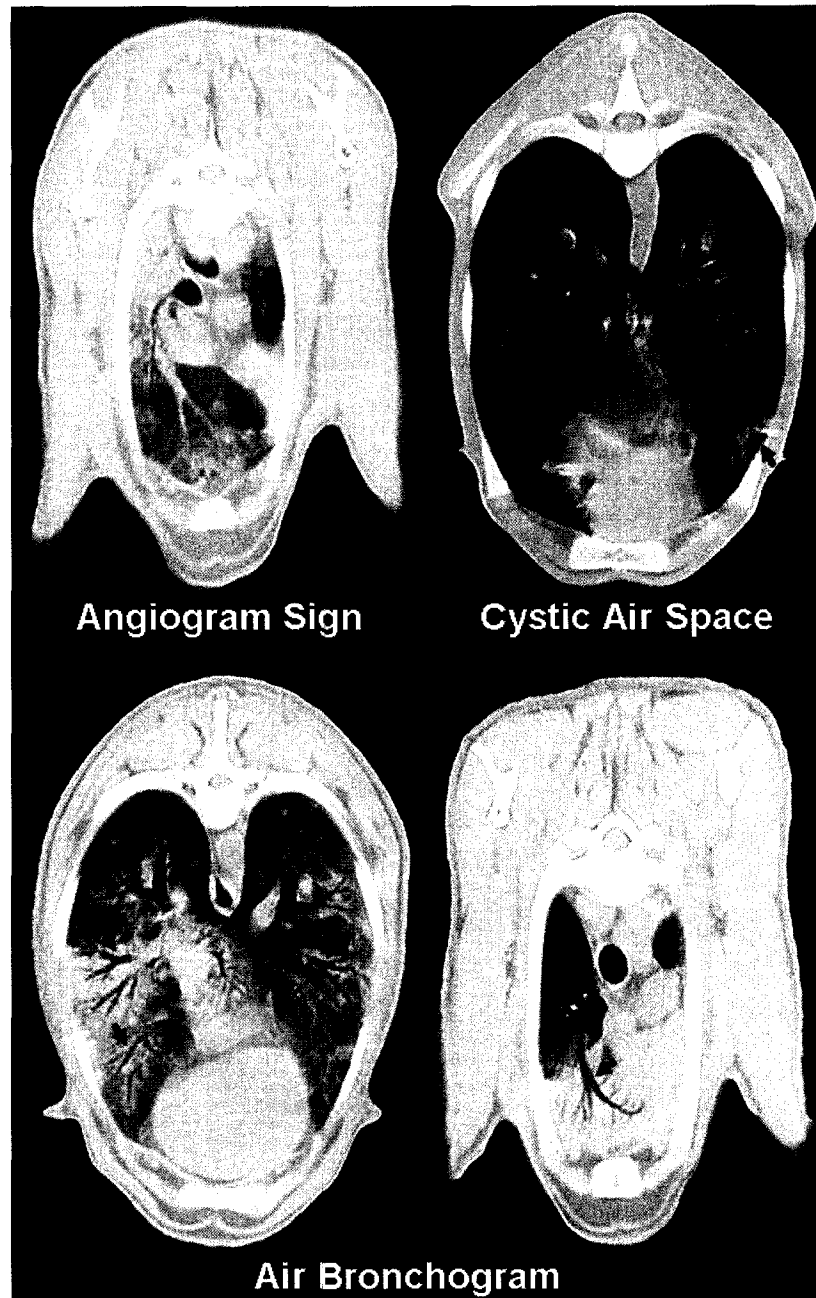


Figure 2.12: CT scan features, including angiogram sign, cystic air space, and air bronchograms, seen during disease development. Black arrows indicate features.

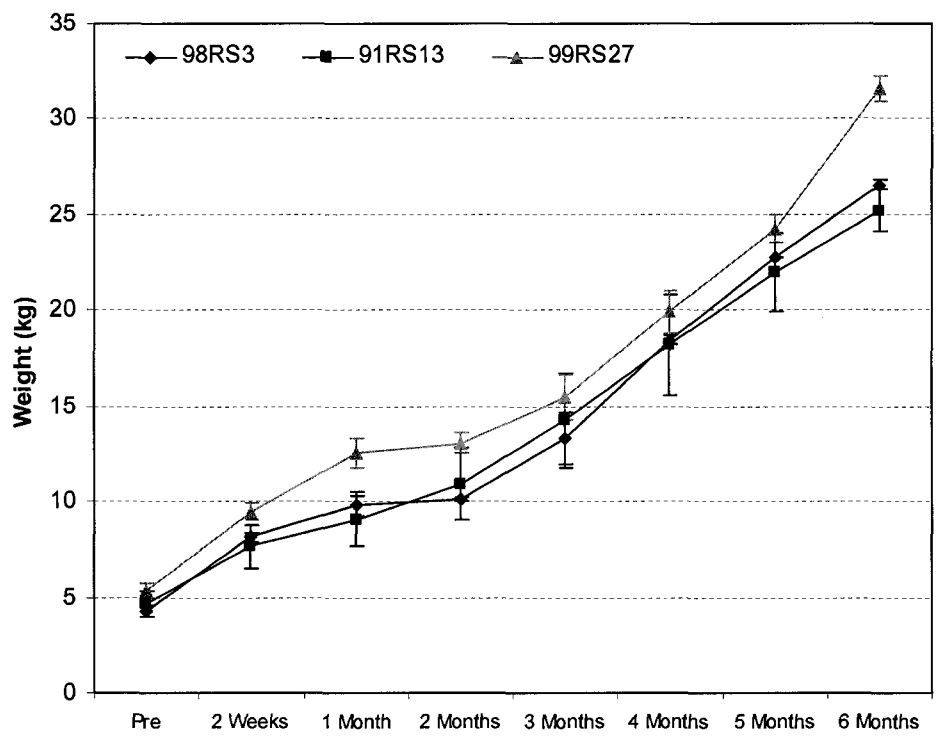


Figure 2.13: Sheep weights over time, grouped by inoculum source. Each point represents the mean weight of live sheep  $\pm$  standard error.

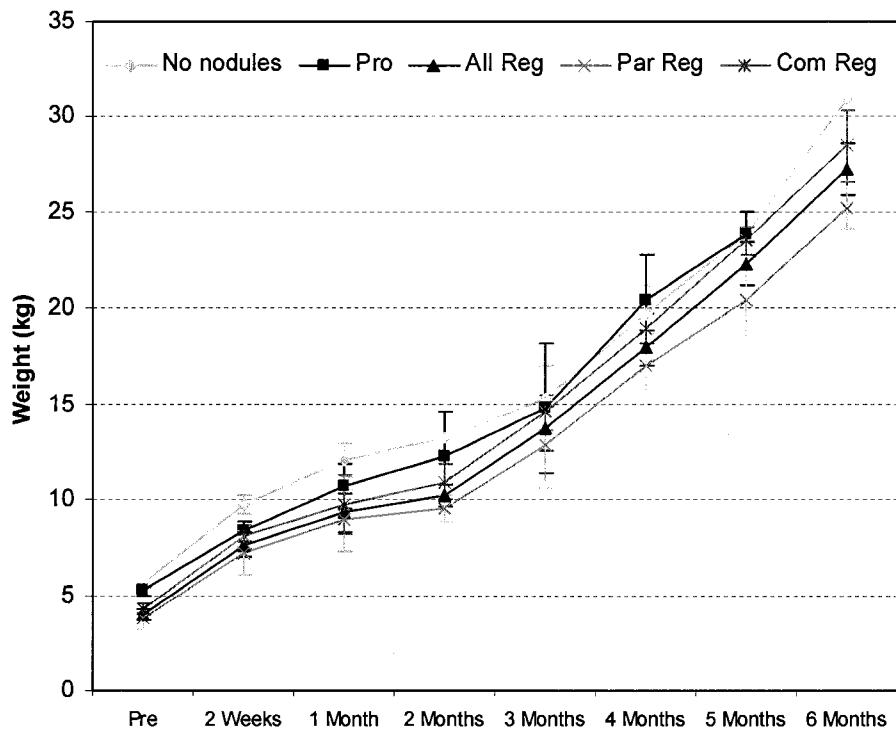


Figure 2.14: Sheep weights over time, grouped by nodular disease development: no nodules, progressors (pro), regressors (all reg), partial regressors (par reg), and complete regressors (com reg). Each point represents the mean weight of live sheep  $\pm$  standard error.

## **CHAPTER III**

### **HISTOPATHOLOGY OF OVINE PULMONARY ADENOCARCINOMA AND IMMUNE RESPONSE TO JAAGSIEKTE SHEEP RETROVIRUS**

#### **INTRODUCTION**

The tropism of a retrovirus is primarily determined by the envelope gene and the LTR. The envelope gene encodes the viral glycoprotein that specifically interacts with the cellular receptors necessary for viral entry (Weiss and Taylor 1995) and, for JSRV, this receptor has been cloned and identified as Hyal2, a glycosylphosphatidylinositol-linked cell surface protein that is expressed in many cell types (Lepperdinger et al. 1998; Strobl et al. 1998; Rai et al. 2001). Accordingly, JSRV can infect a variety of cells, but primarily targets differentiated epithelial cells of the lungs (Palmarini et al. 1995; Platt et al. 2002). Also, using sensitive PCR assays, JSRV DNA and RNA transcripts have been detected in lymphoreticular organs, PBMCs, and in lymphoid cells isolated from the mediastinal lymph nodes of both natural and experimental OPA cases (Palmarini

et al. 1996b; Holland et al. 1999; Garcia-Goti et al. 2000; Gonzalez et al. 2001; Salvatori et al. 2004). Notably, there is no evidence of viral transformation in any of these cell types (Palmarini et al. 1996b; Holland et al. 1999). Instead, in OPA-affected sheep, JSRV expression and subsequent transformation are restricted to alveolar type II cells/type II pneumocytes in the alveoli and Clara cells in the bronchioli (Palmarini et al. 1995; Platt et al. 2002). This restriction is due to the preferential activation of the JSRV LTR in these cells, as viral expression is driven more efficiently in cells that express transcription factors that interact with the viral promoter and enhancer elements contained in the LTR (Palmarini et al. 2000a). Remarkably, JSRV appears to be unique among retroviruses in inducing transformation of the differentiated epithelial cells of the lungs (Rosenberg and Jolicoeur 1997).

The gross pathology of OPA is well established; neoplastic areas are localized at the periphery of the lungs and tend to be multifocal, varying from small discrete nodules (1 – 30mm) to extensive tumors involving entire lung lobes (De las Heras et al. 2003; Leroux et al. 2007). Histopathologically, OPA originates from differentiated alveolar type II cells and non-ciliated bronchiolar epithelial (Clara) cells (Nisbet et al. 1971; Perk et al. 1971; Sharp 1987; Platt et al. 2002). In human lung cancer, transformation of these cell types is indicative of nonmucinous BAC (Travis et al. 2006) and, classically, OPA has been compared with this subtype of adenocarcinoma (Palmarini and Fan 2001). However, in the 1999 WHO classification of lung tumors, the BAC criteria underwent a major change, requiring that all BACs demonstrate pure lepidic (bronchioloalveolar)

growth without invasion of the stroma, blood vessels, or pleural (Travis et al. 1999). Accordingly, OPA is now classified as a mixed-subtype adenocarcinoma, as these ovine tumors have both bronchioloalveolar and invasive (acinar and papillary) growth patterns (Mornex et al. 2003). The stroma of the tumor is generally thin but may be infiltrated by various amounts of lymphocytes, plasma cells and connective tissue fibers (De Las Heras et al. 1995; De las Heras et al. 2003).

Despite the highly productive infection in the lungs and the disseminated lymphoid infection, the immune response to JSRV and OPA appears to be minimal. Following natural or experimental infection with the virus, no JSRV capsid-specific humoral response has been detected in sera or lung fluid of affected sheep (Sharp and Herring 1983; Ortin et al. 1998; Summers et al. 2002; Sharp and DeMartini 2003). This lack of systemic immunity has been proposed to be a consequence of transcriptionally active endogenous JSRV-related sequences expressed in utero, resulting in central tolerance to exogenous JSRV (Spencer et al. 2003; Palmarini et al. 2004). However, a recent study has shown that inoculation of sheep with recombinant JSRV capsid protein in adjuvant can successfully induce a JSRV-specific humoral response; thus, the ovine immune system appears to be capable of recognizing and responding to JSRV antigens (Summers et al. 2005). In all mentioned studies, it is important to note that only JSRV capsid antigens, from natural sources or protein recombination, have been used for the detection of circulating antibodies. Thus far, there has been no

investigation of antibodies against the envelope protein, the oncogenic component of JSRV.

Locally, in the lung parenchyma, diffuse interalveolar septal thickening by lymphocytes, macrophages, plasma cells, and neutrophils has been reported; additionally, a similar inflammatory response, as well as lymphoid proliferation, has been consistently documented around both affected and non-affected bronchioles (Payne and Verwoerd 1984; Rosadio et al. 1988; De Las Heras et al. 1995; Garcia-Goti et al. 2000; De las Heras et al. 2003). However, these influxes are probably due to concurrent infections, such as OvLV or mycoplasma, commonly present in OPA cases (Cutlip and Young 1982; Demartini et al. 1988; Verwoerd 1990). A recent study that experimentally infected specific pathogen-free lambs with JSRV found no influx of dendritic cells, B cells, CD4<sup>+</sup> T cells, CD8<sup>+</sup> T cells, or  $\gamma\delta$  T cells in the neoplastic nodules or in their periphery (Summers et al. 2005). Alternatively, this study found that the local immune response during OPA development is mediated predominantly by infiltrating macrophages that secrete high levels of IFN- $\gamma$  (Summers et al. 2005).

The absence of an immune response against JSRV in infected sheep could provide a permissive environment for the development of neoplasms in the lung (Ortin et al. 1998). Interestingly, it has been shown that the JSRV envelope can transduce not only sheep cells but also human, monkey, bovine, dog, and rabbit cells *in vitro*; yet, there is an absence of evidence of infection with JSRV *in vivo*, possibly due to the development of a strong immune response leading to virus clearance (Rai et al. 2000). In a study using immunodeficient mice, lung

adenocarcinomas were induced by a replication-defective AAV6 vector that expresses the JSRV envelope protein (ARJenv); the consequent mouse tumors were similar, both in location and histology, to OPA (Wootton et al. 2005; Wootton et al. 2006). However, in the same study, immunocompetent mice mounted a strong serum antibody response against JSRV envelope and tumor development was almost entirely blocked, indicating that JSRV envelope tumorigenesis can be controlled by the normal immune system of these mice (Wootton et al. 2005).

In the present study, H&E and immunohistochemical sections from sheep involved in the radiographic imaging of OPA disease development study [(04RS1-04RS12) detailed in Chapter II] were evaluated. Specifically, we looked for evidence of JSRV-transformed tumor cells to determine whether the nodules visible on CT were indicative of OPA. Additionally, features suggestive of a local immune response in the lung, possibly against JSRV-induced tumor cells, were also noted, particularly in relation to nodular disease development status. For comparison, we looked at these features in archival tissue sections from JSRV-infected sheep with confirmed OPA and no documented regression to determine if there were any characteristics that were histologically unique to either the tumor cells or immune infiltrate in our sheep lungs that might correlate with nodular disease progression or regression. To evaluate evidence of an antiviral humoral immune response, serum samples from 04RS1-04RS12 were analyzed for the presence of antibodies against the JSRV envelope and OvLV.

## MATERIALS AND METHODS

### *Animal samples*

Serum samples were obtained from JSRV-inoculated lambs 04RS1 through 04RS12, used in the radiographic imaging of OPA disease development study (Chapter II), at each imaging time point. Sera were rapidly frozen in liquid nitrogen, stored at -80°C, and used for subsequent analysis of antibodies against JSRV and OvLV.

The lungs of JSRV-inoculated lambs 04RS1 through 04RS12, used in the radiographic imaging of OPA disease development study (Chapter II), were examined grossly at necropsy to identify any lesions suggestive of OPA. Samples from neoplastic-like areas and/or tissue from all lobes were taken for microscopic examination. For this purpose, tissue samples were fixed in 10% neutral-buffered formalin, processed routinely, sectioned at 5µm, and stained with haematoxylin and eosin (H&E) or used for immunohistochemical analyses. In addition, 22 formalin-fixed, paraffin-embedded tissue sections from previous studies of natural and experimental OPA were provided by Dr. James DeMartini (Colorado State University).

C57BL/6 ARJenv (+) lung tumor tissue sections, collected as part of a previous study (Wootton et al. 2005), were generously provided by A. Dusty Miller, Fred Hutchinson Cancer Research Center.

### *Immunohistochemistry*

Immunohistochemical (IHC) staining of lung tissue was performed using standard techniques on an automated stainer (Discovery, Ventanna Medical Systems, Tucson, AZ). Briefly, 5 $\mu$ m sections were cut and mounted on positively charged slides. The sections were deparaffinized and then rehydrated in a descending series of alcohol concentrations. Heat-induced epitope retrieval with citrate buffer (pH 6.0) for 30 minutes was followed by endogenous peroxidase blocking with 3% hydrogen peroxide and incubation with antiserum at room temperature for 12 hours. A prediluted, universal biotinylated secondary antibody and 3, 3'-diaminobenzidine tetrahydrochloride (DAB) (DAB Map™ Kit, Ventanna Medical Systems, Tucson, AZ) were utilized to detect the immunoreactive complexes. The slides were counterstained with Mayer's hematoxylin and dehydrated before microscopic examination. Normal lung tissue from disease-free sheep was used as a negative control. A second negative lung control had the primary antibody replaced by antibody diluent only.

The antiserum against the JSRV envelope, generously provided by A. Dusty Miller, Fred Hutchinson Cancer Research Center, was mouse immune serum collected from C57BL/6 mice infected with ARJenv at 8 weeks post-infection (Wootton et al. 2005). The antiserum was diluted 1:500. Lung tumor tissue sections from these mice were used as a positive control.

The pan T-cell antibody used was a polyclonal rabbit anti-human CD3 antibody (Biocare, Cat. No. CP 215), diluted 1:50. Sheep lymph node tissue sections were used as a positive control.

Slides were analyzed using an image analysis workstation (AxioVision Release 4.6, Carl Zeiss). Polychromatic high-resolution images (1300 x 1030 pixel) were obtained at 20X magnification. The percent of tissue surface area that stained positive for CD3 was recorded from five independent image analyses. The mean percent of CD3 staining was used for statistical analysis [one-way analysis of variance (ANOVA) with Bonferroni's multiple comparison post test].

#### *Ovine lentivirus detection*

Serum antibodies to OvLV were tested for using agar-gel immunodiffusion (AGID) serology at Colorado State University's Diagnostic Laboratory.

#### *Jaagsiekte sheep retrovirus (JSRV) envelope neutralization*

The neutralization assay was performed as described previously (Wootton et al. 2005). Briefly, sheep serum samples were diluted in PBS to give a final volume of 20 $\mu$ l. Next, 20 $\mu$ l of JSRV-pseudotype virus [LAPSN(PJ4), packaged with gag-pol proteins from MoMLV and envelope protein from JSRV (Rai et al. 2000)] encoding alkaline phosphatase (AP) was added to the serum samples and incubated at room temperature for 30 min. The serum/virus mixture was then added to cells in a 6-well plate seeded the day before at  $5 \times 10^4$  cells per well. Infections were done in the presence of 4 $\mu$ g/ml polybrene. Two days after virus exposure, the cells were stained for AP expression and positive foci were counted. Serum dilutions were calculated based on the amount of serum in the

40µl incubation mixture. Antibody titers were expressed as the reciprocal of the highest dilution of serum that reduced the number of viral foci by 50%.

## RESULTS

### *Tumor histopathology*

At euthanasia, of the eight sheep (04RS1 – 04RS8) that received inocula with detectable JSRV DNA (prepared from the tumor homogenates of 98RS3 and 91RS13), three (04RS4, 04RS5, and 04RS6) had grossly apparent lesions, five (04RS1, 04RS2, 04RS4, 04RS5, and 04RS6) had evident nodules on CT, and these same five had histopathologically visible tumor (Table 3.1). Of the remaining three animals with no grossly or histopathologically perceptible tumor at euthanasia, two (04RS3 and 04RS7) had radiographically detectable nodules at some point during the study that completely regressed by six months post inoculation and one (04RS8) was sacrificed early, at one month post inoculation. The four sheep (04RS9 – 04RS12) receiving the inoculum with no detectable JSRV DNA (from 99RS27) did not have nodules on their final CT scan nor grossly or histopathologically discernable tumor at euthanasia.

As for the five sheep with histopathologically confirmed cancer, the tumor presentation varied from a few tiny, well-circumscribed neoplasms to innumerable, discrete to coalescing tumor masses. In terms of nodular disease development groups, two (04RS1 and 04RS2) of the partial regressors showed the former pattern while the other partial regressor (04RS6) as well as the two

(04RS5 and 04RS5) progressors showed the latter (Figure 3.1). The cells that comprised these neoplasms were cuboidal to low columnar, with basally-located round to oval nuclei having an open chromatin pattern and a central nucleolus. The majority of neoplasms appeared with a regular alveolar pattern and general preservation of the pulmonary architecture; only rarely were there papillary formations in small and terminal bronchioles or a tubulopapillary pattern superimposed on the alveolar appearance. Mitoses were very rare but perceptible in four of five animals with tumor and thus, not specific to a nodular disease development group, although a progressor (04RS5) had the most mitotic figures [2-3 per 10 high power fields (hpfs)]. Apoptosis was almost never seen, except in one partial regressor (04RS6), in which one apoptotic cell per 10 hpfs was observed. For comparison, we also looked at these features in archival H&E-stained sections from 22 JSRV-infected sheep with confirmed OPA and no documented regression; observations were similar to those found in our tumor-bearing sheep: lung neoplasms varied greatly, from one or a few tiny tumors to large coalescing masses, and mitotic figures and apoptotic cells were rare (Table 3.2). Regarding the ARJenv (+) sample, we saw several moderately large tumors (Figure 3.2A) with one mitotic figure and one apoptotic cell per 10 hpfs (Table 3.1).

#### *JSRV envelope immunohistochemistry*

To investigate the presence of JSRV, we stained the lung tissue samples with an antibody specific for the envelope protein of this virus. We found tumor-

specific staining in three samples (04RS4, 04RS5, and 04RS6); as for the other two samples (04RS1 and 04RS2) with visible tumor in the H&E-stained sections, neither had tumor in the IHC sections (Table 3.3). Thus, of the three animals with evident tumor on the IHC sections, all stained positive for the JSRV envelope protein (Figure 3.3). However, the staining intensity differed between nodular disease development groups; the two progressors (04RS4 and 04RS5), as well as the ARJenv (+) sample (Figure 3.2B), showed strong staining intensity while the partial regressor (04RS6) only showed moderate staining intensity. In all animals, this staining was homogenous throughout the cytoplasm of the tumor cells; no staining was observed in the nuclei.

#### *Pulmonary histopathology*

In addition to tumor, other striking features seen in the H&E-stained lung sections include follicular hyperplasia (FH) (Figure 3.4A), hypertrophy of the bronchus associated lymphoid tissue (BALT) (Figure 3.4B), and alveolar septae thickening due to collagen deposition, occasional neutrophils, and infiltration of mononuclear leukocytes, including mature plasma cells, macrophages, and lymphocytes. These lymphocytes were seen in the lung parenchyma as well as intratumorally (Figure 3.5). In eleven of twelve sheep, both FH and lung parenchyma lymphocyte infiltration were observed at euthanasia (Table 3.1). As for the intratumor lymphocyte infiltration, one partial regressor with neoplasms <500 $\mu$ m only showed minimal lymphocyte infiltration; however, the two progressors exhibited marked lymphocyte infiltration and the other two partial

regressors exhibited severe lymphocyte infiltration. Thus, infiltration of lymphocytes within the neoplasms was not specific to a nodular disease development group. Additionally, this feature was also noted in the archival sections from 22 JSRV-infected sheep with confirmed OPA and no documented regression (Table 3.2). Concerning the ARJenv (+) sample, we found minimal lung parenchyma lymphocyte infiltration and no atypical intratumor lymphocyte infiltration (Table 3.1).

### *CD3 immunohistochemistry*

Next, we sought to further characterize the lung parenchyma and intratumor lymphocytes by IHC staining of the ovine lung tissue samples with an antibody specific for CD3, a pan T-cell marker. There were no obvious differences in lung parenchyma CD3<sup>+</sup> T-cell infiltration between nodule disease development groups, although the sheep with the greatest CD3<sup>+</sup> infiltrate at euthanasia (04RS11) did not develop nodules during the study (Table 3.3). Of the three sheep with tumor in the IHC sections, the partial regressor (04RS6) had more intratumor CD3<sup>+</sup> lymphocytes than both progressors (04RS4 and 04RS5) (Figure 3.6, Table 3.3). In fact, when intratumor CD3<sup>+</sup> cells were quantified with image analysis software, over 40% of the tissue surface area examined was comprised of CD3<sup>+</sup> T-cells in the partial regressor whereas, in both progressors, CD3<sup>+</sup> T-cells only constituted only ~7% of the tissue surface area (Figures 3.7 and 3.8).

*Correlation between OPA-associated lesions and humoral antibody against the JSRV envelope*

As mentioned previously, we confirmed the presence of the JSRV envelope protein in the lung tumor tissue of sheep infected with the virus. Subsequently, we looked for the presence of circulating antibodies against this protein by measuring the ability of the sheep serum to neutralize the infectivity of a retroviral vector bearing the JSRV envelope [LAPSN(PJ4)] (Rai et al. 2000; Wootton et al. 2005) (Table 3.4). For eleven of twelve pre-inoculation serum samples, the dilution that reduced the titer of the vector by 50% was  $\leq 1:10$ , signifying low amounts of JSRV envelope-specific antibodies in the serum of these animals. However, for one sheep (04RS2), the same neutralization was accomplished by a 1:100 dilution of the pre-inoculation serum sample. Perplexed by this relatively high antibody titer against JSRV envelope in the serum of a neonate, we tested the dam of this lamb and found that her serum was also able to halve the titer of the vector at a 1:100 dilution. These results suggest vertical transmission of the anti-JSRV envelope antibodies from the dam to the lamb, most likely via colostrum. We tested the serum of 04RS2 again at three months post inoculation and the effective dilution for 50% vector titer reduction was decreased to 1:20, providing further evidence that the initial high serum titer most likely represented time-dependent degradation of maternal IgG antibodies and was not a result of antibody production by the lamb. However, at six months post inoculation, this animal was independently making antibodies against the JSRV

envelope, as a 1:100 serum dilution was again able to reduce the titer of the vector by half.

Interestingly, in terms of nodular disease development, lamb 04RS2 showed partial regression of radiographically visible nodules at four and six months post inoculation. Additionally, another partial regressor (04RS6) also produced high titers of anti-JSRV envelope antibodies that coincided with nodule clearance; by three months post inoculation and through the remaining three months of the study, the serum of this sheep was capable of 50% neutralization at a 1:100 dilution. During this time, dramatic nodule regression was observed, specifically at five and six months post inoculation. As for the other partial regressor (04RS1), nodules regressed much earlier, at two months post inoculation, and then progressed until euthanasia at four months post inoculation. At this time, the serum of this sheep was only able to reduce the vector titer by 50% at a dilution of < 1:10, indicating that there was not a significant humoral immune response when the nodules were progressing toward the end of the study. Similarly, serum antibody titers were low at euthanasia for the two animals with nodular disease progression (04RS4 and 04RS5), again suggesting an inadequate immune response that was not able to combat JSRV-induced tumor.

Regarding the three complete regressors, nodule clearance occurred early (two months post inoculation) in two (04RS7 and 04RS10) and, at euthanasia four months later, these sheep did not have appreciable antibody levels (neutralizing dilutions of  $\leq$  1:20). As for the other complete regressor (04RS3), nodules were apparent at three months post inoculation and were cleared by the

next CT scan, at six months post inoculation. At this time, the serum of this sheep was able to halve the vector titer at a 1:20 dilution. However, due to the three month gap in CT scanning, it is unclear when nodule regression occurred, therefore, we cannot make an obvious association with anti-JSRV envelope antibody titer in this animal.

Of the four sheep with no radiographically visible nodules during the study, three (04RS8, 04RS9, and 04RS12) had low circulating antibody titers at euthanasia (neutralizing dilutions of  $\leq 1:20$ ). Conversely, 04RS11 had a relatively high titer at this time (neutralizing dilution of 1:100), possibly suggesting an active humoral immune response against JSRV in this animal that may have prevented tumor development.

#### *Ovine lentivirus (OvLV)*

OvLV is the causative pathogen of ovine progressive pneumonia (OPP), a common infection in sheep. In an attempt to avoid confounding data resulting from the presence of two viruses (OvLV in addition to JSRV), we acquired the lambs used in this study from an alleged OPP-negative flock. Nevertheless, one (04RS8) of the twelve did test positive (via serology) for OvLV antibodies prior to virus inoculation. Also, as mentioned in Chapter II, the three inocula used in this study tested positive (via PCR) for OvLV. Consequently, all lambs were inadvertently inoculated with OvLV. At two weeks post inoculation, no OvLV antibodies were detected in the serum of any animals with the exception of 04RS8 (Table 3.5). This lamb was subsequently euthanized to prevent OvLV

transmission to the other eleven animals. However, by two months post inoculation, ten of the remaining eleven sheep had seroconverted and, at euthanasia, all animals were seropositive for antibodies against OvLV.

## CONCLUSIONS

In the preceding study, H&E and immunohistochemical sections from sheep involved in the radiographic imaging of OPA disease development study [(04RS1-04RS12) detailed in Chapter II] were evaluated. Of the eight sheep that received inocula with detectable JSRV DNA, five had evident nodules on CT as well as histopathologically visible tumor at euthanasia, confirming that the nodules observed on CT were indicative of OPA. Furthermore, the four sheep receiving the inoculum with no detectable JSRV DNA did not have nodules on their final CT scan nor grossly or histopathologically discernable tumor at euthanasia, providing further corroboration that the nodules seen on CT during this study signified the presence of OPA. Of the three animals with tumor on the IHC sections, all stained positive for the JSRV envelope protein, indicating that the tumors were indeed OPA induced by JSRV.

Additionally, features suggestive of a local immune response in the lung, possibly against JSRV-induced tumor cells, were also noted, including lung parenchyma and intratumor lymphocyte infiltration. Varying degrees of both were seen and neither correlated with nodular disease development status. However, the sheep with the greatest CD3<sup>+</sup> lung parenchyma T-cell infiltration did not

develop nodules during the study and, the partial regressor with tumor on the IHC section did have significantly more intratumoral CD3<sup>+</sup> cells than both progressors. Taken together, these results suggest a possible role for a T-cell mediated immune response against JSRV and OPA tumor development.

Regarding a humoral immune response, serum samples from 04RS1-04RS12 were analyzed for the presence of antibodies against the JSRV envelope. The sheep with the greatest CD3<sup>+</sup> lung parenchyma T-cell infiltration also had a relatively high anti-JSRV envelope antibody titer; additionally, two partial regressors produced relatively high antibody titers that coincided with nodule clearance. Again, these results propose a potential association between an immune response against JSRV and OPA tumor development. However, all sheep were also seropositive for OvLV antibodies and, thus, from our study, it cannot be determined if the local immune infiltrate observed in the lungs was directed toward OvLV infection, JSRV infection, or even OPA tumor antigens.

Table 3.1: Radiographic development and histologic features of lung disease in sheep receiving inoculum with JSRV (04RS1 – 04RS8) and without JSRV (04RS9 – 04RS12) and histologic features of lung disease in mice receiving a vector expressing the JSRV envelope [ARJenv (+)].

Sheep	Computed Tomography		Histology					
	Nodule Development	Nodules at Euthanasia	Tumor	Mitotic Figures	Apoptosis	Follicular Hyperplasia	Lung Parenchyma Lymphocyte Infiltration	Intratumor Lymphocyte Infiltration
04RS8	No nodules		0	Ø	Ø	3	5	Ø
04RS9	No nodules		0	Ø	Ø	5	5	Ø
04RS11	No nodules		0	Ø	Ø	5	5	Ø
04RS12	No nodules		0	Ø	Ø	2	3	Ø
04RS4	Progression	✓	4	1	0	3	4	4
04RS5	Progression	✓	4	2	0	4	5	4
04RS1	Partial regression	✓	1	1	0	4	4	1
04RS2	Partial regression	✓	1	0	0	2	3	5
04RS6	Partial regression	✓	4	1	1	5	5	5
04RS3	Complete regression		0	Ø	Ø	3	3	Ø
04RS7	Complete regression		0	Ø	Ø	1	2	Ø
04RS10	Complete regression		0	Ø	Ø	0	0	Ø
ARJenv (+)	---	---	4	1	1	0	1	0

Pathological scoring for tumor: 0 = no apparent tumor; 1 = one or a few very tiny tumors; 2 = several small tumors; 3 = one or more moderately large tumors; 4 = one very large or several moderately large tumors; 5 = several large and/or coalescing tumors. Pathological scoring for mitotic figures (mf) and apoptotic cells (ac): 0 = <1 mf or ac per 20 high power fields (hpf); 1 = 1 mf or ac per 10 hpf; 2 = 2-3 mf or ac per 10 hpf; 3 = 4-5 mf or ac per 10 hpf; 4 = 6-8 mf or ac per 10 hpf; 5 = >8 mf or ac per 10 hpf. Pathological scoring for other features: 0 = no apparent change from normal; 1 = minimal change from normal; 2 = mild change from normal; 3 = moderate change from normal; 4 = marked change from normal; 5 = severe change from normal. Ø indicates no tumor present histologically so features not applicable.

Table 3.2: Histologic features of lung disease induced by JSRV infection in sheep.

Sheep	JSRV Source	Age at Euthanasia	Tumor	Mitotic Figures	Apoptosis	Follicular Hyperplasia	Lung Parenchyma Lymphocyte Infiltration	Intratumor Lymphocyte Infiltration
85RS7	LH	1 month	5	1	0	0	0	1
85RS14	LH	2 months	5	0	0	2	2	3
85RS21	LF	3 months	4	0	0	0	5	4
85RS22	LF	3 months	4	0	0	0	5	2
85RS11	LH	4 months	3	0	0	2	2	2
86RS44	LH	4 months	4	1	0	4	5	4
85RS8	LH	5 months	3	0	0	4	5	3
85RS13	LF	5 months	4	1	0	0	2	3
85RS2	LF	6 months	2	0	1	2	3	2
85RS42	LH	6 months	1	0	0	2	3	2
85RS43	LH	6 months	1	0	0	2	3	2
86RS50	LH	6 months	2	1	0	0	1	3
00RS28	LH	6 months	2	2	0	0	0	2
84RS16	LH	7 months	3	1	1	3	2	2
84RS17	LF	7 months	5	0	0	5	5	4
85RS1	LF	7 months	3	0	0	2	3	3
85RS6	LH	7 months	1	0	0	2	2	1
85RS19	LH	7 months	4	1	0	4	4	2
85RS50	LH	7 months	5	0	0	4	5	4
00RS25	LH	7 months	3	2	0	0	1	3
00RS26	LH	7 months	1	1	0	0	1	3
85RS52	LH	8 months	1	0	0	3	3	2

Pathological scoring for tumor: 0 = no apparent tumor; 1 = one or a few very tiny tumors; 2 = several small tumors; 3 = one or more moderately large tumors; 4 = one very large or several moderately large tumors; 5 = several large and/or coalescing tumors. Pathological scoring for mitotic figures (mf) and apoptotic cells (ac): 0 = <1 mf or ac per 20 high power fields (hpf); 1 = 1 mf or ac per 10 hpf; 2 = 2-3 mf or ac per 10 hpf; 3 = 4-5 mf or ac per 10 hpf; 4 = 6-8 mf or ac per 10 hpf; 5 = >8 mf or ac per 10 hpf. Pathological scoring for other features: 0 = no apparent change from normal; 1 = minimal change from normal; 2 = mild change from normal; 3 = moderate change from normal; 4 = marked change from normal; 5 = severe change from normal.

Table 3.3: Correlation of radiographic development of nodular disease in sheep receiving inoculum with JSRV (04RS1 – 04RS8) and without JSRV (04RS9 – 04RS12) with immunohistochemical (IHC) detection of JSRV envelope (Env) and CD3, a pan T-cell marker.

Sheep	Computed Tomography		Histology			
	Nodule Development	Nodules at Euthanasia	Tumor via H&E	JSRV Env	CD3	
					Lung Parenchyma	Intratumor
04RS8	No nodules			0	4	∅
04RS9	No nodules			0	2	∅
04RS11	No nodules			0	5	∅
04RS12	No nodules			0	3	∅
04RS4	Progression	✓	✓	3	2	2
04RS5	Progression	✓	✓	3	2	1
04RS1	Partial regression	✓	✓	§	3	∅
04RS2	Partial regression	✓	✓	§	2	∅
04RS6	Partial regression	✓	✓	2	2	3
04RS3	Complete regression			0	2	∅
04RS7	Complete regression			0	1	∅
04RS10	Complete regression			0	2	∅
ARJenv (+)	---	---	✓	3	---	---

Pathological scoring for intensity of JSRV Env IHC: 0 = no staining; 1 = weak staining intensity; 2 = moderate staining intensity; 3 = strong staining intensity. Pathological scoring for CD3 IHC: 0 = no positive cells present; 1 = few scattered positive cells (within normal limits); 2 = slight increase in positive cells above normal; 3 = moderate increase in positive cells above normal; 4 = marked increase in positive cells above normal; 5 = very severe increase in positive cells above normal. ∅ indicates no tumor present so features not applicable. § indicates tumor seen in H&E section not present in IHC section.

Table 3.4: Correlation of JSRV envelope antibody titers with radiographic disease development, and histologically detected tumor in sheep receiving inoculum with JSRV (04RS1 – 04RS8) and without JSRV (04RS9 – 04RS12).

Sheep	Date of Serum Sample	Antibody Titer	Computed Tomography			Histology
			Nodule Development	Visible Regression Dates	Nodules at Euthanasia	Tumor via H&E
04RS8	Pre-inoculation	<10	No nodules	∅		
	1 month	<10				
04RS9	Pre-inoculation	<10				
	4 months	10				
04RS11	Pre-inoculation	<10	No nodules	∅		
	5 months	100				
04RS12	Pre-inoculation	≤10	No nodules	∅		
	6 months	20				
04RS4	Pre-inoculation	<10	Progression	∅	✓	✓
	5 months	<10				
04RS5	Pre-inoculation	<10	Progression	∅	✓	✓
	5 months	20				
04RS1	Pre-inoculation	<10	Partial regression	2 months, then progression	✓	✓
	4 months	<10				
04RS2	Pre-inoculation	100	Partial regression	4 & 6 months	✓	✓
	3 months	20				
	6 months	100				
04RS6	Pre-inoculation	<10	Partial regression	5 & 6 months	✓	✓
	1 month	<10				
	2 months	20				
	3 months	100				
	4 months	100				
	5 months	100				
	6 months	100				
04RS3	Pre-inoculation	<10	Complete regression	6 months		
	6 months	20				
04RS7	Pre-inoculation	<10	Complete regression	2 months		
	6 months	20				
04RS10	Pre-inoculation	<10	Complete regression	2 months		
	6 months	<10				

JSRV envelope antibody titers were expressed as the reciprocal of the highest dilution of serum that reduced the titer of the LAPSN(PJ4) JSRV retroviral vector by 50%. ∅ indicates not applicable.

Table 3.5: OvLV AGID serology results from sheep receiving inoculum with JSRV (04RS1 – 04RS8) and without JSRV (04RS9 – 04RS12).

<b>Sheep</b>	<b>Pre</b>	<b>Post-JSRV Inoculation</b>			<b>Age at Sacrifice</b>
		<b>2 Weeks</b>	<b>2 Months</b>	<b>At Sacrifice</b>	
04RS1	-	-	+	+	4 months
04RS2	-	-	+	+	6 months
04RS3	-	-	+	+	6 months
04RS4	-	-	+	+	5 months
04RS5	-	-	-	+	5 months
04RS6	-	-	+	+	6 months
04RS7	-	-	+	+	6 months
04RS8	+	+		+	1 month
04RS9	-	-	+	+	4 months
04RS10	-	-	+	+	6 months
04RS11	-	-	+	+	5 months
04RS12	-	-	+	+	6 months

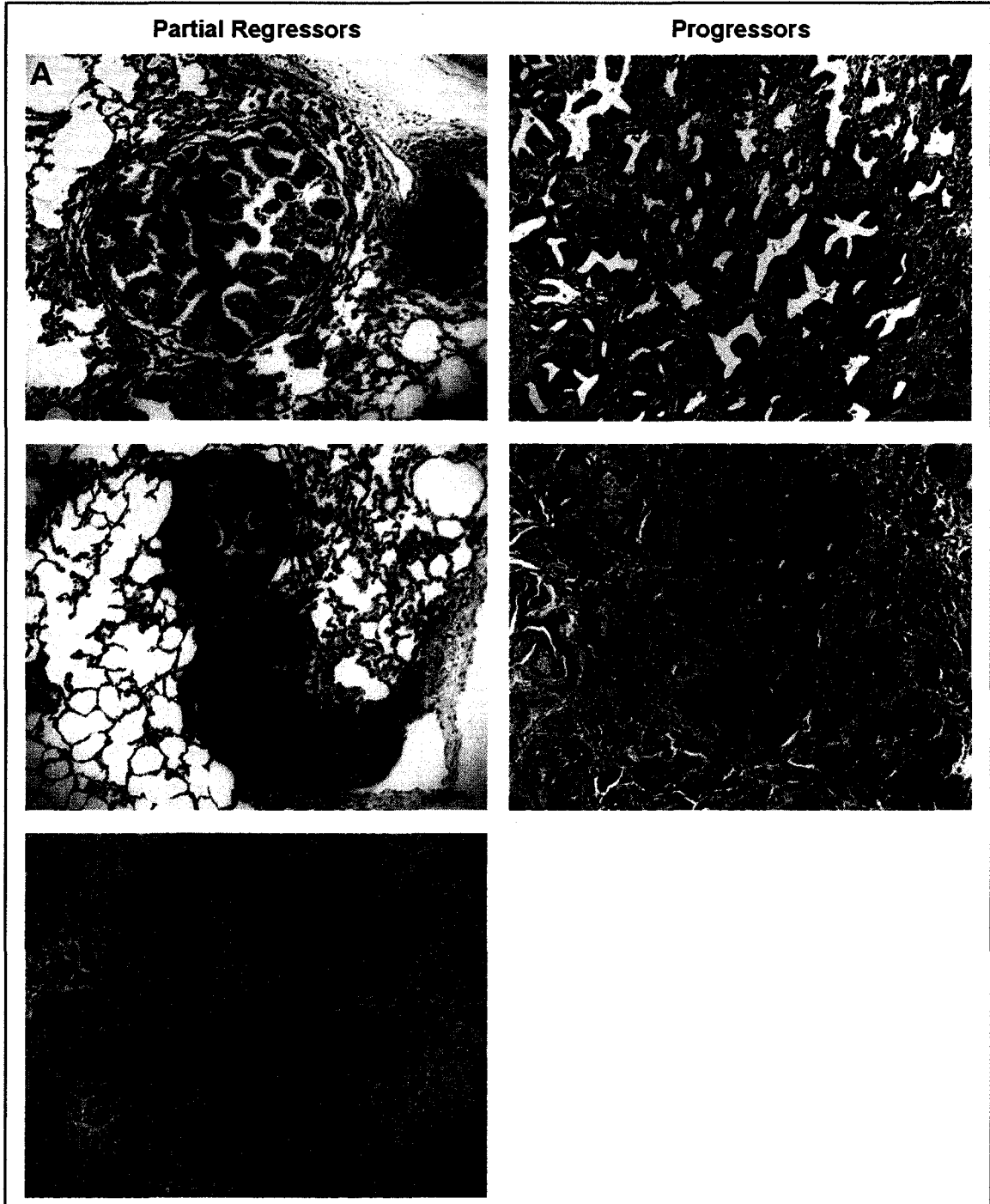


Figure 3.1: Hematoxylin and eosin staining of lung tissue from tumor partial regressors (A = 04RS1, B = 04RS2, C = 04RS6) and tumor progressors (D = 04RS4, E = 04RS5). Slides are viewed at 10X. 100µm scale bars are provided in the bottom right of each microphotograph.

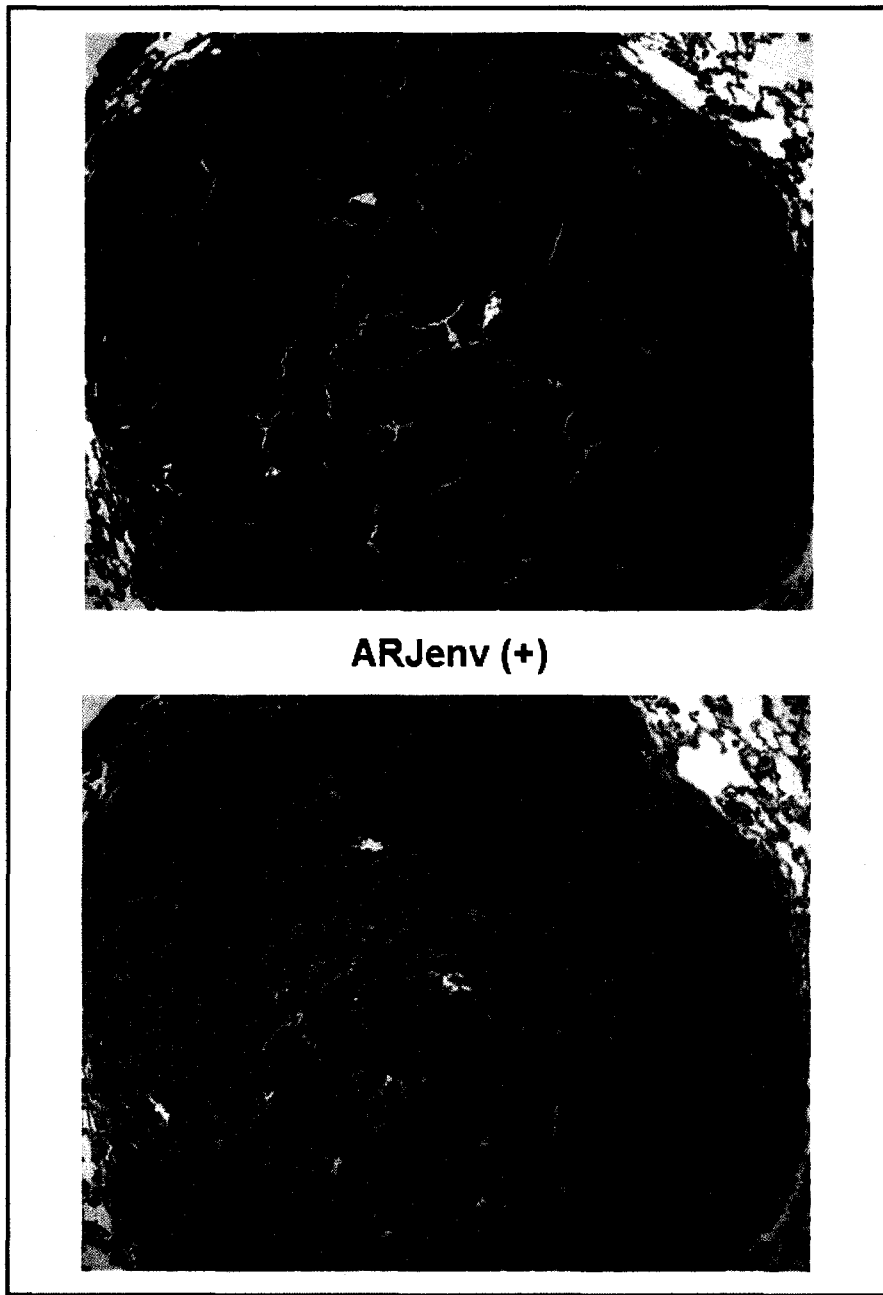


Figure 3.2: (A) Hematoxylin and eosin staining and (B) JSRV envelope (brown stain) immunostaining of ARJenv (+) lung tumor tissue viewed at 10X. 100 $\mu$ m scale bars are provided in the bottom right of each microphotograph.

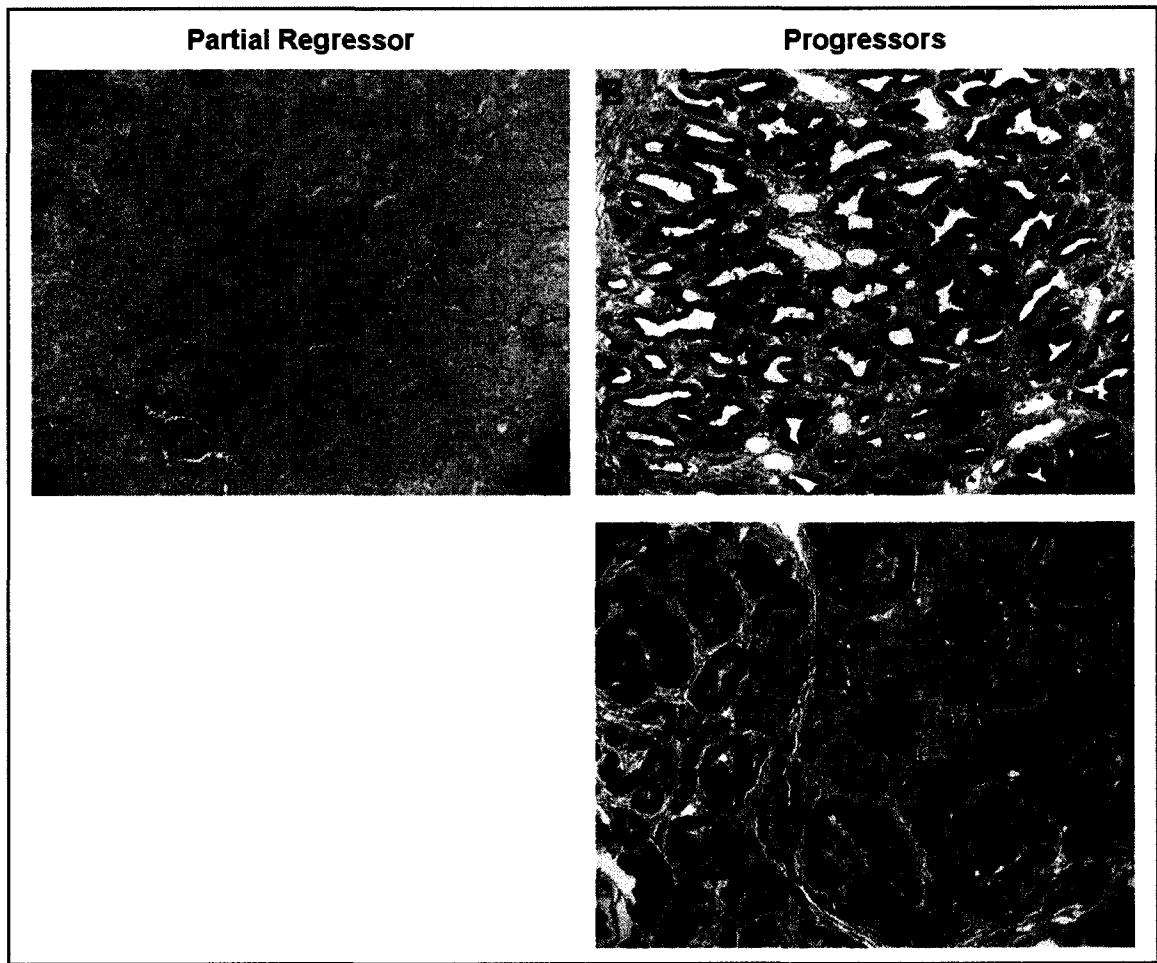


Figure 3.3: JSRV envelope (brown stain) immunostaining of lung tumor tissue from nodular disease partial regressor (A = 04RS6) and nodular disease progressors (B = 04RS4, C = 04RS5). Slides are viewed at 10X. 100µm scale bars are provided in the bottom right of each microphotograph.

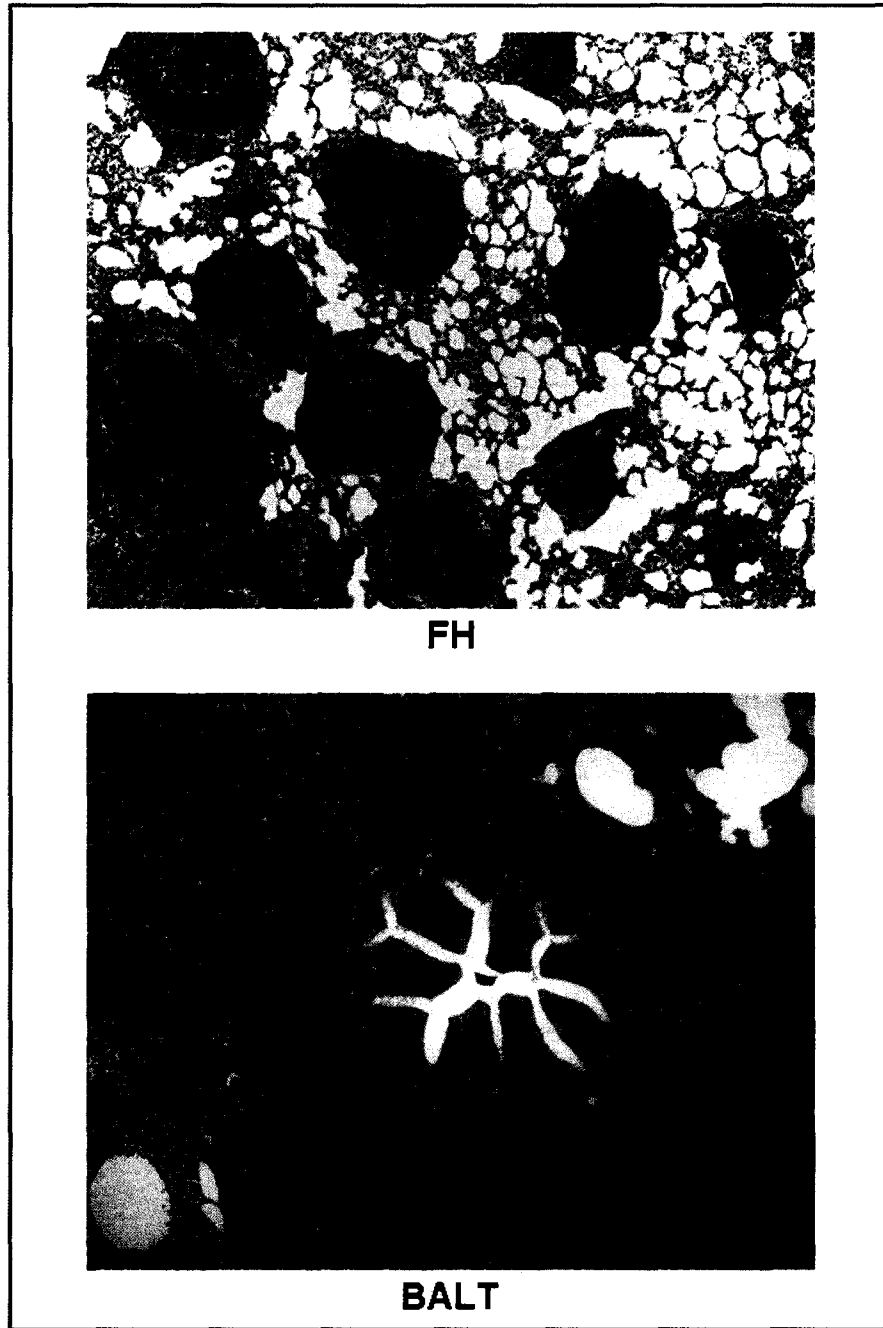


Figure 3.4: Hematoxylin and eosin staining of histological features seen in virus-inoculated sheep lungs. A = follicular hyperplasia (FH) viewed at 4X (04RS6); B = bronchus associated lymphoid tissue (BALT) hyperplasia viewed at 10X (04RS11). 100µm scale bars are provided in the bottom right of each microphotograph.

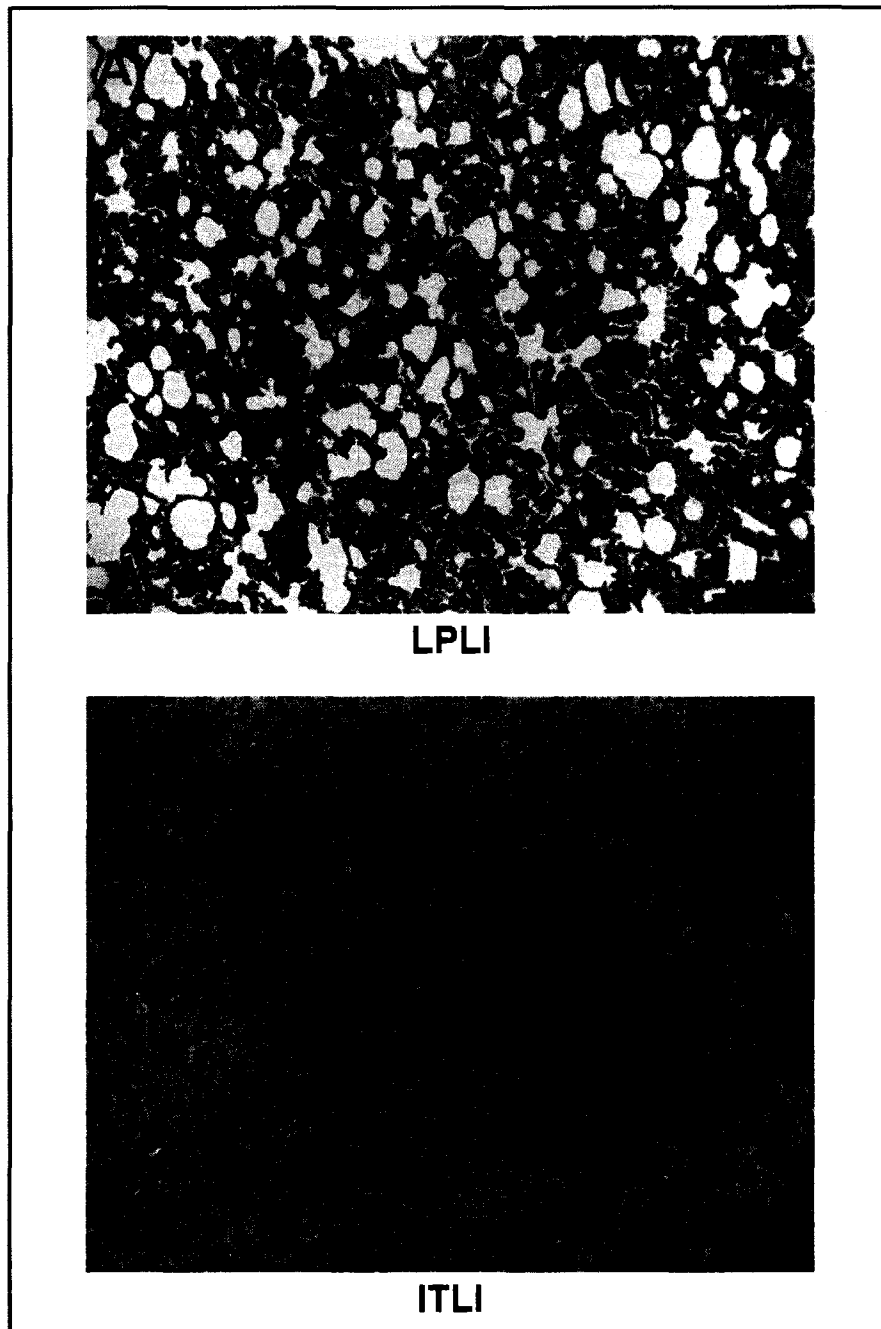


Figure 3.5: Hematoxylin and eosin staining of histological features seen in virus-inoculated sheep lungs. A = lung parenchyma lymphocyte infiltration (LPLI) viewed at 10X (04RS6); B = intratumor lymphocyte infiltration (ITLI) viewed at 10X (04RS6). 100µm scale bars are provided in the bottom right of each microphotograph.

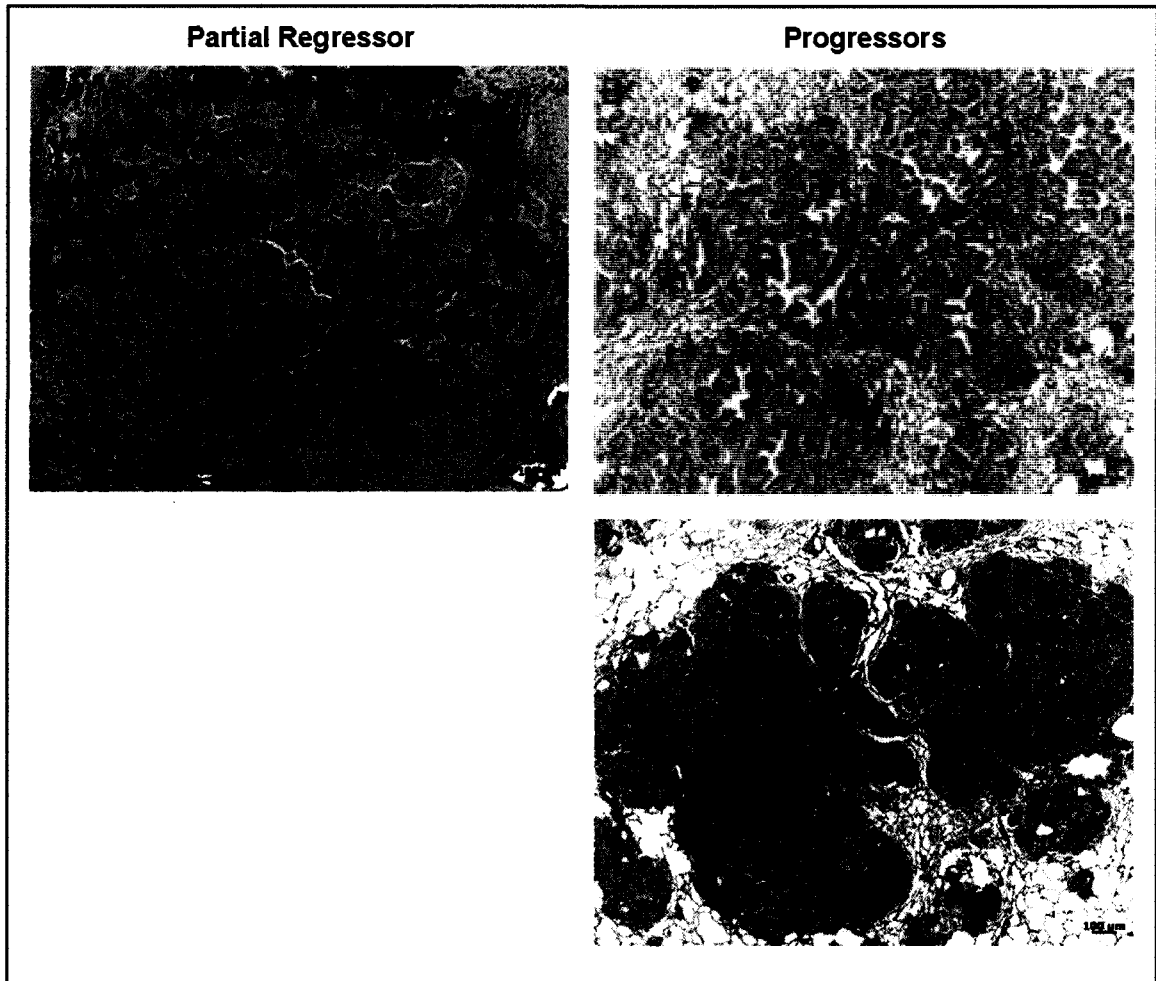


Figure 3.6: CD3 (brown stain) immunostaining of lung tumor tissue from nodular disease partial regressor (A = 04RS6) and nodular disease progressors (B = 04RS4, C = 04RS5). Slides are viewed at 10X. 100µm scale bars are provided in the bottom right of each microphotograph.

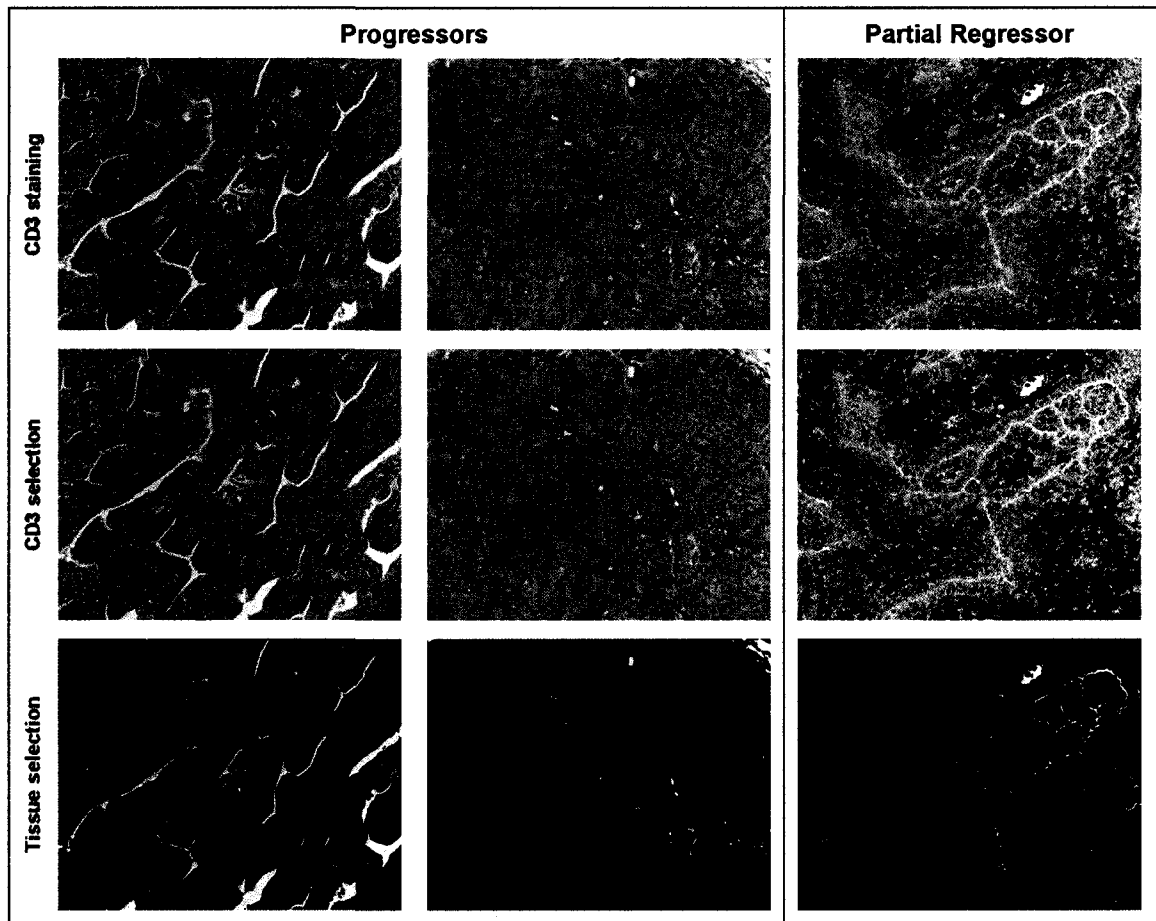


Figure 3.7: CD3 immunostaining of tumor tissue from progressors (A = 04RS4, B = 04RS5) and a partial regressor (C = 04RS6). Top row: CD3-stained cells (brown) and tumor cells (blue). Middle row: digital image analysis of CD3-stained cell selection (red). Bottom row: digital image analysis of tissue selection (blue). Slides are viewed at 20X. 50 $\mu$ m scale bars provided in the bottom right of each micrograph.

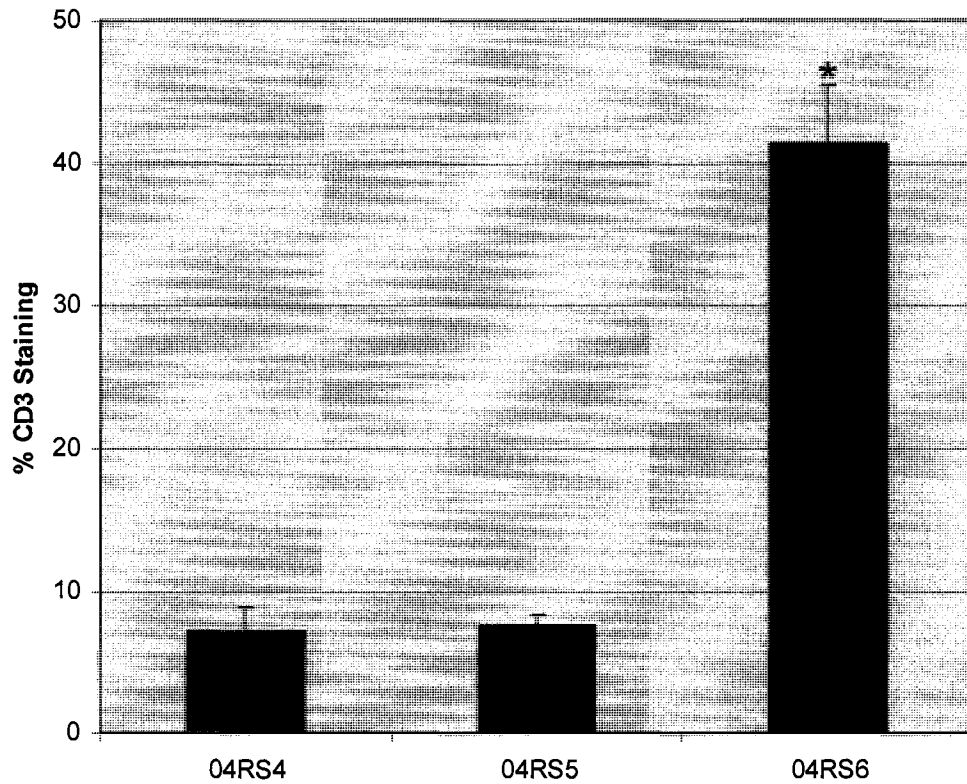


Figure 3.8: Graphical representation of the percent of tissue surface area (blue in bottom row of Figure 3.7) that stained positive for CD3 (pan T cell marker) (red in middle row of Figure 3.7). Sheep 04RS4 and 04RS5 were nodular disease progressors whereas 04RS6 was a nodular disease partial regressor. Columns are the mean of five independent images analyses  $\pm$  standard error. Asterisk (\*) indicates a significant difference ( $P < 0.001$ ) from 04RS4 and 04RS5.

## **CHAPTER IV**

### **GENETIC PROFILING OF OVINE PULMONARY ADENOCARCINOMA**

#### **INTRODUCTION**

OPA shares both symptomatic and histopathologic characteristics with human lung adenocarcinoma (De las Heras et al. 2000; Palmarini and Fan 2001; Fan et al. 2003; Mornex et al. 2003; Sharp and DeMartini 2003). Based on these commonalities as well as possible molecular signaling parallels, including aberrant activation of the PI3K-Akt and Ras-MEK-Erk1/2 pathways, we aimed to determine if OPA harbors mutations similar to those found in human lung adenocarcinomas. Recently, activating mutations in the TK domain (exons 18-21) of the EGFR gene have been found in patients that respond to the TKIs gefitinib and erlotinib (Lynch et al. 2004; Paez et al. 2004). These mutations target functionally important structures of the TK domain that are in close proximity to the ATP-binding cleft of the receptor (Lynch et al. 2004) and consist of three very different types: multinucleotide in-frame deletions that eliminate four

highly conserved amino acids (LREA) encoded by exon 19, duplications/insertions involving a small region in exon 20, and missense mutations in exons 18, 19, and 21, especially a single point mutation, L858R, in exon 21 (Kosaka et al. 2004; Lynch et al. 2004; Paez et al. 2004; Pao et al. 2004; Tokumo et al. 2005). The LREA deletion, exon 20 duplications/insertions, and L858R missense point mutation constitute ~95% of the mutations identified to date (Gazdar et al. 2004).

Another gene aberrantly activated by mutations in 30-50% of lung adenocarcinomas is the RAS family member, KRAS (Rodenhuis et al. 1988). The majority of these mutations occur in codons 12 and 13 in exon 1 (Rodenhuis et al. 1988; Pao et al. 2005) and are predominantly G to T transversions that result in the substitution of a single amino acid at these critical positions in the encoded protein (Barbacid 1987; Rodenhuis and Slebos 1990). These substitutions abolish GAP-induced GTP hydrolysis, leading to constitutive activation of Kras and thus, continuous stimulation of cellular proliferation.

In contrast to EGFR and KRAS, mutations in P53, a tumor suppressor gene, often lead to inactivation. P53 is mutated in many cancers, including approximately 50% of NSCLCs (Takahashi et al. 1989; Hollstein et al. 1991; Bodner et al. 1992; Greenblatt et al. 1994; Brambilla and Brambilla 1997; Mao 2001) and, more specifically, 33% of lung adenocarcinomas (Greenblatt et al. 1994). The majority of these mutations are found in the highly conserved core domain of the gene within exons 5-8 (Hollstein et al. 1991) and result in altered

DNA binding and reduced transactivation of p53-dependent genes (Unger et al. 1992).

To be a valid animal model for human lung adenocarcinoma, OPA should harbor genetic alterations similar to those found in the human disease. Thus, for this work, we obtained lung tissue samples (tumor, if available) from sheep either naturally or experimentally infected with JSRV, isolated the DNA, and sequenced the TK domain (exons 18-21) of the EGFR, exon 1 of KRAS, with particular interest in codons 12 and 13, and the DNA-binding domain (exons 5-8) of P53. In addition to the ovine samples, we analyzed DNA from lung tumor tissue of C57BL/6 mice that developed lesions similar to OPA after being inoculated with a vector encoding the envelope protein of JSRV [ARJenv (+)] (Wootton et al. 2005).

## **MATERIALS AND METHODS**

### *Animal samples*

All ovine tissue samples and C57BL/6 DNA samples were obtained from archival materials collected as part of previous studies (Table 4.1). Tissue was collected at the time of sacrifice, rapidly frozen in liquid nitrogen, and stored at -80°C. If present, tumor tissue was grossly dissected to enrich the tumor cell population. DNA was extracted from ovine lung tissue using a DNeasy Tissue Kit (Qiagen, Cat. No. 69504). DNA samples from C57BL/6 ARJenv (+) lung tumors and C57BL/6 ARAP4 [ARJenv negative (-) control] lung tissue (Wootton et al.

2005) were generously provided by A. Dusty Miller, Fred Hutchinson Cancer Research Center.

*Mutational profiling of EGFR, KRAS, and P53*

The first four exons (exons 18-21) of the TK domain of the EGFR gene, exon 1 of the KRAS gene, and exons 5-8 of the highly conserved core domain of the P53 gene were amplified in a one-step PCR using the MultiBlock PCR System (MBS) (Thermo Electron Corporation). Each 50 $\mu$ L PCR reaction contained 45 $\mu$ L Platinum<sup>®</sup> PCR SuperMix (22U/ml complexed recombinant *Taq* DNA polymerase with Platinum<sup>®</sup> *Taq* Antibody, 22mM Tris-HCl (pH 8.4), 55mM KCl, 1.65mM MgCl<sub>2</sub>, 220 $\mu$ M dGTP, 220 $\mu$ M dATP, 220 $\mu$ M dTTP, 220 $\mu$ M dCTP, and stabilizers) (Invitrogen, Cat. No. 11306-016), 200nM (final concentration) forward primer and 200nM (final concentration) reverse primer (Table 4.1), and 500ng template DNA.

PCR cycling parameters were: one template denaturation/enzyme activation cycle at 94°C for 2 minutes, 35 cycles of denaturation at 94°C for 30 seconds, annealing at respective temperature (Table 4.2) for 30 seconds and extension at 72°C for 60 seconds, followed by one final extension cycle at 72°C for 10 minutes.

The resulting PCR products were purified using a QIAquick 96 PCR Purification Kit (Qiagen, Cat No. 28181). High-throughput (96-well plate) bidirectional dideoxynucleotide sequencing of PCR-amplified gene products was performed at Polymorphic DNA Technologies, Inc (Alameda, CA) using a

BigDye® Terminator v3.1 Cycle Sequencing Kit (Applied Biosystems, Cat. No. 4337454) and an ABI 3730xl DNA Analyzer (Applied Biosystems). Sequence variants were confirmed by an additional, independent PCR amplification and sequencing reaction in both sense and antisense directions. Readable sequences were compared against the following reference sequences (prefix NM), reference assemblies (prefix NC), and expressed sequence tag (prefix EE) listed in the NCBI database:

Homo sapiens EGFR: NM\_005228.3

Mus musculus EGFR: NC\_000077.4 (reference assembly for C57BL/6J)

Homo sapiens KRAS: NM\_004985.3

Ovis aries KRAS: EE767129

Mus musculus KRAS: NC\_000072.4 (reference assembly for C57BL/6J)

Homo sapiens P53: NM\_000546.3

Ovis aries P53: NM\_001009403.1

Mus musculus P53: NC\_000077.4 (reference assembly for C57BL/6J)

\*The first and last 15 nucleotides (5 amino acids) of ovine EGFR exon 20 were unreadable.

\*\*The first 27 nucleotides (9 amino acids) and last 18 nucleotides (6 amino acids) of ovine and C57BL/6 ARJenv (+ and -) KRAS exon 1 were unreadable.

#### *Quantitative real-time polymerase chain reaction (qPCR)*

DNA was extracted from ovine lung tissue using a DNeasy Tissue Kit (Qiagen, Cat. No. 69504).

Integrated exogenous JSRV (exJSRV) copy number was detected using a fluorogenic probe in combination with real-time PCR. Each 25 $\mu$ L PCR reaction contained 12.5 $\mu$ L Platinum<sup>®</sup> Quantitative PCR Supermix-UGD with ROX (60U/ml Platinum<sup>®</sup> *Taq* DNA polymerase, 40mM Tris-HCl (pH 8.4), 6mM MgCl<sub>2</sub>, 400 $\mu$ M dGTP, 400 $\mu$ M dATP, 400 $\mu$ M dCTP, 800 $\mu$ M dUTP, 40U/ml uracil DNA glycosylase (UDG), 1 $\mu$ M ROX Reference Dye, and stabilizers) (Invitrogen, Cat. No. 11743-100), 200nM (final concentration) forward primer, 200nM (final concentration) reverse primer, 100nM (final concentration) fluorogenic probe, and 250ng template DNA.

The following primers, based on GenBank accession number AF105220 and specific for the transmembrane (TM) region of exJSRV, were used for the qPCRs:

exJSRV env (forward) (TA7F-B): 5'-TTGGTGTAGGAATACTTGTGTT-3'

exJSRV env (reverse) (TA8R): 5'-TATTTCTATATTTTCATATGCAGCA-3'

The following probe, based on GenBank accession number AF105220 and specific for the TM region of exJSRV, was used for the qPCRs: 5'-FAM-CTCGTTC GTGGCATGGTTCG-TAMRA-3' (TAProbe-1), where 6-carboxyfluorescein (FAM) serves as the reporter fluorochrome and tetramethyl-6-carboxyrhodamine (TAMRA) serves as the quencher.

PCR cycling parameters were: one UDG incubation cycle at 50°C for 2 minutes, one template denaturation/enzyme activation cycle at 95°C for 2 minutes, 45 cycles of denaturation at 95°C for 15 seconds and annealing at 55°C for 45 seconds (this step was enabled for data collection). Reactions were done

in triplicate. A full length JSRV envelope provirus clone (pBlue-JSRV) was serially diluted and used as a standard. DNA from an ovine skin fibroblast (OSF) cell line, which contains endogenous JSRV (enJSRV) sequences, was used as a viral specificity control and as a negative control for exJSRV.

## RESULTS

### *JSRV DNA*

Viral DNA was detected and quantitated in 32 lung tissue samples from sheep either naturally or experimentally infected with JSRV. Tumor tissue was available from 24 animals; the remaining 8 samples were of lung tissue, as these sheep did not have grossly visible tumor at necropsy. As a negative control, we used lung tissue from seven uninfected sheep. In addition to ovine samples, we analyzed DNA from lung tumor tissue of immunodeficient C57BL/6 mice that developed lesions similar to OPA after being inoculated with a vector encoding the envelope protein of JSRV [ARJenv (+)]; as a negative control, lung tissue DNA from a mouse inoculated with a vector containing only the gene encoding alkaline phosphatase [ARJenv (-)] was used. In the sheep samples, JSRV DNA copy number varied greatly, ranging from approximately 3 copies (04RS3) to over 7050 copies (00RS25) per 250ng of DNA (Figure 4.1). As for OPA, tumor tissue was evident histologically in 26 sheep; no tumor tissue was found in six sheep. Interestingly, in these six sheep, less than 100 copies of JSRV DNA were detected in all but one animal, suggesting a correlation between JSRV copy

number and OPA development. In the mouse samples, we found 601 copies of JSRV DNA in the ARJenv (+) mouse lung tumor tissue and no JSRV DNA in the ARJenv (-) sample.

### *Mutational profiling of EGFR*

The EGFR is a cell-surface receptor that is often aberrantly activated in NSCLC, particularly in adenocarcinomas. In humans, the EGFR protein is composed of 1210 amino acids, coded by a gene comprised of 28 exons. Of these, exons 18-21 code for the TK domain of the protein, a region frequently found to contain activating mutations that confer a selective growth advantage to the affected lung cells. In this study, we sequenced the TK domain of the EGFR gene isolated from lung tumor DNA of JSRV-positive (+) sheep as well as DNA isolated from the JS7 cell line, derived from the tumor of an animal with a natural case of OPA. Additionally, we sequenced the lung tumor tissue of an ARJenv (+) C57BL/6 mouse. As our controls, we used lung tissue from JSRV-negative (-) sheep and an ARJenv (-) mouse. For comparison in our alignments, we included the reference sequence from human (*Homo sapiens*) EGFR and the reference assembly from C57BL/6 mouse (*Mus musculus*) EGFR.

In EGFR exon 18, five of the 30 JSRV (+) sheep had the same two heterozygous single base substitutions (Figure 4.2). One of the sheep harboring these substitutions was a female natural case of OPA while the other four (two males and two females) were experimentally-induced OPA cases. Interestingly, these two substitutions were also found in one of the six female JSRV (-) sheep.

One substitution was a G to A transition at nucleotide position 2325 and the other was a C to T transition at nucleotide position 2355 (Figure 4.3A). Both of these base changes occurred at the third position of the resultant codons, changing ACG to ACA and CTC to CTT, respectively. However, due to the redundancy of the genetic code, the consequent amino acid was not altered in either case; at amino acid position 693, both ACG and ACA code for threonine and, at amino acid position 703, both CTC and CTT code for lysine (Figure 4.4).

In exon 19 of the EGFR, two female experimentally-induced OPA cases out of a total of 31 JSRV (+) sheep had the same three heterozygous single base substitutions (Figure 4.5). The first substitution was a C to T transition at nucleotide position 2451, the second was a G to A transition at nucleotide position 2499, and the third was a C to A transversion at nucleotide position 2505 (Figure 4.3B). All of these base changes occurred at the third position of the resultant codons, changing GGC to GGT, ACG to ACA, and CCC to CCA, respectively. However, similar to the EGFR exon 18 substitutions, the codons were synonymous; both GGC and GGT code for glycine at amino acid position 735, both ACG and ACA code for threonine at amino acid position 751, and both CCC and CCA code for proline at amino acid position 753 (Figure 4.4).

The EGFR exon 20 sequence analyses excluded the first and last 15 nucleotides of the exon, as this data was unreadable. Yet, the sequencing results of the internal 156 nucleotides revealed an identical solitary heterozygous single base substitution present in one of 32 JSRV (+) sheep and one of five JSRV (-) sheep (Figure 4.6). The JSRV (+) sheep was a male with experimentally-induced

OPA whereas the JSRV (-) sheep was a female. The substitution was a C to T transition at nucleotide position 2673, which falls in the third position of a codon (Figure 4.3C). As seen before, a synonymous codon was the outcome; at amino acid position 807, both ACT and ATT code for an aspartic acid (Figure 4.4).

In EGFR exon 21, three of 32 JSRV (+) sheep and one of six JSRV (-) sheep had the same heterozygous single base substitution (Figure 4.7). Of the JSRV (+) sheep, one was an experimentally-infected male, one was an experimentally-infected female, and one was a female natural case of OPA. The substitution was a C to T transition at nucleotide position 2727 (Figure 4.3D). This corresponds to the third position of a codon, changing TAC to TAT. As with the previously-mentioned EGFR substitutions, both codons code for the same amino acid; in this case, a tyrosine at amino acid position 827 (Figure 4.4).

Regarding the mouse samples and the EGFR TK domain exons, we found no nucleotide disparities between ARJenv (+) and ARJenv (-) DNA nor between these sequences and the C57BL/6 reference sequence.

Thus, in this study, we found a total of seven different heterozygous single base substitutions in the TK domain of the EGFR (Table 4.3). However, these substitutions were not exclusive to JSRV (+) sheep, as four of the seven were also seen in JSRV (-) sheep. Curiously, none of the three substitutions seen in exon 19 were observed in JSRV (-) sheep. Of the seven total JSRV (+) sheep with EGFR substitutions, four had substitutions in more than one exon; two JSRV (+) sheep (04RS6 and 04RS8) had substitutions in exons 18 and 19, and two JSRV (+) sheep (86RS50 and 98RS3) had substitutions in exons 18 and 21. Of

the two JSRV (-) sheep with EGFR substitutions, one (05RS2) had substitutions in two exons (18 and 21). Overall, the relevance of the substitutions found in exons 18-21 of the EGFR is unclear, as all seven were silent substitutions and did not have an effect on the amino acid sequence of the EGFR protein; additionally, most substitutions were present in both JSRV-infected and uninfected sheep.

### *Mutational profiling of KRAS*

KRAS is an important regulator of cell proliferation, differentiation, motility, and apoptosis that is often found to be mutated in human cancers, including lung adenocarcinomas. This member of the small guanosine triphosphatase (GTPase) superfamily is comprised of 188 amino acids, translated from four coding exons. Of the mutations found in KRAS, the vast majority are in codons 12 and 13. For this work, we sequenced the interior of KRAS exon one isolated from lung tumor DNA of JSRV (+) sheep and ARJenv (+) C57BL/6 mice, lung tissue DNA of JSRV (-) sheep and ARJenv (-) C57BL/6 mice, and JS7 cell line DNA; in particular, we focused on the sequence of codons 12 and 13. For comparison in our alignments, we included the reference sequence from human (*Homo sapiens*) KRAS, the reference assembly from C57BL/6 mouse (*Mus musculus*) KRAS, and the expressed sequence tag from sheep (*Ovis aries*) KRAS.

The first 27 and last 18 nucleotides of KRAS exon one are excluded from the subsequent analyses, as these sequences were unreadable. For nucleotides

28 through 93, we found no variants in any of the samples; specifically, codons 12 and 13 were not found to be mutated in the lung tumors of JSRV (+) sheep and ARJenv (+) mice (Figure 4.8). Accordingly, there was no change in the amino acid translation (Figure 4.9).

### *Mutational profiling of P53*

P53 is a DNA-binding protein that plays an essential role in cell cycle regulation, functioning as a tumor suppressor. In many human cancers, the P53 gene is plagued by inactivating mutations, causing the loss of tumor suppressor activity and consequent promotion of carcinogenesis. These mutations are commonly found in the DNA binding domain, encoded by exons 5-8. Thus, in this study, we sequenced these P53 exons isolated from lung tumor DNA of JSRV (+) sheep and ARJenv (+) C57BL/6 mice, lung tissue DNA of JSRV (-) sheep and ARJenv (-) C57BL/6 mice, and JS7 cell line DNA. For comparison in our alignments, we included the reference sequences from human (*Homo sapiens*) and sheep (*Ovis aries*) P53, and the reference assembly for C57BL/6 mouse (*Mus musculus*) P53.

In all four exons sequenced, we found no nucleotide alterations, and thus no amino acid differences, between JSRV (+) and JSRV (-) sheep nor between ARJenv (+) and ARJenv (-) C57BL/6 mice (Figures 4.10 - 4.14). Thus, P53 DNA-binding domain mutations do not appear to be essential for JSRV-induced OPA.

## CONCLUSIONS

In this chapter, we analyzed lung tissue DNA (tumor tissue, if available) from sheep infected with JSRV for alterations in three genes commonly mutated in human lung adenocarcinomas. In the TK domain of the EGFR (exons 18-21), we found seven different heterozygous single base substitutions. However, all were silent substitutions and did not alter the amino acid sequence of the EGFR protein. Furthermore, most of these substitutions were not exclusive to JSRV-infected sheep and were found in uninfected sheep as well. As for the other two genes, we observed no alterations in exon one (codons 12 and 13, in particular) of the KRAS gene or in the DNA-binding domain (exons 5-8) of the P53 tumor suppressor gene. Additionally, we also sequenced these genes in DNA isolated from the lung tumor tissue of mice inoculated with a vector encoding the envelope protein of JSRV [ARJenv(+)]; no nucleotide variants were observed. Thus, JSRV-induced OPA in sheep and JSRV envelope-induced lung adenocarcinomas in mice do not harbor genetic mutations similar to those commonly found in human lung adenocarcinomas.

Table 4.1: Characteristics of sheep infected with JSRV and analyzed for mutations.

<b>Sheep</b>	<b>Sex</b>	<b>JSRV Source</b>	<b>Age at Sacrifice</b>
84RS16	Female	Lung homogenate	7 months
84RS17	?	Lung fluid	7 months
85RS1	Female	Lung fluid	7 months
85RS2	Female	Lung fluid	6 months
85RS6	Male	Lung homogenate	7 months
85RS7	Male	Lung homogenate	1 month
85RS8	Male	Lung homogenate	5 months
85RS11	Male	Lung homogenate	4 months
85RS13	Male	Lung fluid	5 months
85RS14	Male	Lung homogenate	2 months
85RS19	Male	Lung homogenate	7 months
85RS21	Male	Lung fluid	3 months
85RS22	Male	Lung fluid	3 months
85RS50	Male	Lung homogenate	7 months
86RS44	Female	Lung homogenate	4 months
86RS50	Male	Lung homogenate	6 months
87RS1	Male	Lung homogenate	3 months
91RS13	Male	Lung homogenate	2 months
98RS3	Female	Natural case	Adult
00RS25	Male	Lung homogenate	7 months
00RS28	Female	Lung homogenate	6 months
04RS1	Female	Lung homogenate	4 months
04RS2	Female	Lung homogenate	6 months
04RS3	Female	Lung homogenate	6 months
04RS4	Female	Lung homogenate	5 months
04RS5	Female	Lung homogenate	5 months
04RS6	Female	Lung homogenate	6 months
04RS7	Female	Lung homogenate	6 months
04RS8	Female	Lung homogenate	1 month
04RS9	Female	Lung homogenate	4 months
04RS10	Female	Lung homogenate	6 months
04RS11	Female	Lung homogenate	5 months

Table 4.2: Primer sets and annealing temperatures used for amplification in polymerase chain reactions.

Gene	Exon	Animal	Oligonucleotides		Annealing Temperature (°C)
			F: Forward	R: Reverse	
EGFR	18	Sheep	F: 5'-TCTCACCAGTTCCTAGAACAGG-3'	R: 5'-TCCCTCCAGGAAATCATCTGTGC-3'	57.5
		Mouse	F: 5'-CCACTGCTCCTTTGAACAC-3'	R: 5'-CACTGGTCCAGAAAGCCTA-3'	55
	19	Sheep	F: 5'-CTCTGATTCCTGGGACACAACAG-3'	R: 5'-TGCCAACCCACGAGAAAAGGTAG-3'	57.5
		Mouse	F: 5'-AATCCAGCTACAAGGCAAC-3'	R: 5'-CATGAACTAAGGAAGCAAGATTGA-3'	55
	20	Sheep	F: 5'-CCTACGTGATGCCAGTGT-3'	R: 5'-GCGATCTGCACACACCAGT-3'	57.5
		Mouse	F: 5'-TTGTGATTCATCTATTGTCCTTACCT-3'	R: 5'-CAGTGGACAGACCTCCCAAC-3'	55
21	Sheep	F: 5'-GTCCAAGTCACCTGTGCTGTGGAG-3'	R: 5'-CCTCACCTAGAAGGTCTCTGAGATG-3'	57.5	
Mouse	F: 5'-AGATGGTTCACCTCCCTCACG-3'	R: 5'-TTTGGCCTCTGAACAGGTCT-3'	55		
KRAS	1	Sheep & Mouse	F: 5'-GCCTGCTGAAAATGACTGA-3'	R: 5'-GGATCATATTCATCCACAAAGTG-3'	53
	5	Sheep	F: 5'-AGAAGACCTACCCTGGCAACTACG-3'	R: 5'-GCACCCACACACTGTGCTAAAGG-3'	59.5
P53	6	Sheep	F: 5'-AGCACATGACGGAGTTGTGAG-3'	R: 5'-GCAGGAGCTGTACACATGAAGTTG-3'	59.5
	5 & 6	Mouse	F: 5'-TGGTGTGGACAATGTGTT-3'	R: 5'-TAGCACTCAGGAGGGTGAGG-3'	55
		7	Sheep	F: 5'-CGGAACACCTTTAGACACAGTGTGG-3'	R: 5'-AACACGCACCTCAAAGCTGCTC-3'
	8	Sheep	F: 5'-CATCCTCACCATCATCACACTGG-3'	R: 5'-GTGGTTCTCTTTTGGCTGTGGAG-3'	57.5
	7 & 8	Mouse	F: 5'-TGCCGAACAGGTGGAATATC-3'	R: 5'-GTGACTTTGGGGTGAAGCTC-3'	55

Table 4.3: Summary of heterozygous single base substitutions found in ovine EGFR nucleotide sequences.

Exon	Single Base Substitution	Codon Position	Amino Acid Position	Amino Acid Result	Prevalence Total Sheep	Prevalence JSRV (+) Sheep	Affected JSRV (+) Sheep	Prevalence JSRV (-) Sheep	Affected JSRV (-) Sheep
18	G2325A	3	693	T to T	16.7 % (6/36)	16.7% (5/30)	85RS19, 86RS50,	16.7% (1/6)	05RS2
18	C2355T	3	703	L to L	16.7 % (6/36)	16.7% (5/30)	98RS3, 04RS6, 04RS8	16.7% (1/6)	
19	C2451T	3	735	G to G	5.7% (2/35)	6.5% (2/31)		0% (0/4)	
19	G2499A	3	751	T to T	5.7% (2/35)	6.5% (2/31)	04RS6, 04RS8	0% (0/4)	
19	C2505A	3	753	P to P	5.7% (2/35)	6.5% (2/31)		0% (0/4)	
20	C2672T	3	807	D to D	5.4% (2/37)	3.1% (1/32)	91RS13	20% (1/5)	05RS5
21	C2727T	3	827	Y to Y	10.5% (4/38)	9.4% (3/32)	86RS50, 98RS3, 04RS7	16.7% (1/6)	04RS2

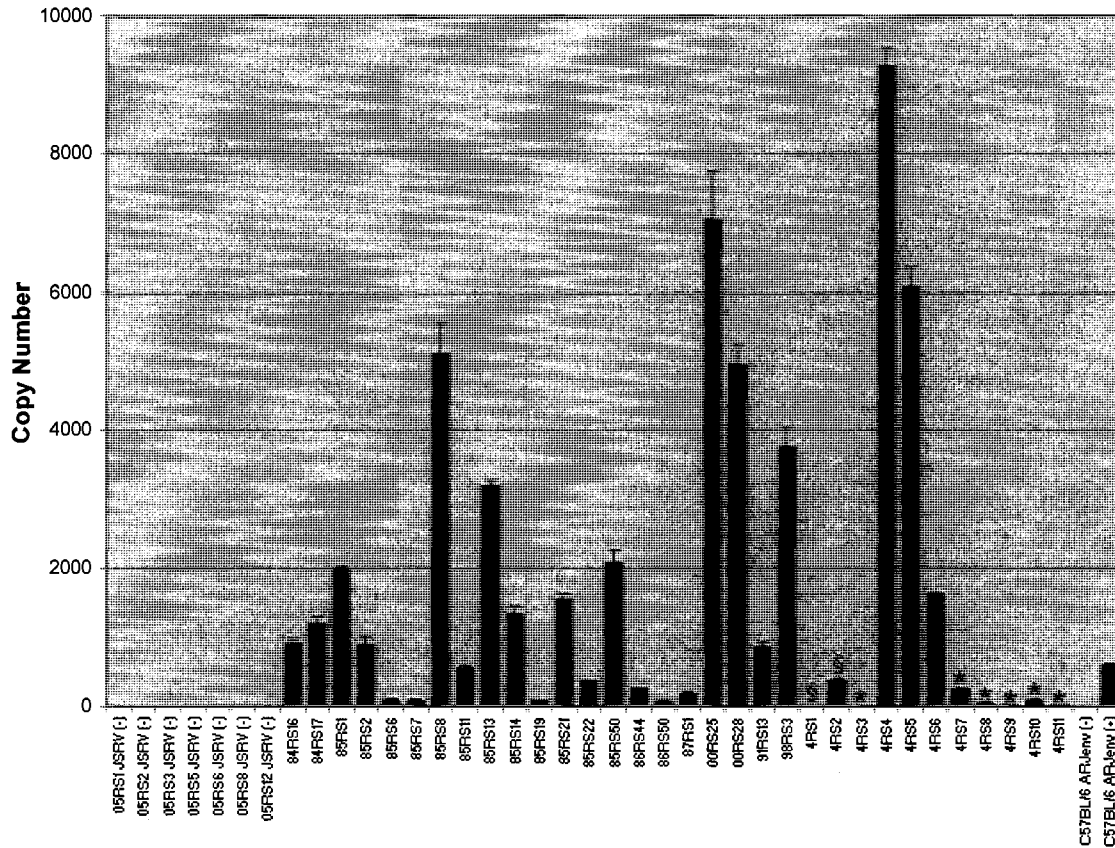


Figure 4.1: JSRV copy numbers per 250ng DNA isolated from sheep and mouse (C57BL/6 ARJenv) lung tissue. Seven sheep (05RS1 – 05RS12) were not infected with JSRV. Thirty-two sheep (84RS16 – 04RS11) were infected with JSRV. Lung tumor tissue was available and used for analyses from 24 of these sheep. The remaining 8 sheep did not have grossly visible tumor at necropsy; thus, lung tissue was used for analysis. Of these sheep, tumor tissue was evident histologically in 2 (§) and was not evident histologically in 6 (\*). JSRV copy numbers are the mean of three replicates  $\pm$  standard error.



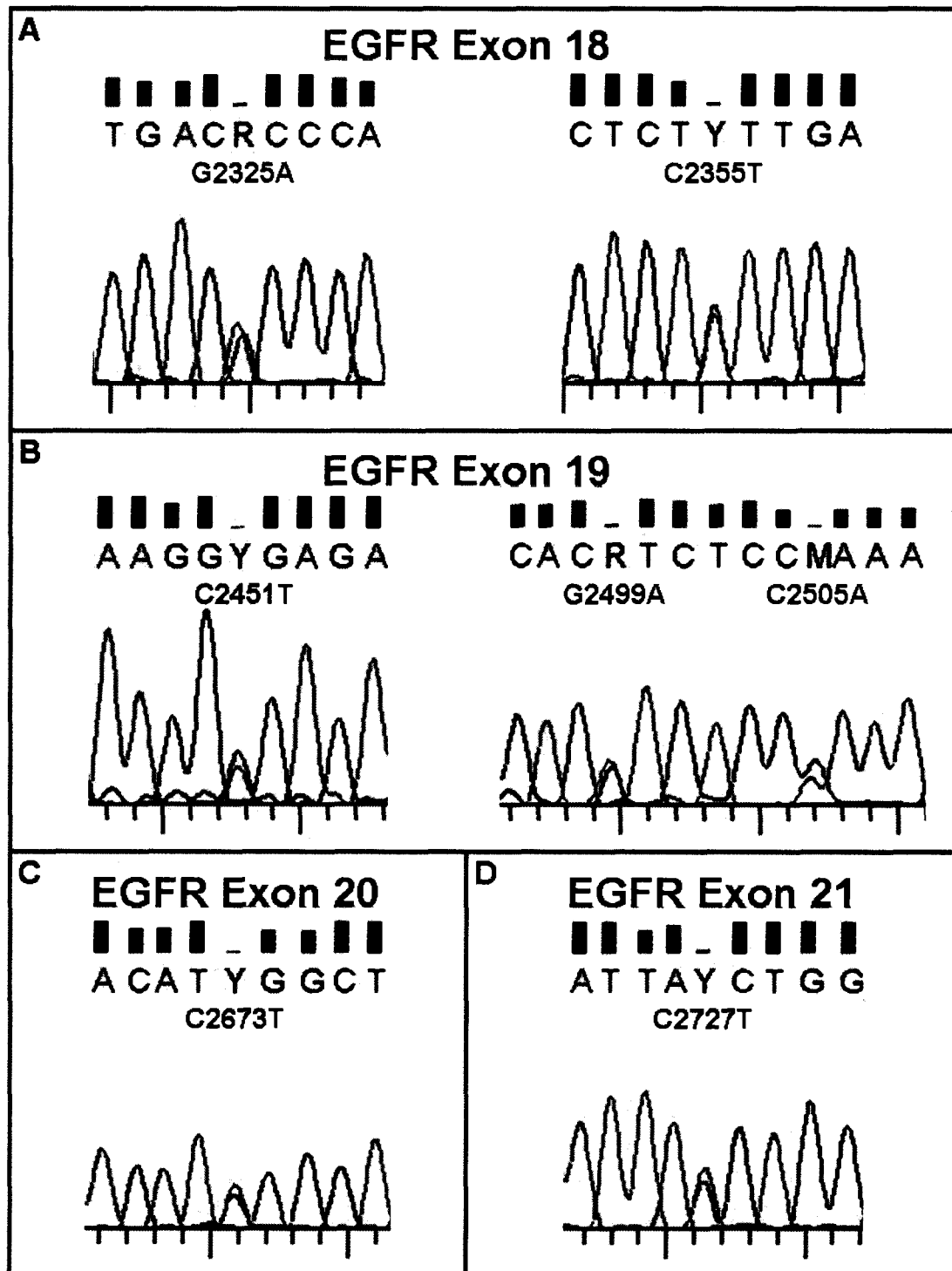


Figure 4.3: Representative chromatograms of heterozygous single base substitutions in ovine EGFR. Yellow highlighting indicates the base substitution.

## EGFR Exons 18-21 Translated

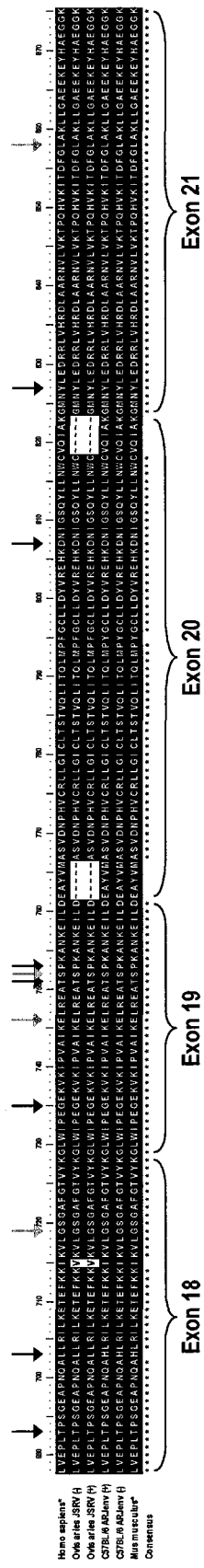


Figure 4.4: EGFR exons 18-21 alignment of amino acid sequences from JSRV (+) and JSRV (-) sheep, ARJenv (+) and ARJenv (-) C57BL/6 mice, and reference sequences from *Homo sapiens*\*, and *Mus musculus*\* C57BL/6. Black arrows indicate the positions at which synonymous substitutions were found in the ovine DNA. Gray arrows indicate the positions of common activating mutations (G719S, Del 746-752, L858R) in human DNA. The first and last 15 nucleotides (5 amino acids) of exon 20 were unreadable and are indicated by (~).













## P53 Exon 6

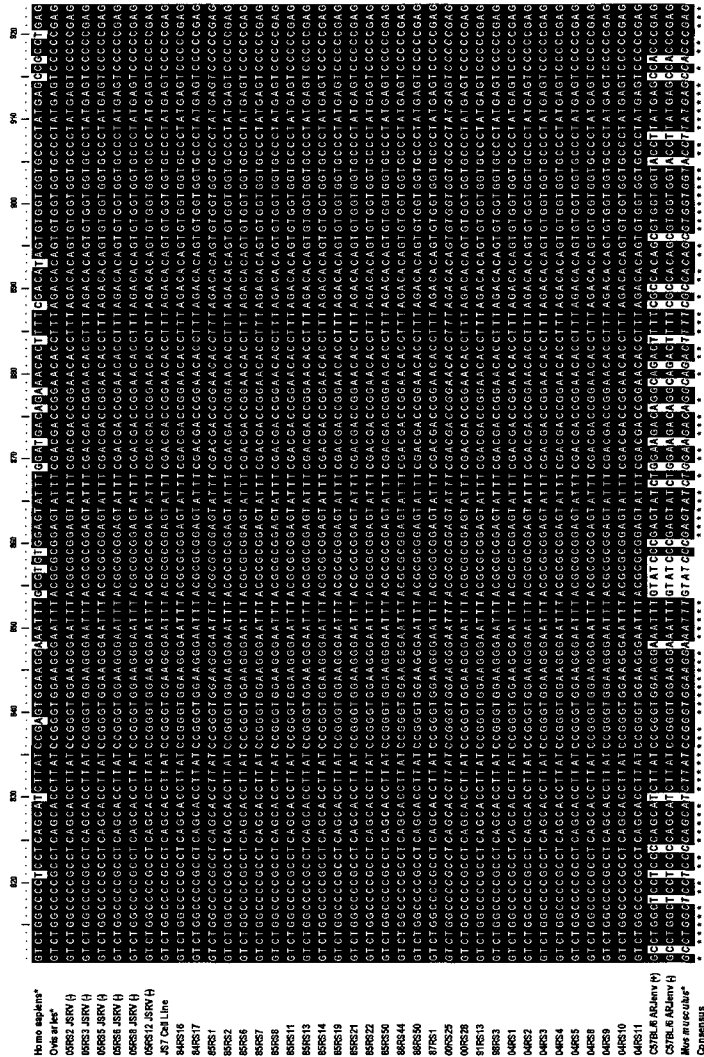


Figure 4.11: P53 exon 6 alignment of nucleotide sequences from 30 JSRV (+) (84RS16 – 04RS11) and 6 JSRV (-) (05RS2 – 05RS12) sheep, the JS7 cell line, ARJenv (+) and ARJenv (-) C57BL/6 mice, reference sequences from *Homo sapiens*\* and *Ovis aries*\*, and a reference assembly for *Mus musculus*\* C57BL/6. No sequence variants were found.



# P53 Exon 8

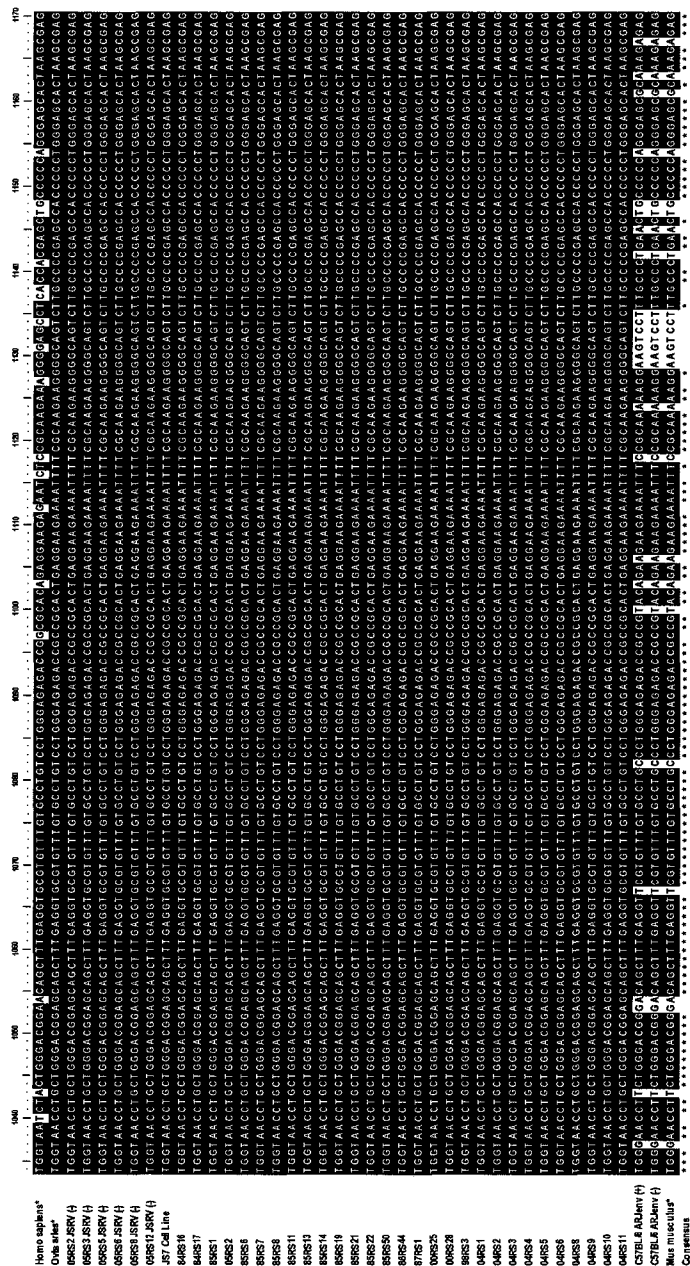


Figure 4.13: P53 exon 8 alignment of nucleotide sequences from 29 JSRV (+) (84RS16 – 04RS11) and 6 JSRV (-) (05RS2 – 05RS12) sheep, the JS7 cell line, ARJenv (+) and ARJenv (-) C57BL/6 mice, reference sequences from *Homo sapiens*\* and *Ovis aries*\*, and a reference assembly for *Mus musculus*\* C57BL/6. No sequence variants were found.

## P53 Exons 5-8 Translated

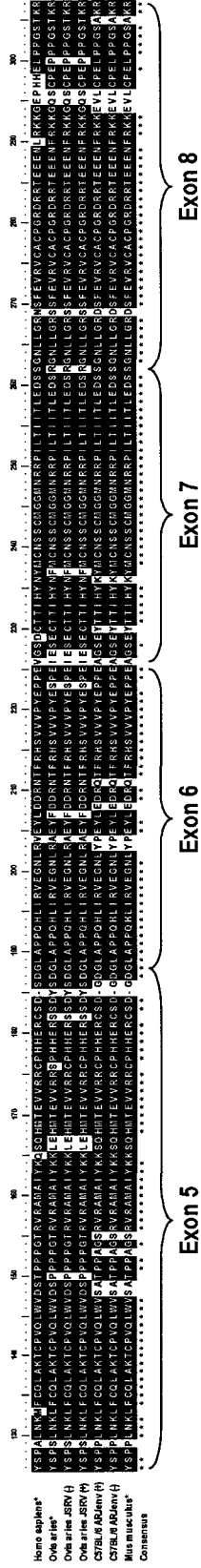
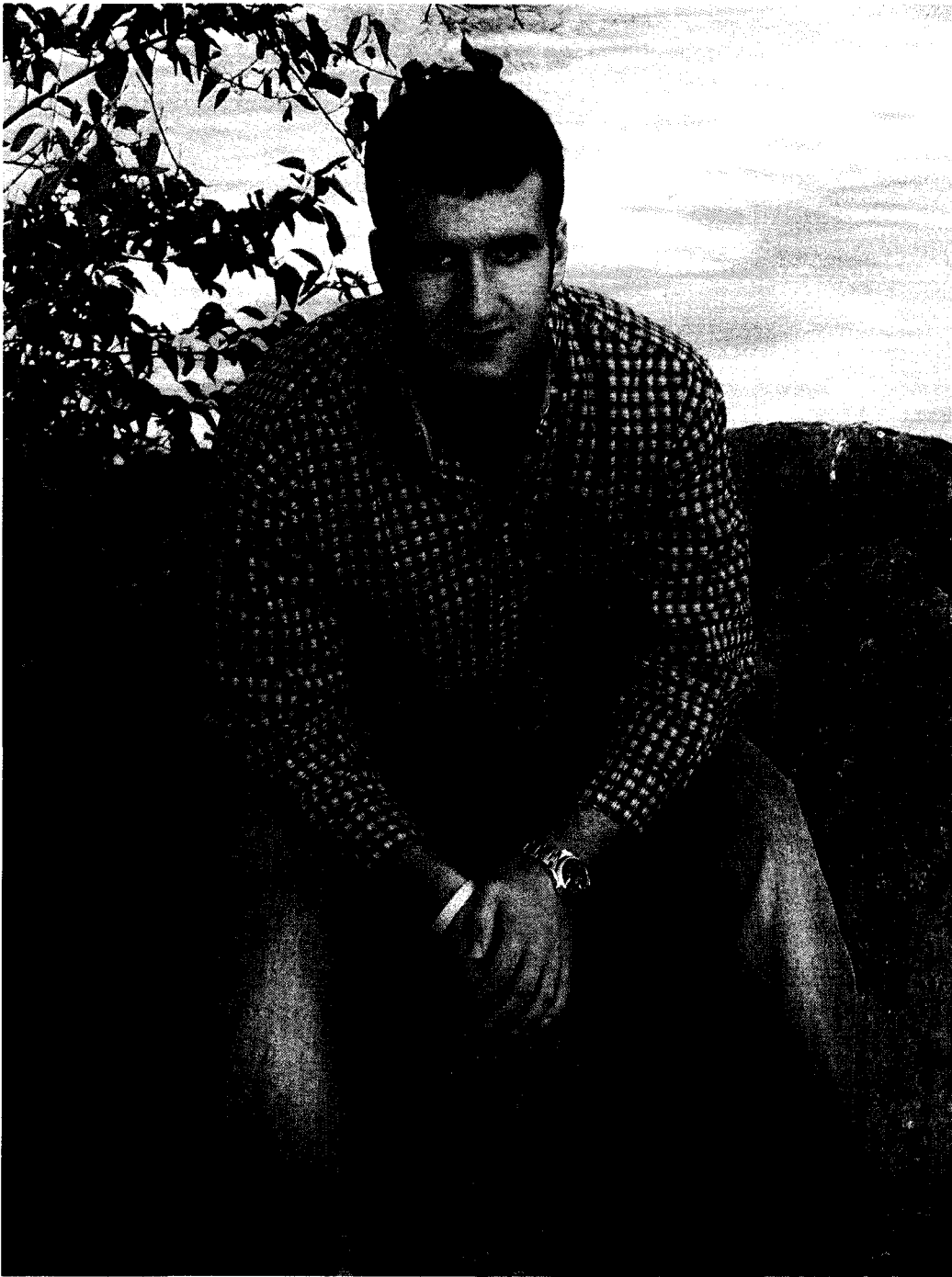


Figure 14.4: P53 exons 5-8 alignment of amino acid sequences from JSRV (+) and JSRV (-) sheep, ARJenv (+) and ARJenv (-) C57BL/6 mice, reference sequences from *Homo sapiens*\* and *Ovis aries*\*, and a reference assembly for *Mus musculus*\* C57BL/6. No sequence variants were found.



## CHAPTER V

### DISCUSSION

Lung cancer remains the leading cause of cancer-related deaths among men and women worldwide. Despite the optimization of treatment techniques over recent decades, the outcome for advanced disease has not changed significantly and remains bleak. Accordingly, the need to develop better, more effective therapies is urgent. To accomplish this, we need to enhance our understanding of the mechanisms involved in lung carcinogenesis. While cell culture studies certainly aid in this pursuit, the complex nature of tumor progression, invasion, and metastasis as well as response to therapy cannot be fully mimicked *in vitro*. Thus, *in vivo* work, capitalizing on animal models as complete, dynamic systems, offers the best potential for insight into cancer development and treatment.

Currently, rodents are widely used for experimental lung cancer research. However, major limitations of these murine models include dissimilarities in terms of lung anatomy and physiology as well as problems of scale inherent with all

small animal models. As an alternative, our work proposed that sheep affected by OPA are a relevant animal model for the study of human lung carcinogenesis and, in particular, for the evaluation of lung cancer therapeutics. Symptomatic and histopathologic similarities between OPA and human lung adenocarcinoma have been previously reported (De las Heras et al. 2000; Palmarini and Fan 2001; Fan et al. 2003; Mornex et al. 2003; Sharp and DeMartini 2003). Additionally, there may be molecular signaling parallels, including aberrant activation of the PI3K-Akt and Ras-MEK-Erk1/2 pathways, between these two lung cancers. Further value of this model is dependent upon its predictability, reproducibility, amenability, and validity. The former two features have been previously reported; OPA induction in sheep is both predictable and reproducible following JSRV inoculation of neonatal lambs (Sharp et al. 1983; DeMartini et al. 1987; Sharp and DeMartini 2003; Salvatori et al. 2004). The overall objective of this body of work was to assess the amenability of this animal model for therapeutic research and to assess the validity of OPA-affected sheep as an animal model for human lung adenocarcinoma in terms of genetic similarities.

To be amenable for therapeutic research, we must be able to detect OPA early, before the cancer reaches an advanced stage and treatment strategies would likely be futile. In addition to early detection, we must also be able to monitor the development of OPA. To be amenable for therapeutic research, we must be able to follow disease development in order to assess therapeutic response after the hypothetical administration of treatment.

For OPA induction, we inoculated three groups (n = 4) of neonatal lambs with virus isolated from the lung tumor homogenate of three sheep with confirmed OPA (Table 2.1). All three inocula had RT activity, indicating infectious retrovirus in the preparations (Figure 2.1). However, JSRV DNA was only detected in the inocula prepared from 98RS3 and 91RS13 (Figure 2.2 and Table 2.4). Conversely, all three inocula tested positive for OvLV, the etiological agent of OPP and, an alternative source of RT. Thus, the RT activity in the inocula prepared from 98RS3 and 91RS13 was attributable to both JSRV and OvLV, and the proportion contributed by either retrovirus could not be differentiated. On the other hand, all of the RT activity in the inoculum from 99RS27 was ascribed to OvLV, as no JSRV DNA was detected in this preparation. Regarding this inoculum, it is possible that the JSRV was inactivated when this preparation was incubated with OvLV antiserum in an attempt to neutralize the OvLV. Overall, lambs receiving inoculum prepared from 98RS3 and 91RS13 were administered JSRV and OvLV whereas lambs receiving inoculum from 99RS27 were administered only OvLV. Thus it is likely that, in addition to JSRV-induced OPA, our sheep had virus-induced pneumonia, possibly in response to JSRV and almost certainly in response to OvLV.

The coexistence of OPA and OPP is a common occurrence. Descriptive evidence of simultaneous infection can be found in the earliest reports of OPA in South Africa (Cowdry and Marsh 1927) and Iceland (Sigurdsson 1958) (Rosadio et al. 1988). Additionally, careful examination of other reports suggests that these diseases have coexisted both naturally and experimentally throughout the world,

including the United States (Cutlip and Young 1982) and Canada (Cutlip et al. 1992) (Rosadio et al. 1988). In one study, these two retroviruses were coadministered to neonatal lambs; animals were euthanized 8-28 weeks after inoculation and all 9 developed multifocal neoplasms characteristic of OPA and lymphoid interstitial pneumonia characteristic of OPP (DeMartini et al. 1987). Consequently, in our study, the disease present in the lungs of inoculated sheep was the manifestation of JSRV-induced OPA and JSRV or OvLV-induced pneumonia.

To investigate OPA development following JSRV inoculation, we used CT as a noninvasive imaging modality to detect disease earlier and more precisely than is possible with clinical observations and to follow the development of neoplastic lesions over time. Although there are no reports describing the radiographic appearance of OPA, the gross lesions are well documented; neoplastic areas are localized at the periphery of the lungs and tend to be multifocal, varying from small discrete nodules (1 – 30mm) to extensive tumors involving entire lung lobes (De las Heras et al. 2003; Leroux et al. 2007). Histopathologically, OPA originates from differentiated alveolar type II cells and non-ciliated bronchiolar epithelial (Clara) cells (Nisbet et al. 1971; Perk et al. 1971; Sharp 1987; Platt et al. 2002). In human lung cancer, transformation of these cell types is indicative of nonmucinous BAC (Travis et al. 2006) and, classically, OPA has been compared with this subtype of adenocarcinoma (Palmarini and Fan 2001). However, in the 1999 WHO classification of lung tumors, the BAC criteria underwent a major change, requiring that all BACs

demonstrate pure lepidic (bronchioloalveolar) growth without invasion of the stroma, blood vessels, or pleura (Travis et al. 1999). Accordingly, OPA is now classified as a mixed-subtype adenocarcinoma, as these ovine tumors have both bronchioloalveolar and invasive (acinar and papillary) growth patterns (Mornex et al. 2003). Regarding human adenocarcinomas, these neoplasms are typically heterogenous and contain more than one subtype in over 80% of cases (Terasaki et al. 2003; Beasley et al. 2005). As for pure BAC, this subtype only accounts for approximately 4% of human lung cancers (Read et al. 2004). However, the strict definition of BAC is prognostically important and derives from a seminal study showing that small (< 2cm) peripheral lung adenocarcinomas with a pure BAC pattern have a 100% 5-year survival rate whereas adenocarcinomas with mixed BAC and invasive components have a survival rate of 75% and those with purely invasive growth patterns have a survival rate of 52% (Noguchi et al. 1995).

Radiographically, human mixed-subtype adenocarcinomas with a BAC component have several gross pathologic and radiographic presentations: a solitary peripheral nodule (43%), multiple nodules (27%), and regional consolidation (30%) (Hill 1984; Travis et al. 2005; Garfield et al. 2006). Multiple nodules can be unilateral or bilateral and may appear as a dominant nodule with satellites within the same lobe or multicentric nodules involving one or more lobes (Travis et al. 2005). The regional consolidation appears as a DLP that is grossly and radiographically difficult to distinguish from pneumonia (Travis et al. 2005; Garfield et al. 2006). In the literature, evidence suggests that there is a

continuum between a solitary nodule, multiple nodules, and DLP consolidation (Hill 1984; Trigaux et al. 1996).

During our CT observations, nodules were seen in eight of twelve sheep (Table 2.5). In terms of presentation, a solitary nodule was detected in only two sheep and this occurred early in the study; the other six sheep presented with multiple nodules at some point during the study (Table 2.8). As with the human disease, nodules were random and found most frequently in the periphery of the lungs (Table 2.8). The number of nodules visualized on CT varied and was often greater than 30 (Table 2.8). In both human and sheep adenocarcinomas presenting with multiple nodules, it is unclear if this manifestation is due to intrapulmonary metastasis or a multiclonal origin (Bonomo et al. 1998; Palmarini and Fan 2001). In our sheep, nodule size also varied considerably, ranging from 1mm to 13mm (Table 2.8). In humans, lung nodule size is a good indicator of prognosis; if a nodule measures more than 2cm, it has a greater likelihood of being malignant, compared with a 50% rate of malignancy in all nodules less than 2cm (Shure and Fedullo 1983; Mohammed et al. 2005).

In our study, nodule attenuation was also noted and ranged from pure GGO to mixed (GGO/solid) to solid, with mixed attenuation nodules being the most common (Table 2.8). In humans, adenocarcinomas that consist mostly of a BAC component typically show GGO attenuation on CT and an ill-defined gross appearance whereas solid attenuation on CT and a circumscribed gross appearance is characteristic of purely invasive adenocarcinomas (Travis et al. 2006). Regarding mixed-subtype adenocarcinomas with both BAC and invasive

components, a mixture of these CT and gross pathologic features is seen (Travis et al. 2006). As the majority of nodules visualized in our study showed mixed attenuation, it would follow that these were indicative of mixed-subtype adenocarcinomas. However, a definitive prognosis of very small (subcentimeter) lung cancers in relation to CT attenuation remains difficult (Asamura et al. 2003; Yoon et al. 2005) and, based on CT alone, it is not possible to determine if nodules are benign or malignant. Thus, when an intrathoracic nodule is encountered on CT, a myriad of diagnoses should be considered, including neoplastic, infectious, and inflammatory lesions (Mohammed et al. 2005). Regarding the latter two, in a study assessing the HRCT appearance of different types of pneumonia, nodules were seen in 78% of patients with viral pneumonias; all nodules were centrilobar and no random nodules were detected (Reittner et al. 2003). Also, in humans, interstitial pneumonias caused by viruses are associated with a reticulonodular pattern (Fraser and Fraser 1994; Reittner et al. 2003). In our study, nodules were random as opposed to centrilobar and a reticulonodular pattern was not evident, again suggesting that the nodules were OPA and not pneumonic. Additionally, histopathological evaluation revealed that the five sheep with nodules evident on CT at euthanasia did indeed have tumor characteristic of OPA (Table 3.1 and Figure 3.1), providing further evidence for the assumption that the nodules visualized on CT during this study are manifestations of OPA. Moreover, these five animals were from the groups receiving the JSRV-positive/OvLV-positive inocula (98RS3 and 91RS13); no sheep receiving the JSRV-negative/OvLV-positive inoculum (99RS27) had

radiographically detectable nodules or histopathologically discernable tumor at euthanasia.

In addition to nodules, we also noticed a DLP in the lungs of our sheep during this study (Table 2.5 and Table 2.9). Actually, a DLP was seen more frequently than nodular disease and was observed in all twelve sheep on the majority of post inoculation CT scans. As with nodular disease, the appearance of the DLP varied, ranging from mild diffuse GGO to severe solid consolidation (Table 2.9). As mentioned previously, it is difficult to distinguish the DLP form of adenocarcinoma from pneumonia on CT (Travis et al. 2005; Garfield et al. 2006). Early DLP, occurring within two weeks of inoculation, probably represented an inflammatory reaction (pneumonia) to the inoculum.

In a study comparing the CT patterns of diffuse BAC with pneumonia, consolidation and coexisting areas of GGO were characteristic of both (Aquino et al. 1998). However, a peripheral distribution of consolidation and associated nodules in the same lobe or in other areas of the lung were significantly more common in patients with BAC (Aquino et al. 1998). In our sheep inoculated with JSRV and showing a DLP with a mixed and/or solid attenuation, the consolidation was typically seen in the lung periphery and, nodules were often found concurrently, both within the DLP and/or independent of the DLP (Table 2.9 and Table 2.10). In the sheep presumably inoculated with only OvLV, mixed and/or solid attenuation DLP was also found in the periphery but, in all four sheep, nodules were never found concurrently. Accordingly, in our study, the implication of the mixed and or/solid DLP observed in tandem with nodules could

be adenocarcinoma whereas the mixed and or/solid DLP observed without associated nodules is most likely pneumonia, although a definitive diagnosis cannot be made based on CT alone.

Certain other findings on CT help to identify pulmonary consolidation as a BAC-containing tumor, including the CT angiogram sign (Im et al. 1990; Murayama et al. 1993), cystic air spaces (Ohba et al. 1972; Zwirewich et al. 1990; Adler et al. 1992; Weisbrod et al. 1995), and air bronchograms (Wong et al. 1994; Akata et al. 1995) (Trigaux et al. 1996; Aquino et al. 1998). All of these features were observed within the DLPs seen in our JSRV-inoculated sheep (Figure 2.12), again signifying the likely presence of adenocarcinoma rather than pneumonia. However, air bronchograms were also prevalent in the DLPs of the sheep inoculated with only OvLV, again making an explicit diagnosis of the mixed and/or solid DLPs as either adenocarcinoma or pneumonia impossible.

In the same study cited previously that assessed the HRCT appearance of different types of pneumonia, areas of GGO were a common finding in viral pneumonias (Reittner et al. 2003). The presence of this DLP implies that the disease is causing infiltration of the lung, without completely obliterating the air spaces; more specifically, in most DLPs, GGO is due to inflammatory infiltration involving the alveolar septa and/or the alveolar lumen (Lynch 2000). In our study, all twelve sheep were seropositive for OvLV antibodies (Table 3.5) and showed a DLP with a GGO component at euthanasia (Table 2.5 and Table 2.9). In eleven of these animals, histopathology revealed significant FH (Table 3.1 and Figure 3.4A), lung parenchyma lymphocyte infiltration (Table 3.1 and Figure 3.5A),

primarily within the alveolar septa, and hypertrophy of the BALT (Figure 3.4B), all of which are hallmarks of OPP (DeMartini et al. 1993). This implicates viral pneumonia in response to OvLV as the cause of the DLP-associated GGO detected in our study.

Regarding OPP specifically, the radiographic presentation of this disease has been detailed using HRCT; in this study, five newborn lambs were experimentally infected with OvLV and were HRCT scanned and then euthanized at three months post inoculation (Cadore et al. 1997). The HRCT scans showed abnormal features in infected animals, including increased parenchymal density, alveolar edema, thickened interlobular septa, and increased density in peribronchiolar areas. No nodules were seen in these experimentally-infected lambs at three months post inoculation on HRCT. On anatomic-pathological examination of post-mortem lung tissue specimens, peribronchovascular lymphoid nodules were present in three sheep and present but minor in two sheep, and intraparenchymatous lymphoid nodules were present but minor in only one sheep. This suggests that the lymphoid nodule development due to OPP is not visible on HRCT at this early stage of disease development and, thus, lends support to the notion that the nodules seen in our study were OPA. As for the DLP, the reported increased parenchymal density is similar to the GGO DLP seen in our study, suggesting that this disease presentation is the manifestation of OvLV-induced pneumonia.

In sheep experimentally-infected with OvLV, there is evidence of an acute phase of infection during the first weeks or months post inoculation (Blacklaws et

al. 1995; Thormar 2005). In our sheep, a GGO DLP appeared at two weeks post inoculation and progressed by one month post inoculation; the development of this DLP could be the result of an early inflammatory response to components of the inoculum. Subsequently, this DLP regressed, possibly indicative of a reduced inflammatory response, as the number of OvLV-infected cells has been shown to decrease after the development of a specific immune response (Blacklaws et al. 1995). However, this early response does not eliminate the virus (Thormar 2005), and thus, the ultimate progression of the DLP seen in our sheep could be the result of the slowly-progressing secondary inflammatory reaction that is typical of OPP.

In summary, we were able to monitor pulmonary disease development after inoculation with JSRV using CT. Diffuse lung disease and discrete nodules were detectable as early as two weeks post inoculation. At this time point, no clinical signs of OPA were evident. In fact, other than mild audible breathing, our animals did not develop any symptoms characteristic of OPA during the study. Even at euthanasia, the sheep with the most advanced lung lesions did not “pass” the wheelbarrow test, a common field assessment for OPA. Thus, our results clearly demonstrate that CT is a suitable imaging modality for visualizing OPA disease development and can detect pulmonary abnormalities before the onset of clinical signs. However, a definitive diagnosis using CT alone cannot be made and, in this study, the interpretation of the radiographic images was confounded by the presence of another virus in the inoculum and, thus, another disease manifestation. The CT appearance in conjunction with histopathological

evidence at euthanasia suggests that the nodules seen radiographically were indicative of OPA and the GGO DLPs were indicative of OPP; as for the mixed and/or solid attenuation DLPs, a distinction between JSRV-induced adenocarcinoma and OvLV-induced OPP cannot be made and, in the JSRV-positive/OvLV positive inoculation groups, it is likely that both diseases contributed to the mixed and/or solid DLPs.

Surprisingly, not all sheep with radiographically visible nodules during the course of the study had progressive disease. In fact, only two of eight animals exhibited progressive nodular disease; the CT scans from the other six sheep showed nodules that apparently regressed over time, either partially (n = 3) or completely (n = 3) (Table 2.5). Nodular disease development was not associated with the inocula and, hence, different virus strains: one progressor, two partial regressors, and one complete regressor received inoculum prepared from 98RS3; one progressor, one partial regressor, and one complete regressor received inoculum prepared from 91RS13; and, one complete regressor, presumably exposed to JSRV by contact with infected lambs, received inoculum prepared from 99RS27. However, as for features seen on CT, we found a correlation between nodular disease development and presentation (Table 2.8); the more extensive the disease, in terms of multiple nodules versus a solitary nodule and bilateral versus unilateral lung involvement, the more likely it was that the nodular disease progressed as opposed to regressed. On the other hand, nodule number, size, and attenuation were not found to be good predictors of nodular disease progression or regression (Table 2.8). Also, we noticed no

obvious connection between a DLP and nodule presence or development (Table 2.10).

In addition to presentation, nodular disease development was found to be associated with JSRV DNA copy number in the lung tissue (tumor tissue, if available) at euthanasia; sheep with the most JSRV DNA had progressive disease while sheep with the least amount of JSRV DNA had complete regression of visible nodules (Table 2.7). However, in the sheep with progressive disease, we were able to obtain and analyze lung tumor tissue at euthanasia whereas, for the complete regressors, no tumor tissue was available so non-tumor lung tissue was used for the JSRV DNA analysis. Also, regarding the partial regressors, only one had grossly visible tumor at euthanasia so, for the other two, lung tissue was used for analysis. In total, for JSRV DNA quantitation, we analyzed tumor tissue from three animals and lung tissue with no grossly apparent tumor from the other nine. We found that the tumor tissue had considerably more JSRV DNA than the lung tissue. Also, the tumor tissue from the two progressors had appreciably more JSRV DNA than the tumor tissue from the partial regressor (04RS6). These results are not surprising in light of the immunohistochemical staining results, showing that the JSRV envelope is only present in tumor tissue; no staining was seen in non-neoplastic lung tissue (Table 3.3). Additionally, the JSRV envelope staining was more intense in the progressors than in the partial regressor (Figure 3.3). Thus, the nodular progressors had more extensive nodular disease and more JSRV DNA than the regressors. This suggests that the quantity of JSRV is directly proportional to the

pathogenesis of this virus and, consequently, the progression of OPA. In further support of this notion, the level of JSRV envelope staining was correlated with tumor size in ARJenv (+) mice, again signifying that more JSRV results in faster tumor growth (Wootton et al. 2005).

Regarding the histological appearance of OPA, two of the partial regressors showed one or a few very tiny (< 500µm) neoplasms while the other partial regressor as well as the two progressors showed coalescing tumor masses (Table 3.1 and Figure 3.1). Within the lesions, there were no differences in mitotic figures or apoptotic cells between progressors and regressors. These features are consistent with the histopathological appearance of OPA reported in the literature (De las Heras et al. 2003). Additionally, for comparison, we also looked at these features in archival sections from 22 JSRV-infected sheep with confirmed OPA and no documented regression; observations were similar to those found in our tumor-bearing sheep. Therefore, there was nothing histologically unique about the tumor cells in our sheep that correlated with nodular disease progression or regression.

In addition to tumor, other striking features seen in the H&E-stained sections include FH (Figure 3.4A), hypertrophy of the BALT (Figure 3.4B), and alveolar septae thickening due to collagen deposition, occasional neutrophils, and infiltration of mononuclear leukocytes, including mature plasma cells, macrophages, and lymphocytes. These features have been previously reported in the lung parenchyma of JSRV-infected sheep (Payne and Verwoerd 1984; Rosadio et al. 1988; De Las Heras et al. 1995; Garcia-Goti et al. 2000; De las

Heras et al. 2003); however, it is clear that such mononuclear cell influxes are predominantly due to concurrent infections, such as OvLV (Cutlip and Young 1982; Demartini et al. 1988; Verwoerd 1990). Further evidence for this comes from a recent study in which lambs were experimentally infected with only JSRV; as for a local immune response to OPA, no influx of dendritic cells, B-cells or T-cells was found in the neoplastic nodules or in their periphery. Thus, it is probable that the lymphoid proliferation and infiltration seen in the lung parenchyma of our sheep is a result of OvLV infection.

In addition to lung parenchyma lymphocyte infiltration, we also saw intratumor lymphocyte infiltration (Table 3.1 and Figure 3.5B). One partial regressor with neoplasms <500µm only showed minimal lymphocyte infiltration; however, the two progressors exhibited marked lymphocyte infiltration and the other two partial regressors exhibited severe lymphocyte infiltration. Thus, infiltration of lymphocytes within the neoplasms was not specific to a nodular disease development group. Additionally, this feature was also noted in the archival sections from the JSRV-infected sheep with confirmed OPA and no documented regression (Table 3.2), indicating that intratumor lymphocyte infiltration was not unique to the animals in our study.

To further characterize the intratumor lymphocyte infiltration in the three sheep with coalescing tumor masses, we did immunohistochemical staining for CD3, a pan T-cell marker (Table 3.3). The partial regressor had more intratumor CD3<sup>+</sup> T-cells than both progressors and, when quantitated, the difference was

significant (Figures 3.6 – 3.8), suggesting a possible role for CD3<sup>+</sup> T-cells in the spontaneous regression of lung cancer seen in our study.

Spontaneous regression of cancer is a rare phenomenon, with an estimated incidence of less than 1 in 60,000 to 100,000 cases (Cole 1981). In a review of the literature from 1900 to 1964, only 176 cases of spontaneous regression were reported (Everson and Cole 1966), with more than half of the cases belonging to four cancer types: renal cell cancer, neuroblastoma, malignant melanoma, and choriocarcinoma (Cole 1976). Despite its global high incidence, only one case involved lung cancer (Everson and Cole 1966). In a later review of the literature, only 15 cases of spontaneous regression of lung cancer were reported (Kappauf et al. 1997).

The process of spontaneous regression of cancer remains unclear. Mechanisms proposed include tumor inhibition by growth factors and/or cytokines, induction of differentiation, hormonal mediation, elimination of a carcinogen, tumor necrosis, angiogenesis inhibition, psychological factors, apoptosis, epigenetic events, and immune mediation (Papac 1998). Stimulation of the host immune response is often implicated (Cole 1981). In animal models of cancer, there is substantial evidence showing that spontaneous and carcinogen-induced tumors arise more frequently in immunodeficient mice (Zitvogel et al. 2006). In humans, the increased risk of tumor development in immunosuppressed patients, regression following reduction of immunosuppressive agents, instances of spontaneous tumor regression, and the association of tumor-infiltrating lymphocytes with improved prognosis all point

towards a role for the immune system in suppressing tumor growth (Swann and Smyth 2007).

In human cancer cases, tumor-infiltrating lymphocytes have been shown to inhibit tumor growth and are associated with improved prognoses in melanoma (Clemente et al. 1996), breast cancers (Marrogi et al. 1997), colorectal cancers (Jass 1986; Baier et al. 1998; Naito et al. 1998; Diederichsen et al. 2003), esophageal cancers (Schumacher et al. 2001), and ovarian cancers (Zhang et al. 2003; Sato et al. 2005). In a recent study, the density of T-cells infiltrating colorectal tumors was a better predictor of survival than traditional staging based on tumor size and spread; patients with high densities of CD3<sup>+</sup> T-cells within the tumor region (in the center of the tumor and in the invasive margin) had a 5-year survival rate of 73% compared with a 5-year survival rate of 30% for patients with low densities of CD3<sup>+</sup> T-cells (Galon et al. 2006). Additionally, in primary lung cancers, intratumoral infiltration by CD3<sup>+</sup> T-cells has been associated with a better patient outcome (Johnson et al. 2000).

In further support of the role of the T-cell in an anti-tumor immune response, several studies in animals can be cited (Boon et al. 1994). First, specific immune memory against tumor challenge can be conferred to syngeneic animals by adoptive transfer of splenic T lymphocytes of immunized animals (Rouse et al. 1972). Also, tumor rejection can be prevented and tumor growth favored by inactivation of T-cells (Rouse et al. 1972). Further, tumors can also be eradicated by adoptive transfer of T lymphocytes (Greenberg et al. 1988). Lastly,

tumor variants that have escaped rejection *in vivo* have proven resistant to relevant anti-tumor cytotoxic T lymphocytes (CTLs) (Uyttenhove et al. 1983).

CTLs are the effector cells of the immune system that lyse tumor cells and virus-infected cells in a major histocompatibility complex (MHC)-restricted fashion (Baxevanis and Papamichail 1994). Mechanisms by which CTLs destroy their targets include direct killing involving Fas/Fas ligand and perforin/granzyme mediated apoptosis and indirect killing involving cytokine production and helper functions for other effector cells (Berke 1991; Baxevanis and Papamichail 1994).

Activation of T lymphocytes is a key event for an efficient response of the immune system. For proliferation and differentiation into activated, cytolytic cells, stimulation of naïve T-cells is required and involves the T-cell receptor, costimulatory molecules, and antigen (Favero and Lafont 1998). Numerous antigens could act as stimulants to the immune system and thus cause regression of cancer, including trauma, infection, and tumor cells themselves (Cole 1981). A large array of immunogenic human tumor antigens has been identified, including differentiation antigens, mutational antigens, overexpressed/amplified antigens, and viral antigens (Boon and van der Bruggen 1996; Old and Chen 1998; Rosenberg 1999; Dunn et al. 2004). In syngeneic hosts, neoplasms induced by viruses, including polyoma virus (Sjogren et al. 1961) and Simian virus 40 (SV40) (Khera et al. 1963), have been shown to bear antigens that cause tumor rejection (Boon et al. 1994). Also, specific transplantation immunity was elicited by mouse tumors induced with retroviruses

(Klein and Klein 1964). Generally, CTLs recognize viral antigens (Boon et al. 1994), as opposed to tumor antigens.

Thus, the spontaneous regression of JSRV-induced OPA observed in our sheep could be the result of the tumoricidal activity of CTLs in response to cell surface-expressed JSRV or tumor antigens. In our study, the notion of tumor rejection mediated by T-cells is supported by the significantly greater number of intratumor CD3<sup>+</sup> cells in the partial regressor than in the progressors. However, CD3<sup>+</sup> cells were also present within the tumor of the progressors and intratumor lymphocyte infiltration was additionally seen in the archival sections from the JSRV-infected sheep with confirmed OPA and no documented regression. The progressive cancer seen in these animals could have resulted from an evasion of the host's immune response by the tumor cells, possibly by immunoselection (that is, selection of non-immunogenic tumor cell variants) or by immunosubversion (that is, active suppression of the immune response) (Dunn et al. 2004; Zitvogel et al. 2006). There are numerous examples suggesting that tumor cells can escape CTL-mediated control by either down-regulating the accessory molecules required for T-cell stimulation (Azuma et al. 1992; Baskar et al. 1993) or blocking the intracellular processing of tumor-specific antigens (Restifo et al. 1993; Khanna et al. 1994; Rowe et al. 1995). The Epstein-Barr virus (EBV)-associated tumor Burkitt's lymphoma (BL) is a classic example of a human tumor that evades CTL surveillance; this resistance has been attributed to the cell phenotype-related down-regulation of viral antigens, adhesion molecules, and certain class I

alleles (Rickinson et al. 1992; Khanna et al. 1996). Overall, the relationship between CD3<sup>+</sup> T-cells and tumor regression seen in our study could be a direct reflection of the host's ability to respond to JSRV and/or OPA antigens by a CTL-mediated mechanism. Conversely, it has been postulated that the lymphocyte influxes observed in the lungs of OPA-affected sheep are due to concurrent infections and not JSRV or tumor antigens. Further evidence supporting this notion comes from a recent study in which lambs were experimentally infected with only JSRV; as for a local immune response to OPA, no influx of dendritic cells, B-cells or T-cells was found in the neoplastic nodules or in their periphery (Summers et al. 2005). Thus, it is also possible that the host does not elicit an immune response against JSRV or OPA and the lymphocyte influx, including CD3<sup>+</sup> T-cells, is the result of immune stimulation by another antigen.

The host CTL immune response in sheep affected by OPA and OPP could also be directed against OvLV, which may inadvertently have a role in OPA tumor rejection. The infiltration of alveolar macrophages surrounding neoplastic foci is a consistent histological feature of OPA (Rosadio et al. 1988) and, these macrophages may serve as an important target for OvLV replication (Dawson et al. 1985; DeMartini et al. 1987), since alveolar macrophages have been demonstrated to be the preferential target cells of OvLV infection (Gendelman et al. 1985). Furthermore, in sheep infected with OvLV, there is known to be a CTL-mediated immune response (Reyburn et al. 1992). Thus, if CTLs are in the vicinity of OPA tumor tissue in response to OvLV-infection of nearby macrophages, it is possible that the tumor cells may also fall under siege as

bystanders. Interestingly, there are a number of spontaneous cancer regression cases closely related to secondary infections like measles, viral hepatitis, herpes zoster, and chickenpox (Weintraub 1969; Bluming and Ziegler 1971; Horning and Rosenberg 1984; Drobyski and Qazi 1989; Kappauf et al. 1997). In fact, the leading hypothesis regarding the spontaneous regression of non-Hodgkin's lymphoma involves modulation of the host immune system induced by concurrent viral or bacterial infection (Krikorian et al. 1980), and to traumatic effect including biopsy (Grem et al. 1986; Kumamoto et al. 1994). Spontaneous regression following local infection may be attributable to local cytokine release and cellular immune activation resulting in inflammatory necrosis or T-cell mediated apoptosis of tumor cells (Kappauf et al. 1997).

If OvLV-induced OPP promoted regression of OPA tumors, this would indicate an antagonistic relationship between these two diseases. Previously, synergism between JSRV and OvLV has been hypothesized, including the enhancement of JSRV infection by OvLV-induced host immunosuppression (Myer et al. 1988), but firm evidence is lacking (Myer et al. 1988; Dawson et al. 1990; Sharp and DeMartini 2003). Additionally, the absence of OvLV-induced OPP in Scotland, where OPA causes significant losses, suggests that these two diseases are not invariably coexistent (Rosadio et al. 1988). Interestingly, in OPA-affected flocks in Scotland, the incidence of cancer is relatively high, with approximately 30% of the sheep having histologically confirmed lesions (Sharp and DeMartini 2003). If the immune response induced by OvLV infection does

have deleterious effects on JSRV-induced tumor, the absence of OPP in this country could account for the high incidence of OPA.

In addition to intratumoral T-cell infiltration, we also found a noteworthy humoral response against the JSRV envelope in two sheep with nodular disease regression and one sheep that did not develop nodules but tested positive for JSRV DNA, albeit low levels (~15 copies). In prior work, only the presence of antibodies against the JSRV capsid protein has been investigated and, a specific humoral response has never been detected in sera or lung fluid of affected sheep (Sharp and Herring 1983; Ortin et al. 1998; Summers et al. 2002; Sharp and DeMartini 2003). Thus, our study is the first demonstration of a humoral response against JSRV in OPA-affected sheep. Significantly, this response was directed against the envelope protein, the oncogenic component of JSRV. However, the antibody titers observed in our sheep was not nearly as high as that mounted by normal, immunocompetent C57BL/6 mice after inoculation with ARJenv; serum from our best responders reduced by titer of the JSRV retroviral vector by 50% at a 1:100 dilution whereas serum from ARJenv (+) mice demonstrated the same titer reduction at a 1:3000 dilution (Wootton et al. 2005). Furthermore, of the four immunocompetent mice that were administered ARJenv, only one developed very small tumors, indicating that JSRV-envelope induced tumorigenesis can be controlled by the normal immune system of these mice (Wootton et al. 2005). Additionally, although the JSRV envelope can transduce human, monkey, bovine, dog, and rabbit cells *in vitro*, there is an absence of evidence of JSRV infection *in vivo* in these species, possibly due to the development of a strong

immune response leading to virus clearance (Rai et al. 2000). As for the potential role of a humoral response in spontaneous regression of cancer, it has been established that tumor rejection is most notably mediated by CTLs (Pardoll 1992; Baxevanis and Papamichail 1994; Slingluff et al. 1994) but, antibody responses have been shown to be a requisite component of effective antitumor immune responses in murine systems (Reilly et al. 2001) and are associated with clinical course in human antitumor vaccine protocols (DiFronzo et al. 2002; Chung et al. 2003).

Supporting the notion that OPA development may be adversely effected by the immune system, an age-dependent susceptibility to OPA has been reported in experimental transmission studies (Verwoerd et al. 1980; Sharp et al. 1983; DeMartini et al. 1987; Rosadio et al. 1988); in comparison to aged sheep, neonatal lambs inoculated with JSRV produce more virus, leading to earlier detection of viremia and earlier development of neoplastic lesions (Salvatori et al. 2004). This age-related susceptibility of lambs to develop experimental OPA is likely related to the presence of more JSRV target cells in newborn lambs than in older animals (Salvatori et al. 2004) as well as to the immaturity of the neonatal immune response to viral infections (Rosadio et al. 1988). In particular, suboptimal interactions between antigen-presenting cells and T-cells, and the inability of these cells to secrete some cytokines, result in responses that are qualitatively different from those in adults, with decreased cytotoxic effector cell function and B-cell help (Upham et al. 2002).

In addition to age-susceptibility, there also appears to be differences in host-susceptibility to the development of OPA. In our work using age-matched sheep, animals receiving the same inoculum and thus, the same JSRV strain, had radically different viral loads and courses of disease. Similar outcomes have been reported in other experimental transmission studies; sheep of the same age that receive the same inoculum develop varying degrees of clinical signs and lesions associated with OPA; in fact, some sheep inoculated with JSRV never develop OPA (Wandera 1968; Sharp et al. 1983; DeMartini et al. 1987; Salvatori et al. 2004). In flocks with naturally occurring, endemic disease, the prevalence of JSRV infection is 40% - 80%, although only 30% of sheep develop OPA lesions (Sharp and DeMartini 2003). This considerable difference between virus prevalence and disease incidence in the natural setting may also reflect variations in host susceptibility (Sharp and DeMartini 2003). It is probable that the ability to mount an effective immune response against JSRV or OPA plays a significant role in the vulnerability of the host to disease development. Accordingly, both natural and experimental JSRV infection may have several outcomes: if an insufficient immune response is mounted, OPA progression results; if a sufficient immune response is mounted early, OPA is prevented; or, if a sufficient immune response is mounted after tumorigenesis, OPA regression results.

In addition to assessing the amenability of this animal model for therapeutic research by monitoring disease development via CT, our other objective was to assess the validity of OPA-affected sheep as an animal model

for human lung adenocarcinoma in terms of genetic similarities. Specifically, OPA tumors were screened for mutations commonly found in human lung cancers, including activating mutations in the EGFR and KRAS genes and inactivating mutations in the P53 tumor suppressor gene.

In the TK domain of the EGFR (exons 18-21), we found seven different heterozygous single base substitutions. However, all were silent substitutions and did not alter the amino acid sequence of the EGFR protein. Furthermore, most of these substitutions were not exclusive to JSRV-infected sheep and were found in uninfected sheep as well. In human lung cancer, EGFR TK domain mutations correlate with increased sensitivity of these cancers to TKIs (Lynch et al. 2004; Paez et al. 2004) and preferentially involve a subset of lung cancers, which are clinicopathologically characterized by female sex, East Asian ethnicity, non-smoking, and adenocarcinoma histology (Fukuoka et al. 2003; Kris et al. 2003; Perez-Soler et al. 2004). The morphological features of adenocarcinomas harboring the mutations were reported to be frequent in those cancers with bronchioloalveolar features (Miller et al. 2004), and, more specifically, those with alveolar type II cell and Clara cell involvement (Yatabe et al. 2005; Yatabe and Mitsudomi 2007). Thus, in humans, EGFR TK domain mutations are found in subtypes of lung cancer that are histologically similar to OPA and, like the sheep lung cancer, do not involve tobacco smoke as the likely carcinogen. In fact, from time to time, JSRV has been postulated to be the etiological agent of human BAC (Stinson et al. 1972; Geddes 1987; Morabia and Wynder 1992; Peterschmitt et al. 1994; Nuorva et al. 1995). Antibodies against the JSRV major capsid

protein were found to react with about 30% (39 of 129) of human BACs and 26% (17 of 65) of human pulmonary adenocarcinoma samples (De las Heras et al. 2000). However, attempts to identify such viruses by PCR have been unsuccessful thus far (Yousem et al. 2001; Hiatt and Highsmith 2002; Morozov et al. 2004). Thus, based on some of the features of human lung adenocarcinomas that are associated with EGFR TK domain mutations, we speculated that similar mutations may be involved in OPA tumorigenesis. However, in light of our work, we now know that the amino acid sequence of the EGFR protein is not altered in OPA tumors, and thus, mutations in this gene do not appear to play a critical role in JSRV-induced oncogenesis.

As for the other two genes, we observed no alterations in exon 1 (codons 12 and 13, in particular) of the KRAS gene or in the DNA-binding domain (exons 5-8) of the P53 tumor suppressor gene. Additionally, we also sequenced these genes in DNA isolated from the lung tumor tissue of ARJenv (+) mice; no nucleotide variants were observed. Studies have suggested that KRAS codon 12 and 13 point mutations may be a direct result of one or more carcinogenic ingredients of tobacco smoke (Rodenhuis et al. 1987; Rodenhuis et al. 1988). Additionally, P53 mutations are correlated with carcinogens in tobacco smoke and, consequently, are more common in lung malignancies of smokers than never-smokers (Husgafvel-Pursiainen et al. 2000). In OPA, the carcinogen that promotes tumorigenesis is a virus, and not tobacco smoke; thus, it was unlikely that these mutations would be present in JSRV-induced neoplasms. However, the mechanism by which JSRV induces transformation is uncertain and, as has

been shown for other retrovirus-induced tumors (Hoatlin et al. 1990; Li et al. 1990; Ruscetti et al. 1990; Aguilar-Cordova et al. 1991), OPA development is likely to be a multistep process resulting from an accumulation of events (Cousens et al. 2004). One such event could be insertional mutagenesis and, in studies exploring this mechanism, a multiclonal pattern of JSRV integration sites was found (Cousens et al. 2004; Philbey et al. 2006), suggesting random integration and polyclonality of JSRV-induced tumors. Thus, it is possible that in some JSRV-induced tumors, the virus could insert within KRAS or P53, resulting in activation of the former or inactivation of the latter and consequently promote transformation. In support of this concept, oncogenic retroviruses have been shown to alter the expression and/or structure of host-cell proto-oncogenes by insertional activation mechanisms (Varmus 1984; Nusse 1986; Bishop 1987). Regarding RAS family members, transcriptional activation of proto-oncogenes has been shown to result from retroviral insertion in HRAS (Ihle et al. 1989; Bera et al. 1998), NRAS (Sorensen et al. 1996; Martin-Hernandez et al. 2001), and KRAS (George et al. 1986; Trusko et al. 1989). In tumor suppressor genes, including P53, inactivation by retroviral integration has been demonstrated in neoplasms and derived cell lines (Wolf and Rotter 1984; Hicks and Mowat 1988; Lu et al. 1994; Cho et al. 1995). However, like EGFR, it does not appear that mutations in these genes play a critical role in JSRV-induced oncogenesis. However, it must be mentioned that in this study, the genetic profiling results are allegedly from tumor cells but it is possible that the sequences are from non-

tumor cells within the lesions and thus, mutations in the actual tumor cells were simply missed.

In conclusion, sheep affected by OPA are a relevant animal model for the study of human lung adenocarcinoma based on symptomatic, histopathologic, and possible molecular signaling similarities. Also, this animal model is valuable for investigative research in that it is predictable and reproducible following JSRV inoculation of neonatal lambs. In the preceding work, we determined that this animal model is amenable for therapeutic studies because OPA can be detected early, before the onset of clinical signs, and, after the hypothetical administration of treatment, the cancer development could be followed and therapeutic response could be monitored noninvasively using CT. However, not only did we observe OPA disease progression during this study, but surprisingly, we also witnessed spontaneous regression of OPA. In fact, the latter was the more common outcome seen in our research after JSRV inoculation of neonatal lambs. We propose that the immune system, particularly CD3<sup>+</sup> T-cells, is an important mediator of the spontaneous regression of JSRV-induced OPA seen in our work. It is unclear if the tumoricidal activity is directed toward JSRV, OPA tumor antigens, or coinfecting OvLV; thus, further studies are certainly warranted to unlock the mystery of immune-mediated spontaneous regression of OPA. Regardless of the cause, the mere occurrence of spontaneous regression of cancer in OPA-affected sheep severely restricts the use of this animal model for therapeutic research. Even with the most intricate of experimental designs, it would be challenging to conclude if cancer regression seen after the

administration of treatment was due to the therapy, spontaneous regression, or a combination of both factors. That being said, OPA-affected sheep may not be an ideal animal model for therapeutic research but are undoubtedly interesting candidates as animal models for the exploration of the spontaneous regression phenomenon as well as immune-mediate tumoricide.

In addition to assessing the amenability of OPA-affected sheep for therapeutic research, we also found that OPA tumors do not harbor genetic mutations in the TK domain of EGFR, KRAS codons 12 and 13, or the DNA-binding domain of P53 and therefore, are not genetically similar to human lung adenocarcinomas that contain these mutations. Based on these genetic disparities, OPA-affected sheep are not an ideal animal model for human lung adenocarcinoma. Nevertheless, the mechanism of JSRV envelope-induced oncogenesis is still uncertain and further elucidation of the means by which this virus acts as a carcinogen will surely aid in our understanding of human lung cancer. Overall, the genetic profile combined with the disease development data provided further characterization of OPA and facilitated an assessment of the utility and relevance of this animal model for human lung cancer studies.

## REFERENCES

- Adjei, A. A. (2001). "Blocking oncogenic Ras signaling for cancer therapy." *J Natl Cancer Inst* **93**(14): 1062-74.
- Adler, B., S. Padley, et al. (1992). "High-resolution CT of bronchioloalveolar carcinoma." *AJR Am J Roentgenol* **159**(2): 275-7.
- Aguilar-Cordova, E., R. Strange, et al. (1991). "Viral Ha-ras mediated mammary tumor progression." *Oncogene* **6**(9): 1601-7.
- Ahrendt, S. A., P. A. Decker, et al. (2001). "Cigarette smoking is strongly associated with mutation of the K-ras gene in patients with primary adenocarcinoma of the lung." *Cancer* **92**(6): 1525-30.
- Aizawa, S., Y. Suda, et al. (1990). "Env-derived gp55 gene of Friend spleen focus-forming virus specifically induces neoplastic proliferation of erythroid progenitor cells." *Embo J* **9**(7): 2107-16.
- Akata, S., A. Fukushima, et al. (1995). "CT scanning of bronchioloalveolar carcinoma: specific appearances." *Lung Cancer* **12**(3): 221-30.
- Alberti, A., C. Murgia, et al. (2002). "Envelope-induced cell transformation by ovine betaretroviruses." *J Virol* **76**(11): 5387-94.
- Alian, A., D. Sela-Donenfeld, et al. (2000). "Avian hemangioma retrovirus induces cell proliferation via the envelope (env) gene." *Virology* **276**(1): 161-8.
- Allen, T. E., K. J. Sherrill, et al. (2002). "The jaagsiekte sheep retrovirus envelope gene induces transformation of the avian fibroblast cell line DF-1 but does not require a conserved SH2 binding domain." *J Gen Virol* **83**(Pt 11): 2733-42.
- American Cancer Society. Cancer Reference Information. Detailed Guide: All About Lung Cancer - Non-Small Cell. What is Non-Small Cell Lung Cancer? Accessed 2007.
- American Cancer Society (2007). Cancer Facts and Figures 2007. Atlanta, American Cancer Society.
- Aquino, S. L., C. Chiles, et al. (1998). "Distinction of consolidative bronchioloalveolar carcinoma from pneumonia: do CT criteria work?" *AJR Am J Roentgenol* **171**(2): 359-63.

- Arteaga, C. L. (2001). "The epidermal growth factor receptor: from mutant oncogene in nonhuman cancers to therapeutic target in human neoplasia." *J Clin Oncol* **19**(18 Suppl): 32S-40S.
- Asamura, H., K. Suzuki, et al. (2003). "A clinicopathological study of resected subcentimeter lung cancers: a favorable prognosis for ground glass opacity lesions." *Ann Thorac Surg* **76**(4): 1016-22.
- Austin, J. H., N. L. Muller, et al. (1996). "Glossary of terms for CT of the lungs: recommendations of the Nomenclature Committee of the Fleischner Society." *Radiology* **200**(2): 327-31.
- Azuma, M., M. Cayabyab, et al. (1992). "CD28 interaction with B7 costimulates primary allogeneic proliferative responses and cytotoxicity mediated by small, resting T lymphocytes." *J Exp Med* **175**(2): 353-60.
- Bai, J., J. V. Bishop, et al. (1999). "Sequence comparison of JSRV with endogenous proviruses: envelope genotypes and a novel ORF with similarity to a G-protein-coupled receptor." *Virology* **258**(2): 333-43.
- Bai, J., R. Y. Zhu, et al. (1996). "Unique long terminal repeat U3 sequences distinguish exogenous jaagsiekte sheep retroviruses associated with ovine pulmonary carcinoma from endogenous loci in the sheep genome." *J Virol* **70**(5): 3159-68.
- Baier, P. K., S. Wimmenauer, et al. (1998). "Analysis of the T cell receptor variability of tumor-infiltrating lymphocytes in colorectal carcinomas." *Tumour Biol* **19**(3): 205-12.
- Bakhai, A., D. J. Sheridan, et al. (2002). ""Bronchial artery delivery of viral vectors for gene delivery in cystic fibrosis; superior to airway delivery?"" *BMC Pulm Med* **2**(1): 2.
- Balmain, A. and C. C. Harris (2000). "Carcinogenesis in mouse and human cells: parallels and paradoxes." *Carcinogenesis* **21**(3): 371-7.
- Barbacid, M. (1987). "ras genes." *Annu Rev Biochem* **56**: 779-827.
- Barsky, S. H., D. A. Grossman, et al. (1994). "The multifocality of bronchioloalveolar lung carcinoma: evidence and implications of a multiclonal origin." *Mod Pathol* **7**(6): 633-40.
- Baskar, S., S. Ostrand-Rosenberg, et al. (1993). "Constitutive expression of B7 restores immunogenicity of tumor cells expressing truncated major histocompatibility complex class II molecules." *Proc Natl Acad Sci U S A* **90**(12): 5687-90.

- Baxevanis, C. N. and M. Papamichail (1994). "Characterization of the anti-tumor immune response in human cancers and strategies for immunotherapy." *Crit Rev Oncol Hematol* **16**(3): 157-79.
- Beasley, M. B., E. Brambilla, et al. (2005). "The 2004 World Health Organization classification of lung tumors." *Semin Roentgenol* **40**(2): 90-7.
- Begin, R., M. Rola-Pleszczynski, et al. (1981). "Sequential analysis of the bronchoalveolar milieu in conscious sheep." *J Appl Physiol* **50**(3): 665-71.
- Belani, C. P. (2000). "Chemotherapy regimens in advanced non small-cell lung cancer: recent randomized trials." *Clin Lung Cancer* **2 Suppl 1**: S7-S10.
- Belinsky, S. A., T. R. Devereux, et al. (1992). "Role of the alveolar type II cell in the development and progression of pulmonary tumors induced by 4-(methylnitrosamino)-1-(3-pyridyl)-1-butanone in the A/J mouse." *Cancer Res* **52**(11): 3164-73.
- Bera, T. K., T. Tsukamoto, et al. (1998). "Defective retrovirus insertion activates c-Ha-ras protooncogene in an MNU-induced rat mammary carcinoma." *Biochem Biophys Res Commun* **248**(3): 835-40.
- Berke, G. (1991). "T-cell-mediated cytotoxicity." *Curr Opin Immunol* **3**(3): 320-5.
- Bestor, T. H. (1988). "Cloning of a mammalian DNA methyltransferase." *Gene* **74**(1): 9-12.
- Bischof, R. J., K. Snibson, et al. (2003). "Induction of allergic inflammation in the lungs of sensitized sheep after local challenge with house dust mite." *Clin Exp Allergy* **33**(3): 367-75.
- Bishop, J. M. (1987). "The molecular genetics of cancer." *Science* **235**(4786): 305-11.
- Blacklaws, B. A., P. Bird, et al. (1995). "Initial lentivirus-host interactions within lymph nodes: a study of maedi-visna virus infection in sheep." *J Virol* **69**(3): 1400-7.
- Bluming, A. Z. and J. L. Ziegler (1971). "Regression of Burkitt's lymphoma in association with measles infection." *Lancet* **2**(7715): 105-6.
- Bodner, S. M., J. D. Minna, et al. (1992). "Expression of mutant p53 proteins in lung cancer correlates with the class of p53 gene mutation." *Oncogene* **7**(4): 743-9.
- Bogdan, S. and C. Klambt (2001). "Epidermal growth factor receptor signaling." *Curr Biol* **11**(8): R292-5.

- Bonne, C. (1939). "Morphological resemblance of pulmonary adenomatosis (Jaagsiekte) in sheep and certain cases of cancer of the lung in man." *Am J Cancer* **35**: 491-501.
- Bonner, A. E., W. J. Lemon, et al. (2004). "Molecular profiling of mouse lung tumors: association with tumor progression, lung development, and human lung adenocarcinomas." *Oncogene* **23**(5): 1166-76.
- Bonomo, L., M. L. Storto, et al. (1998). "Bronchioloalveolar carcinoma of the lung." *Eur Radiol* **8**(6): 996-1001.
- Boon, T., J. C. Cerottini, et al. (1994). "Tumor antigens recognized by T lymphocytes." *Annu Rev Immunol* **12**: 337-65.
- Boon, T. and P. van der Bruggen (1996). "Human tumor antigens recognized by T lymphocytes." *J Exp Med* **183**(3): 725-9.
- Brambilla, E. and C. Brambilla (1997). "p53 and lung cancer." *Pathol Biol (Paris)* **45**(10): 852-63.
- Breathnach, O. S., B. Freidlin, et al. (2001). "Twenty-two years of phase III trials for patients with advanced non-small-cell lung cancer: sobering results." *J Clin Oncol* **19**(6): 1734-42.
- Cadore, J. L., P. Loubeyre, et al. (1997). "Early diagnosis of lentivirus-induced infiltrative lung disease in sheep by high resolution computed tomography." *Eur Respir J* **10**(7): 1456-9.
- Caporale, M., C. Cousens, et al. (2006). "Expression of the jaagsiekte sheep retrovirus envelope glycoprotein is sufficient to induce lung tumors in sheep." *J Virol* **80**(16): 8030-7.
- Cappuzzo, F., V. Gregorc, et al. (2003). "Gefitinib in pretreated non-small-cell lung cancer (NSCLC): analysis of efficacy and correlation with HER2 and epidermal growth factor receptor expression in locally advanced or metastatic NSCLC." *J Clin Oncol* **21**(14): 2658-63.
- Chang, F., S. Syrjanen, et al. (1995). "Implications of the p53 tumor-suppressor gene in clinical oncology." *J Clin Oncol* **13**(4): 1009-22.
- Charan, N. and P. Carvalho (1992). Anatomy of the normal bronchial circulatory system in humans and animals. The bronchial circulation. J. Butler. New York, M. Dekker: 45-77.
- Chen, J. X., Y. Zheng, et al. (1998). "Carcinogens preferentially bind at methylated CpG in the p53 mutational hot spots." *Cancer Res* **58**(10): 2070-5.

- Cho, B. C., J. D. Shaughnessy, Jr., et al. (1995). "Frequent disruption of the Nf1 gene by a novel murine AIDS virus-related provirus in BXH-2 murine myeloid lymphomas." *J Virol* **69**(11): 7138-46.
- Chou, T. Y., C. H. Chiu, et al. (2005). "Mutation in the tyrosine kinase domain of epidermal growth factor receptor is a predictive and prognostic factor for gefitinib treatment in patients with non-small cell lung cancer." *Clin Cancer Res* **11**(10): 3750-7.
- Chow, Y. H., A. Alberti, et al. (2003). "Transformation of rodent fibroblasts by the jaagsiekte sheep retrovirus envelope is receptor independent and does not require the surface domain." *J Virol* **77**(11): 6341-50.
- Christiani, D. C., et al. (2006). "BAC consensus conference, November 4-6, 2004: epidemiology, pathogenesis, and preclinical models." *J Thorac Oncol* **1**(9 Suppl): S2-7.
- Chung, M. H., R. K. Gupta, et al. (2003). "Humoral immune response to a therapeutic polyvalent cancer vaccine after complete resection of thick primary melanoma and sentinel lymphadenectomy." *J Clin Oncol* **21**(2): 313-9.
- Clemente, C. G., M. C. Mihm, Jr., et al. (1996). "Prognostic value of tumor infiltrating lymphocytes in the vertical growth phase of primary cutaneous melanoma." *Cancer* **77**(7): 1303-10.
- Cole, W. H. (1976). "Relationship of causative factors in spontaneous regression of cancer to immunologic factors possibly effective in cancer." *J Surg Oncol* **8**(5): 391-411.
- Cole, W. H. (1981). "Efforts to explain spontaneous regression of cancer." *J Surg Oncol* **17**(3): 201-9.
- Cousens, C., J. V. Bishop, et al. (2004). "Analysis of integration sites of Jaagsiekte sheep retrovirus in ovine pulmonary adenocarcinoma." *J Virol* **78**(16): 8506-12.
- Cousens, C., N. Maeda, et al. (2007). "In vivo tumorigenesis by Jaagsiekte sheep retrovirus (JSRV) requires Y590 in Env TM, but not full-length orfX open reading frame." *Virology*.
- Cowdry, E. V. and H. Marsh (1927). "COMPARATIVE PATHOLOGY OF SOUTH AFRICAN JAGZIEKTE AND MONTANA PROGRESSIVE PNEUMONIA OF SHEEP." *J. Exp. Med.* **45**(4): 571-585.
- Cox, G., J. L. Jones, et al. (2000). "Matrix metalloproteinase 9 and the epidermal growth factor signal pathway in operable non-small cell lung cancer." *Clin Cancer Res* **6**(6): 2349-55.

- Curt, G. A. (1994). "The use of animal models in cancer drug discovery and development." *Stem Cells* **12**(1): 23-9.
- Cutlip, R. C., H. D. Lehmkuhl, et al. (1992). "Seroprevalence of ovine progressive pneumonia virus in sheep in the United States as assessed by analyses of voluntarily submitted samples." *Am J Vet Res* **53**(6): 976-9.
- Cutlip, R. C. and S. Young (1982). "Sheep pulmonary adenomatosis (jaagsiekte) in the United States." *Am J Vet Res* **43**(12): 2108-13.
- D'Amico, T. A., M. Massey, et al. (1999). "A biologic risk model for stage I lung cancer: immunohistochemical analysis of 408 patients with the use of ten molecular markers." *J Thorac Cardiovasc Surg* **117**(4): 736-43.
- Danilkovitch-Miagkova, A., F. M. Duh, et al. (2003). "Hyaluronidase 2 negatively regulates RON receptor tyrosine kinase and mediates transformation of epithelial cells by jaagsiekte sheep retrovirus." *Proc Natl Acad Sci U S A* **100**(8): 4580-5.
- Dawson, M., S. H. Done, et al. (1990). "Maedi-visna and sheep pulmonary adenomatosis: a study of concurrent infection." *Br Vet J* **146**(6): 531-8.
- Dawson, M., C. Venables, et al. (1985). "Experimental infection of a natural case of sheep pulmonary adenomatosis with maedi-visna virus." *Vet Rec* **116**(22): 588-9.
- De Larco, J. E., R. Reynolds, et al. (1980). "Sarcoma growth factor from mouse sarcoma virus-transformed cells. Purification by binding and elution from epidermal growth factor receptor-rich cells." *J Biol Chem* **255**(8): 3685-90.
- De las Heras, M., S. H. Barsky, et al. (2000). "Evidence for a protein related immunologically to the jaagsiekte sheep retrovirus in some human lung tumours." *Eur Respir J* **16**(2): 330-2.
- De las Heras, M., L. Gonzalez, et al. (2003). "Pathology of ovine pulmonary adenocarcinoma." *Curr Top Microbiol Immunol* **275**: 25-54.
- De Las Heras, M., E. Minguijon, et al. (1995). "Adenomatosis pulmonar ovina (Jaagsiekte): celulas que infiltran el tumor y modificaciones en ganglios linfaticos regionales." *Medicina Veterinaria* **12**(1): 32-36.
- De Las Heras, M., A. Ortin, et al. (2006). "In-situ demonstration of mitogen-activated protein kinase Erk 1/2 signalling pathway in contagious respiratory tumours of sheep and goats." *J Comp Pathol* **135**(1): 1-10.
- De Las Heras, M., A. Ortin, et al. (2005). "A PCR technique for the detection of Jaagsiekte sheep retrovirus in the blood suitable for the screening of ovine pulmonary adenocarcinoma in field conditions." *Res Vet Sci* **79**(3): 259-64.

- DeMartini, J. C., J. V. Bishop, et al. (2001). "Jaagsiekte sheep retrovirus proviral clone JSRV(JS7), derived from the JS7 lung tumor cell line, induces ovine pulmonary carcinoma and is integrated into the surfactant protein A gene." *J Virol* **75**(9): 4239-46.
- DeMartini, J. C., S. J. Brodie, et al. (1993). "Pathogenesis of lymphoid interstitial pneumonia in natural and experimental ovine lentivirus infection." *Clin Infect Dis* **17 Suppl 1**: S236-42.
- Demartini, J. C., R. H. Rosadio, et al. (1988). "The etiology and pathogenesis of ovine pulmonary carcinoma (sheep pulmonary adenomatosis)." *Vet Microbiol* **17**(3): 219-36.
- DeMartini, J. C., R. H. Rosadio, et al. (1987). "Experimental coinduction of type D retrovirus-associated pulmonary carcinoma and lentivirus-associated lymphoid interstitial pneumonia in lambs." *J Natl Cancer Inst* **79**(1): 167-77.
- Denissenko, M. F., J. X. Chen, et al. (1997). "Cytosine methylation determines hot spots of DNA damage in the human P53 gene." *Proc Natl Acad Sci U S A* **94**(8): 3893-8.
- Denissenko, M. F., A. Pao, et al. (1996). "Preferential formation of benzo[a]pyrene adducts at lung cancer mutational hotspots in P53." *Science* **274**(5286): 430-2.
- Diederichsen, A. C., J. B. Hjelmberg, et al. (2003). "Prognostic value of the CD4+/CD8+ ratio of tumour infiltrating lymphocytes in colorectal cancer and HLA-DR expression on tumour cells." *Cancer Immunol Immunother* **52**(7): 423-8.
- DiFronzo, L. A., R. K. Gupta, et al. (2002). "Enhanced humoral immune response correlates with improved disease-free and overall survival in American Joint Committee on Cancer stage II melanoma patients receiving adjuvant polyvalent vaccine." *J Clin Oncol* **20**(15): 3242-8.
- Downward, J. (2003). "Targeting RAS signalling pathways in cancer therapy." *Nat Rev Cancer* **3**(1): 11-22.
- Drobyski, W. R. and R. Qazi (1989). "Spontaneous regression in non-Hodgkin's lymphoma: clinical and pathogenetic considerations." *Am J Hematol* **31**(2): 138-41.
- Dungal, N. (1946). "Experiments with jaagsiekte." *Am J Pathol* **22**: 737-759.
- Dunn, G. P., L. J. Old, et al. (2004). "The immunobiology of cancer immunosurveillance and immunoediting." *Immunity* **21**(2): 137-48.

- Dunn, G. P., L. J. Old, et al. (2004). "The three Es of cancer immunoediting." *Annu Rev Immunol* **22**: 329-60.
- Dykes, J. and J. M'Fadyean (1888). "Lung disease in sheep caused by *Strongylus rufescens*." *J Comp Pathol Ther* **1**: 139-144.
- Emerson, M., L. Renwick, et al. (2003). "Transfection efficiency and toxicity following delivery of naked plasmid DNA and cationic lipid-DNA complexes to ovine lung segments." *Mol Ther* **8**(4): 646-53.
- Everson, T. C. and W. H. Cole (1966). Spontaneous regression of cancer: a study and abstract of reports in the world medical literature and of personal communications concerning spontaneous regression of malignant disease. Philadelphia,, Saunders.
- Fan, H. (1992). Retroviruses and their role in cancer. The retroviridae. J. Levy. New York, Plenum Press. **3**: 313-362.
- Fan, H., M. Palmarini, et al. (2003). "Transformation and oncogenesis by jaagsiekte sheep retrovirus." *Curr Top Microbiol Immunol* **275**: 139-77.
- Favero, J. and V. Lafont (1998). "Effector pathways regulating T cell activation." *Biochem Pharmacol* **56**(12): 1539-47.
- Ferreira, C. G., C. Tolis, et al. (1999). "p53 and chemosensitivity." *Ann Oncol* **10**(9): 1011-21.
- Fontanini, G., M. De Laurentiis, et al. (1998). "Evaluation of epidermal growth factor-related growth factors and receptors and of neoangiogenesis in completely resected stage I-IIIa non-small-cell lung cancer: amphiregulin and microvessel count are independent prognostic indicators of survival." *Clin Cancer Res* **4**(1): 241-9.
- Fraser, R. S. and R. G. Fraser (1994). Synopsis of diseases of the chest. Philadelphia, W.B. Saunders.
- Fujiwara, T., E. A. Grimm, et al. (1993). "A retroviral wild-type p53 expression vector penetrates human lung cancer spheroids and inhibits growth by inducing apoptosis." *Cancer Res* **53**(18): 4129-33.
- Fukuoka, M., S. Yano, et al. (2003). "Multi-institutional randomized phase II trial of gefitinib for previously treated patients with advanced non-small-cell lung cancer (The IDEAL 1 Trial) [corrected]." *J Clin Oncol* **21**(12): 2237-46.
- Galon, J., A. Costes, et al. (2006). "Type, density, and location of immune cells within human colorectal tumors predict clinical outcome." *Science* **313**(5795): 1960-4.

- Garcia-Goti, M., L. Gonzalez, et al. (2000). "Sheep pulmonary adenomatosis: characterization of two pathological forms associated with jaagsiekte retrovirus." *J Comp Pathol* **122**(1): 55-65.
- Garfield, D. H., J. L. Cadranet, et al. (2006). "The bronchioloalveolar carcinoma and peripheral adenocarcinoma spectrum of diseases." *J Thorac Oncol* **1**(4): 344-59.
- Gatzemeier, U., J. von Pawel, et al. (2000). "Phase III comparative study of high-dose cisplatin versus a combination of paclitaxel and cisplatin in patients with advanced non-small-cell lung cancer." *J Clin Oncol* **18**(19): 3390-9.
- Gazdar, A. F., H. Shigematsu, et al. (2004). "Mutations and addiction to EGFR: the Achilles 'heel' of lung cancers?" *Trends Mol Med* **10**(10): 481-6.
- Geddes, D. M. (1987). "Bronchioloalveolar carcinoma." *Br Med J (Clin Res Ed)* **294**(6563): 3.
- Gendelman, H. E., O. Narayan, et al. (1985). "Slow, persistent replication of lentiviruses: role of tissue macrophages and macrophage precursors in bone marrow." *Proc Natl Acad Sci U S A* **82**(20): 7086-90.
- George, D. L., B. Glick, et al. (1986). "Enhanced c-Ki-ras expression associated with Friend virus integration in a bone marrow-derived mouse cell line." *Proc Natl Acad Sci U S A* **83**(6): 1651-5.
- Ginsberg, M. S., R. K. Grewal, et al. (2007). "Lung cancer." *Radiol Clin North Am* **45**(1): 21-43.
- Gonzalez, L., M. Garcia-Goti, et al. (2001). "Jaagsiekte sheep retrovirus can be detected in the peripheral blood during the pre-clinical period of sheep pulmonary adenomatosis." *J Gen Virol* **82**(Pt 6): 1355-8.
- Greatens, T. M., G. A. Niehans, et al. (1998). "Do molecular markers predict survival in non-small-cell lung cancer?" *Am J Respir Crit Care Med* **157**(4 Pt 1): 1093-7.
- Greenberg, P. D., J. P. Klarnet, et al. (1988). "Therapy of disseminated tumors by adoptive transfer of specifically immune T cells." *Prog Exp Tumor Res* **32**: 104-27.
- Greenblatt, M. S., W. P. Bennett, et al. (1994). "Mutations in the p53 tumor suppressor gene: clues to cancer etiology and molecular pathogenesis." *Cancer Res* **54**(18): 4855-78.
- Gregory, H. (1975). "Isolation and structure of urogastrone and its relationship to epidermal growth factor." *Nature* **257**(5524): 325-7.

- Grem, J. L., G. R. Hafez, et al. (1986). "Spontaneous remission in diffuse large cell lymphoma." *Cancer* **57**(10): 2042-4.
- Gschwind, A., O. M. Fischer, et al. (2004). "The discovery of receptor tyrosine kinases: targets for cancer therapy." *Nat Rev Cancer* **4**(5): 361-70.
- Hainaut, P. and M. Hollstein (2000). "p53 and human cancer: the first ten thousand mutations." *Adv Cancer Res* **77**: 81-137.
- Hainaut, P. and G. P. Pfeifer (2001). "Patterns of p53 G-->T transversions in lung cancers reflect the primary mutagenic signature of DNA-damage by tobacco smoke." *Carcinogenesis* **22**(3): 367-74.
- Han, S. W., P. G. Hwang, et al. (2005). "Epidermal growth factor receptor (EGFR) downstream molecules as response predictive markers for gefitinib (Iressa, ZD1839) in chemotherapy-resistant non-small cell lung cancer." *Int J Cancer* **113**(1): 109-15.
- Harris, A. (1997). "Towards an ovine model of cystic fibrosis." *Hum Mol Genet* **6**(13): 2191-4.
- Hernandez-Boussard, T. M. and P. Hainaut (1998). "A specific spectrum of p53 mutations in lung cancer from smokers: review of mutations compiled in the IARC p53 database." *Environ Health Perspect* **106**(7): 385-91.
- Hiatt, K. M. and W. E. Highsmith (2002). "Lack of DNA evidence for jaagsiekte sheep retrovirus in human bronchioloalveolar carcinoma." *Hum Pathol* **33**(6): 680.
- Hicks, G. G. and M. Mowat (1988). "Integration of Friend murine leukemia virus into both alleles of the p53 oncogene in an erythroleukemic cell line." *J Virol* **62**(12): 4752-5.
- Higashiyama, S., J. A. Abraham, et al. (1991). "A heparin-binding growth factor secreted by macrophage-like cells that is related to EGF." *Science* **251**(4996): 936-9.
- Hill, C. A. (1984). "Bronchioloalveolar carcinoma: a review." *Radiology* **150**(1): 15-20.
- Hirsch, F. R., G. V. Scagliotti, et al. (2003). "Epidermal growth factor family of receptors in preneoplasia and lung cancer: perspectives for targeted therapies." *Lung Cancer* **41 Suppl 1**: S29-42.
- Hirsch, F. R., M. Varella-Garcia, et al. (2003). "Epidermal growth factor receptor in non-small-cell lung carcinomas: correlation between gene copy number and protein expression and impact on prognosis." *J Clin Oncol* **21**(20): 3798-807.

- Hoatlin, M. E., S. L. Kozak, et al. (1990). "Activation of erythropoietin receptors by Friend viral gp55 and by erythropoietin and down-modulation by the murine Fv-2r resistance gene." *Proc Natl Acad Sci U S A* **87**(24): 9985-9.
- Hofacre, A. and H. Fan (2004). "Multiple domains of the Jaagsiekte sheep retrovirus envelope protein are required for transformation of rodent fibroblasts." *J Virol* **78**(19): 10479-89.
- Hoffman, R. M. (1999). "Orthotopic metastatic mouse models for anticancer drug discovery and evaluation: a bridge to the clinic." *Invest New Drugs* **17**(4): 343-59.
- Holland, M. J., M. Palmarini, et al. (1999). "Jaagsiekte retrovirus is widely distributed both in T and B lymphocytes and in mononuclear phagocytes of sheep with naturally and experimentally acquired pulmonary adenomatosis." *J Virol* **73**(5): 4004-8.
- Hollstein, M., D. Sidransky, et al. (1991). "p53 mutations in human cancers." *Science* **253**(5015): 49-53.
- Horio, Y., A. Chen, et al. (1996). "Ki-ras and p53 mutations are early and late events, respectively, in urethane-induced pulmonary carcinogenesis in A/J mice." *Mol Carcinog* **17**(4): 217-23.
- Horning, S. J. and S. A. Rosenberg (1984). "The natural history of initially untreated low-grade non-Hodgkin's lymphomas." *N Engl J Med* **311**(23): 1471-5.
- Howard, R. B., J. B. Mullen, et al. (1999). "Characterization of a highly metastatic, orthotopic lung cancer model in the nude rat." *Clin Exp Metastasis* **17**(2): 157-62.
- Hull, S. and H. Fan (2006). "Mutational analysis of the cytoplasmic tail of jaagsiekte sheep retrovirus envelope protein." *J Virol* **80**(16): 8069-80.
- Humphrey, L. L., S. Teutsch, et al. (2004). "Lung cancer screening with sputum cytologic examination, chest radiography, and computed tomography: an update for the U.S. Preventive Services Task Force." *Ann Intern Med* **140**(9): 740-53.
- Hunter, A. R. and R. Munro (1983). "The diagnosis, occurrence and distribution of sheep pulmonary adenomatosis in Scotland 1975 to 1981." *Br Vet J* **139**(2): 153-64.
- Hunter, E., J. Casey, et al. (2000). Retroviridae. [Virus taxonomy : classification and nomenclature of viruses : seventh report of the International Committee on Taxonomy of Viruses](#)

- M. H. V. Van Regenmortel, C. Fauquet, D. H. L. Bishop et al. San Diego, Academic Press: 369-387.
- Husgafvel-Pursiainen, K., P. Boffetta, et al. (2000). "p53 mutations and exposure to environmental tobacco smoke in a multicenter study on lung cancer." *Cancer Res* **60**(11): 2906-11.
- Iggo, R., K. Gatter, et al. (1990). "Increased expression of mutant forms of p53 oncogene in primary lung cancer." *Lancet* **335**(8691): 675-9.
- Ihle, J. N., B. Smith-White, et al. (1989). "Activation of the c-H-ras proto-oncogene by retrovirus insertion and chromosomal rearrangement in a Moloney leukemia virus-induced T-cell leukemia." *J Virol* **63**(7): 2959-66.
- Im, J. G., M. C. Han, et al. (1990). "Lobar bronchioloalveolar carcinoma: "angiogram sign" on CT scans." *Radiology* **176**(3): 749-53.
- Ingenito, E. P., J. J. Reilly, et al. (2001). "Bronchoscopic volume reduction: a safe and effective alternative to surgical therapy for emphysema." *Am J Respir Crit Care Med* **164**(2): 295-301.
- Irvin, C. G. and J. H. Bates (2003). "Measuring the lung function in the mouse: the challenge of size." *Respir Res* **4**(1): 4.
- Janne, P. A., J. A. Engelman, et al. (2005). "Epidermal growth factor receptor mutations in non-small-cell lung cancer: implications for treatment and tumor biology." *J Clin Oncol* **23**(14): 3227-34.
- Jass, J. R. (1986). "Lymphocytic infiltration and survival in rectal cancer." *J Clin Pathol* **39**(6): 585-9.
- Johnson, S. K., K. M. Kerr, et al. (2000). "Immune cell infiltrates and prognosis in primary carcinoma of the lung." *Lung Cancer* **27**(1): 27-35.
- Jorissen, R. N., F. Walker, et al. (2003). "Epidermal growth factor receptor: mechanisms of activation and signalling." *Exp Cell Res* **284**(1): 31-53.
- Kane, M. A. and P. A. Bunn (1998). Overveiw of the biology of lung cancer. Biology of lung cancer. M. A. Kane and P. A. Bunn. New York, M. Dekker: 1-9.
- Kannagi, M., K. Sugamura, et al. (1983). "Establishment of human cytotoxic T cell lines specific for human adult T cell leukemia virus-bearing cells." *J Immunol* **130**(6): 2942-6.
- Kappauf, H., W. M. Gallmeier, et al. (1997). "Complete spontaneous remission in a patient with metastatic non-small-cell lung cancer. Case report, review of

the literature, and discussion of possible biological pathways involved." *Ann Oncol* **8**(10): 1031-9.

- Kastan, M. B., Q. Zhan, et al. (1992). "A mammalian cell cycle checkpoint pathway utilizing p53 and GADD45 is defective in ataxia-telangiectasia." *Cell* **71**(4): 587-97.
- Katz, E., M. H. Lareef, et al. (2005). "MMTV Env encodes an ITAM responsible for transformation of mammary epithelial cells in three-dimensional culture." *J Exp Med* **201**(3): 431-9.
- Kawaguchi, T., M. Kusumoto, et al. (2005). "High-resolution computed tomography appearances of surgically resected pulmonary metastases from colorectal cancer, with histopathologic correlation." *Radiat Med* **23**(6): 418-26.
- Kelly, K., J. Crowley, et al. (2001). "Randomized phase III trial of paclitaxel plus carboplatin versus vinorelbine plus cisplatin in the treatment of patients with advanced non-small-cell lung cancer: a Southwest Oncology Group trial." *J Clin Oncol* **19**(13): 3210-8.
- Khanna, R., S. R. Burrows, et al. (1994). "Endoplasmic reticulum signal sequence facilitated transport of peptide epitopes restores immunogenicity of an antigen processing defective tumour cell line." *Int Immunol* **6**(4): 639-45.
- Khanna, R., S. R. Burrows, et al. (1996). "Peptide transporter (TAP-1 and TAP-2)-independent endogenous processing of Epstein-Barr virus (EBV) latent membrane protein 2A: implications for cytotoxic T-lymphocyte control of EBV-associated malignancies." *J Virol* **70**(8): 5357-62.
- Khera, K. S., A. Ashkenazi, et al. (1963). "Immunity in Hamsters to Cells Transformed in Vitro and in Vivo by Sv40. Tests for Antigenic Relationship among the Papovaviruses." *J Immunol* **91**: 604-13.
- Klein, E. and G. Klein (1964). "Antigenic Properties of Lymphomas Induced by the Moloney Agent." *J Natl Cancer Inst* **32**: 547-68.
- Kosaka, T., Y. Yatabe, et al. (2004). "Mutations of the epidermal growth factor receptor gene in lung cancer: biological and clinical implications." *Cancer Res* **64**(24): 8919-23.
- Krikorian, J. G., C. S. Portlock, et al. (1980). "Spontaneous regression of non-Hodgkin's lymphoma: a report of nine cases." *Cancer* **46**(9): 2093-9.
- Kris, M. G., R. B. Natale, et al. (2003). "Efficacy of gefitinib, an inhibitor of the epidermal growth factor receptor tyrosine kinase, in symptomatic patients

- with non-small cell lung cancer: a randomized trial." *Jama* **290**(16): 2149-58.
- Kumamoto, M., H. Nakamine, et al. (1994). "Spontaneous complete regression of high grade non-Hodgkin's lymphoma. Morphologic, immunohistochemical, and gene amplification analyses." *Cancer* **74**(11): 3023-8.
- Lazo, P. A., J. S. Lee, et al. (1990). "Long-distance activation of the Myc protooncogene by provirus insertion in Mlvi-1 or Mlvi-4 in rat T-cell lymphomas." *Proc Natl Acad Sci U S A* **87**(1): 170-3.
- Leclerc, J. C., E. Gomard, et al. (1973). "Cell-mediated immune reaction against tumors induced by oncornaviruses. II. Nature of the effector cells in tumor-cell cytotoxicity." *Int J Cancer* **11**(2): 426-32.
- Lepperdinger, G., B. Strobl, et al. (1998). "HYAL2, a human gene expressed in many cells, encodes a lysosomal hyaluronidase with a novel type of specificity." *J Biol Chem* **273**(35): 22466-70.
- Leroux, C., N. Girard, et al. (2007). "Jaagsiekte Sheep Retrovirus (JSRV): from virus to lung cancer in sheep." *Vet Res* **38**(2): 211-28.
- Li, J. P., A. D. D'Andrea, et al. (1990). "Activation of cell growth by binding of Friend spleen focus-forming virus gp55 glycoprotein to the erythropoietin receptor." *Nature* **343**(6260): 762-4.
- Liu, J. and M. R. Johnston (2002). "Animal models for studying lung cancer and evaluating novel intervention strategies." *Surg Oncol* **11**(4): 217-27.
- Liu, S. L., F. M. Duh, et al. (2003). "Role of virus receptor Hyal2 in oncogenic transformation of rodent fibroblasts by sheep betaretrovirus env proteins." *J Virol* **77**(5): 2850-8.
- Liu, S. L., M. I. Lerman, et al. (2003). "Putative phosphatidylinositol 3-kinase (PI3K) binding motifs in ovine betaretrovirus Env proteins are not essential for rodent fibroblast transformation and PI3K/Akt activation." *J Virol* **77**(14): 7924-35.
- Liu, S. L. and A. D. Miller (2005). "Transformation of madin-darby canine kidney epithelial cells by sheep retrovirus envelope proteins." *J Virol* **79**(2): 927-33.
- Liu, S. L. and A. D. Miller (2007). "Oncogenic transformation by the jaagsiekte sheep retrovirus envelope protein." *Oncogene* **26**(6): 789-801.
- Lu, S. J., S. Rowan, et al. (1994). "Retroviral integration within the Fli-2 locus results in inactivation of the erythroid transcription factor NF-E2 in Friend

- erythroleukemias: evidence that NF-E2 is essential for globin expression." *Proc Natl Acad Sci U S A* **91**(18): 8398-402.
- Lynch, D. A. (2000). Radiologic differential diagnosis of diffuse lung disease. Imaging of diffuse lung disease. D. A. Lynch, J. D. Newell and J.-S. Lee. Hamilton, Ontario ; Lewiston, NY, B.C. Decker: ix, 322 p.
- Lynch, T. J., D. W. Bell, et al. (2004). "Activating mutations in the epidermal growth factor receptor underlying responsiveness of non-small-cell lung cancer to gefitinib." *N Engl J Med* **350**(21): 2129-39.
- Maeda, N., W. Fu, et al. (2005). "Roles of the Ras-MEK-mitogen-activated protein kinase and phosphatidylinositol 3-kinase-Akt-mTOR pathways in Jaagsiekte sheep retrovirus-induced transformation of rodent fibroblast and epithelial cell lines." *J Virol* **79**(7): 4440-50.
- Maeda, N., Y. Inoshima, et al. (2003). "Transformation of mouse fibroblasts by Jaagsiekte sheep retrovirus envelope does not require phosphatidylinositol 3-kinase." *J Virol* **77**(18): 9951-9.
- Maeda, N., M. Palmarini, et al. (2001). "Direct transformation of rodent fibroblasts by jaagsiekte sheep retrovirus DNA." *Proc Natl Acad Sci U S A* **98**(8): 4449-54.
- Magno, M. (1990). "Comparative anatomy of the tracheobronchial circulation." *Eur Respir J Suppl* **12**: 557s-562s; discussion 562s-563s.
- Malkinson, A. M. (2001). "Primary lung tumors in mice as an aid for understanding, preventing, and treating human adenocarcinoma of the lung." *Lung Cancer* **32**(3): 265-79.
- Mangenev, M., N. de Parseval, et al. (2001). "The full-length envelope of an HERV-H human endogenous retrovirus has immunosuppressive properties." *J Gen Virol* **82**(Pt 10): 2515-8.
- Manning, J. T., Jr., H. J. Spjut, et al. (1984). "Bronchioloalveolar carcinoma: The significance of two histopathologic types." *Cancer* **54**(3): 525-34.
- Mao, L. (2001). "Molecular abnormalities in lung carcinogenesis and their potential clinical implications." *Lung Cancer* **34 Suppl 2**: S27-34.
- Mariassy, A. T., W. M. Abraham, et al. (1994). "Effect of antigen on the glycoconjugate profile of tracheal secretions and the epithelial glycocalyx in allergic sheep." *J Allergy Clin Immunol* **93**(3): 585-93.
- Marrogi, A. J., A. Munshi, et al. (1997). "Study of tumor infiltrating lymphocytes and transforming growth factor-beta as prognostic factors in breast carcinoma." *Int J Cancer* **74**(5): 492-501.

- Martin-Hernandez, J., A. B. Sorensen, et al. (2001). "Murine leukemia virus proviral insertions between the N-ras and unr genes in B-cell lymphoma DNA affect the expression of N-ras only." *J Virol* **75**(23): 11907-12.
- Massey, T. E., T. R. Devereux, et al. (1995). "High frequency of K-ras mutations in spontaneous and vinyl carbamate-induced lung tumors of relatively resistant B6CF1 (C57BL/6J x BALB/cJ) mice." *Carcinogenesis* **16**(5): 1065-9.
- Meert, A. P., B. Martin, et al. (2002). "The role of EGF-R expression on patient survival in lung cancer: a systematic review with meta-analysis." *Eur Respir J* **20**(4): 975-81.
- Meyers, F. J., B. R. Madewell, et al. (1989). "ras p21 expression in ovine pulmonary carcinoma." *Vet Immunol Immunopathol* **23**(3-4): 279-91.
- Miller, V. A., M. G. Kris, et al. (2004). "Bronchioloalveolar pathologic subtype and smoking history predict sensitivity to gefitinib in advanced non-small-cell lung cancer." *J Clin Oncol* **22**(6): 1103-9.
- Mitsuya, H., L. A. Matis, et al. (1983). "Generation of an HLA-restricted cytotoxic T cell line reactive against cultured tumor cells from a patient infected with human T cell leukemia/lymphoma virus." *J Exp Med* **158**(3): 994-9.
- Miyashita, T., S. Krajewski, et al. (1994). "Tumor suppressor p53 is a regulator of bcl-2 and bax gene expression in vitro and in vivo." *Oncogene* **9**(6): 1799-805.
- Mohammed, T. L., C. S. White, et al. (2005). "The imaging manifestations of lung cancer." *Semin Roentgenol* **40**(2): 98-108.
- Morabia, A. and E. L. Wynder (1992). "Relation of bronchioloalveolar carcinoma to tobacco." *Bmj* **304**(6826): 541-3.
- Mornex, J. F., F. Thivolet, et al. (2003). "Pathology of human bronchioloalveolar carcinoma and its relationship to the ovine disease." *Curr Top Microbiol Immunol* **275**: 225-48.
- Morozov, V. A., S. Lagaye, et al. (2004). "Detection and characterization of betaretroviral sequences, related to sheep Jaagsiekte virus, in Africans from Nigeria and Cameroon." *Virology* **327**(2): 162-8.
- Muller, N. L. (2002). "Computed tomography and magnetic resonance imaging: past, present and future." *Eur Respir J Suppl* **35**: 3s-12s.
- Murayama, S., H. Onitsuka, et al. (1993). ""CT angiogram sign" in obstructive pneumonitis and pneumonia." *J Comput Assist Tomogr* **17**(4): 609-12.

- Myer, M. S., H. F. Huchzermeyer, et al. (1988). "The possible involvement of immunosuppression caused by a lentivirus in the aetiology of jaagsiekte and pasteurellosis in sheep." *Onderstepoort J Vet Res* **55**(3): 127-33.
- Naito, Y., K. Saito, et al. (1998). "CD8+ T cells infiltrated within cancer cell nests as a prognostic factor in human colorectal cancer." *Cancer Res* **58**(16): 3491-4.
- Nicholson, R. I., J. M. Gee, et al. (2001). "EGFR and cancer prognosis." *Eur J Cancer* **37 Suppl 4**: S9-15.
- Nisbet, D. I., J. M. Mackay, et al. (1971). "Ultrastructure of sheep pulmonary adenomatosis (Jaagsiekte)." *J Pathol* **103**(3): 157-62.
- Nishizaki, M., T. Fujiwara, et al. (1999). "Recombinant adenovirus expressing wild-type p53 is antiangiogenic: a proposed mechanism for bystander effect." *Clin Cancer Res* **5**(5): 1015-23.
- Nobel, T. A., F. Neumann, et al. (1969). "Histological patterns of the metastases in pulmonary adenomatosis of sheep (jaagsiekte)." *J Comp Pathol* **79**(4): 537-40.
- Nobel, T. A. and K. Perk (1978). "Bronchiolo-alveolar cell carcinoma. Animal model: pulmonary adenomatosis of sheep, pulmonary carcinoma of sheep, pulmonary carcinoma of sheep (Jaagsiekte)." *Am J Pathol* **90**(3): 783-6.
- Noguchi, M., A. Morikawa, et al. (1995). "Small adenocarcinoma of the lung. Histologic characteristics and prognosis." *Cancer* **75**(12): 2844-52.
- Nuorva, K., Y. Soini, et al. (1995). "p53 protein accumulation and the presence of human papillomavirus DNA in bronchiolo-alveolar carcinoma correlate with poor prognosis." *Int J Cancer* **64**(6): 424-9.
- Nusse, R. (1986). "The activation of cellular oncogenes by retroviral insertion." *Trends in Genetics* **2**: 244-247.
- Ohba, S., T. Takashima, et al. (1972). "Multiple cystic cavitory alveolar-cell carcinoma." *Radiology* **104**(1): 65-6.
- Ohsaki, Y., S. Tanno, et al. (2000). "Epidermal growth factor receptor expression correlates with poor prognosis in non-small cell lung cancer patients with p53 overexpression." *Oncol Rep* **7**(3): 603-7.
- Old, L. J. and Y. T. Chen (1998). "New paths in human cancer serology." *J Exp Med* **187**(8): 1163-7.

- Ortin, A., E. Minguijon, et al. (1998). "Lack of a specific immune response against a recombinant capsid protein of Jaagsiekte sheep retrovirus in sheep and goats naturally affected by enzootic nasal tumour or sheep pulmonary adenomatosis." *Vet Immunol Immunopathol* **61**(2-4): 229-37.
- Paez, J. G., P. A. Janne, et al. (2004). "EGFR mutations in lung cancer: correlation with clinical response to gefitinib therapy." *Science* **304**(5676): 1497-500.
- Palmarini, M., C. Cousens, et al. (1996). "The exogenous form of Jaagsiekte retrovirus is specifically associated with a contagious lung cancer of sheep." *J Virol* **70**(3): 1618-23.
- Palmarini, M., S. Datta, et al. (2000a). "The long terminal repeat of Jaagsiekte sheep retrovirus is preferentially active in differentiated epithelial cells of the lungs." *J Virol* **74**(13): 5776-87.
- Palmarini, M., P. Dewar, et al. (1995). "Epithelial tumour cells in the lungs of sheep with pulmonary adenomatosis are major sites of replication for Jaagsiekte retrovirus." *J Gen Virol* **76** ( Pt 11): 2731-7.
- Palmarini, M. and H. Fan (2001). "Retrovirus-induced ovine pulmonary adenocarcinoma, an animal model for lung cancer." *J Natl Cancer Inst* **93**(21): 1603-14.
- Palmarini, M., C. Hallwirth, et al. (2000b). "Molecular cloning and functional analysis of three type D endogenous retroviruses of sheep reveal a different cell tropism from that of the highly related exogenous jaagsiekte sheep retrovirus." *J Virol* **74**(17): 8065-76.
- Palmarini, M., M. J. Holland, et al. (1996b). "Jaagsiekte retrovirus establishes a disseminated infection of the lymphoid tissues of sheep affected by pulmonary adenomatosis." *J Gen Virol* **77** ( Pt 12): 2991-8.
- Palmarini, M., N. Maeda, et al. (2001). "A phosphatidylinositol 3-kinase docking site in the cytoplasmic tail of the Jaagsiekte sheep retrovirus transmembrane protein is essential for envelope-induced transformation of NIH 3T3 cells." *J Virol* **75**(22): 11002-9.
- Palmarini, M., M. Mura, et al. (2004). "Endogenous betaretroviruses of sheep: teaching new lessons in retroviral interference and adaptation." *J Gen Virol* **85**(Pt 1): 1-13.
- Pao, W., V. Miller, et al. (2004). "EGF receptor gene mutations are common in lung cancers from "never smokers" and are associated with sensitivity of tumors to gefitinib and erlotinib." *Proc Natl Acad Sci U S A* **101**(36): 13306-11.

- Pao, W. and V. A. Miller (2005). "Epidermal growth factor receptor mutations, small-molecule kinase inhibitors, and non-small-cell lung cancer: current knowledge and future directions." *J Clin Oncol* **23**(11): 2556-68.
- Pao, W., T. Y. Wang, et al. (2005). "KRAS mutations and primary resistance of lung adenocarcinomas to gefitinib or erlotinib." *PLoS Med* **2**(1): e17.
- Papac, R. J. (1998). "Spontaneous regression of cancer: possible mechanisms." *In Vivo* **12**(6): 571-8.
- Pardoll, D. (1992). "Immunotherapy with cytokine gene-transduced tumor cells: the next wave in gene therapy for cancer." *Curr Opin Oncol* **4**(6): 1124-9.
- Parkin, D. M., F. I. Bray, et al. (2001). "Cancer burden in the year 2000. The global picture." *Eur J Cancer* **37 Suppl 8**: S4-66.
- Parra, H. S., R. Cavina, et al. (2004). "Analysis of epidermal growth factor receptor expression as a predictive factor for response to gefitinib ('Iressa', ZD1839) in non-small-cell lung cancer." *Br J Cancer* **91**(2): 208-12.
- Pastorino, U., S. Andreola, et al. (1997). "Immunocytochemical markers in stage I lung cancer: relevance to prognosis." *J Clin Oncol* **15**(8): 2858-65.
- Payne, A. L. and D. W. Verwoerd (1984). "A scanning and transmission electron microscopy study of jaagsiekte lesions." *Onderstepoort J Vet Res* **51**(1): 1-13.
- Pemberton, A. D., S. M. McAleese, et al. (2000). "cDNA sequence of two sheep mast cell tryptases and the differential expression of tryptase and sheep mast cell proteinase-1 in lung, dermis and gastrointestinal tract." *Clin Exp Allergy* **30**(6): 818-32.
- Perez-Soler, R., A. Chachoua, et al. (2004). "Determinants of tumor response and survival with erlotinib in patients with non--small-cell lung cancer." *J Clin Oncol* **22**(16): 3238-47.
- Perk, K. and I. Hod (1982). "Sheep lung carcinoma: an endemic analogue of a sporadic human neoplasm." *J Natl Cancer Inst* **69**(4): 747-9.
- Perk, K., I. Hod, et al. (1971). "Pulmonary adenomatosis of sheep (jaagsiekte). I. Ultrastructure of the tumor." *J Natl Cancer Inst* **46**(3): 525-37.
- Peterschmitt, A. M., D. G. Moro, et al. (1994). "Bronchoalveolar carcinoma, lymphoid interstitial pneumonia, and retroviruses." *Clin Infect Dis* **19**(6): 1178-9.

- Pfeifer, G. P., E. Spiess, et al. (1985). "Mouse DNA-cytosine-5-methyltransferase: sequence specificity of the methylation reaction and electron microscopy of enzyme-DNA complexes." *Embo J* **4**(11): 2879-84.
- Pfeiffer, P., P. P. Clausen, et al. (1996). "Lack of prognostic significance of epidermal growth factor receptor and the oncoprotein p185HER-2 in patients with systemically untreated non-small-cell lung cancer: an immunohistochemical study on cryosections." *Br J Cancer* **74**(1): 86-91.
- Pfister, D. G., D. H. Johnson, et al. (2004). "American Society of Clinical Oncology treatment of unresectable non-small-cell lung cancer guideline: update 2003." *J Clin Oncol* **22**(2): 330-53.
- Philbey, A. W., C. Cousens, et al. (2006). "Multiclonal pattern of Jaagsiekte sheep retrovirus integration sites in ovine pulmonary adenocarcinoma." *Virus Res* **117**(2): 254-63.
- Plata, F., J. C. Cerottini, et al. (1975). "Primary and secondary in vitro generation of cytolytic T lymphocytes in the murine sarcoma virus system." *Eur J Immunol* **5**(4): 227-33.
- Platt, J. A., N. Kraipowich, et al. (2002). "Alveolar type II cells expressing jaagsiekte sheep retrovirus capsid protein and surfactant proteins are the predominant neoplastic cell type in ovine pulmonary adenocarcinoma." *Vet Pathol* **39**(3): 341-52.
- Politi, K., M. F. Zakowski, et al. (2006). "Lung adenocarcinomas induced in mice by mutant EGF receptors found in human lung cancers respond to a tyrosine kinase inhibitor or to down-regulation of the receptors." *Genes Dev* **20**(11): 1496-510.
- Prenzel, N., E. Zwick, et al. (2000). "Tyrosine kinase signalling in breast cancer. Epidermal growth factor receptor: convergence point for signal integration and diversification." *Breast Cancer Res* **2**(3): 184-90.
- Rai, S. K., J. C. DeMartini, et al. (2000). "Retrovirus vectors bearing jaagsiekte sheep retrovirus Env transduce human cells by using a new receptor localized to chromosome 3p21.3." *J Virol* **74**(10): 4698-704.
- Rai, S. K., F. M. Duh, et al. (2001). "Candidate tumor suppressor HYAL2 is a glycosylphosphatidylinositol (GPI)-anchored cell-surface receptor for jaagsiekte sheep retrovirus, the envelope protein of which mediates oncogenic transformation." *Proc Natl Acad Sci U S A* **98**(8): 4443-8.
- Ramesh, R., T. Saeki, et al. (2001). "Successful treatment of primary and disseminated human lung cancers by systemic delivery of tumor suppressor genes using an improved liposome vector." *Mol Ther* **3**(3): 337-50.

- Read, W. L., N. C. Page, et al. (2004). "The epidemiology of bronchioloalveolar carcinoma over the past two decades: analysis of the SEER database." *Lung Cancer* **45**(2): 137-42.
- Reilly, R. T., J. P. Machiels, et al. (2001). "The collaboration of both humoral and cellular HER-2/neu-targeted immune responses is required for the complete eradication of HER-2/neu-expressing tumors." *Cancer Res* **61**(3): 880-3.
- Reittner, P., S. Ward, et al. (2003). "Pneumonia: high-resolution CT findings in 114 patients." *Eur Radiol* **13**(3): 515-21.
- Restifo, N. P., F. Esquivel, et al. (1993). "Identification of human cancers deficient in antigen processing." *J Exp Med* **177**(2): 265-72.
- Reyburn, H. T., D. J. Roy, et al. (1992). "Characteristics of the T cell-mediated immune response to maedi-visna virus." *Virology* **191**(2): 1009-12.
- Rickinson, A. B., R. J. Murray, et al. (1992). "T cell recognition of Epstein-Barr virus associated lymphomas." *Cancer Surv* **13**: 53-80.
- Riese, D. J., 2nd and D. F. Stern (1998). "Specificity within the EGF family/ErbB receptor family signaling network." *Bioessays* **20**(1): 41-8.
- Rodenhuis, S. and R. J. Slebos (1990). "The ras oncogenes in human lung cancer." *Am Rev Respir Dis* **142**(6 Pt 2): S27-30.
- Rodenhuis, S., R. J. Slebos, et al. (1988). "Incidence and possible clinical significance of K-ras oncogene activation in adenocarcinoma of the human lung." *Cancer Res* **48**(20): 5738-41.
- Rodenhuis, S., M. L. van de Wetering, et al. (1987). "Mutational activation of the K-ras oncogene. A possible pathogenetic factor in adenocarcinoma of the lung." *N Engl J Med* **317**(15): 929-35.
- Rosadio, R. A. and J. M. Sharp (2000). "Adenomatosis pulmonar ovina: evidencias de inmunosupresion retroviral." *Rev Inv Vet Peru* **11**(2): 6-23.
- Rosadio, R. H., M. D. Lairmore, et al. (1988). "Retrovirus-associated ovine pulmonary carcinoma (sheep pulmonary adenomatosis) and lymphoid interstitial pneumonia. I. Lesion development and age susceptibility." *Vet Pathol* **25**(6): 475-83.
- Rosadio, R. H., J. M. Sharp, et al. (1988). "Lesions and retroviruses associated with naturally occurring ovine pulmonary carcinoma (sheep pulmonary adenomatosis)." *Vet Pathol* **25**(1): 58-66.

- Rosati, S., M. Pittau, et al. (2000). "An accessory open reading frame (orf-x) of jaagsiekte sheep retrovirus is conserved between different virus isolates." *Virus Res* **66**(1): 109-16.
- Rosenberg, N. and P. Jolicoeur (1997). Retroviral pathogenesis. Retroviruses J. M. Coffin, S. H. Hughes and H. Varmus. Plainview, N.Y., Cold Spring Harbor Laboratory Press: 475-585.
- Rosenberg, S. A. (1999). "A new era for cancer immunotherapy based on the genes that encode cancer antigens." *Immunity* **10**(3): 281-7.
- Ross, S. R., J. W. Schmidt, et al. (2006). "An immunoreceptor tyrosine activation motif in the mouse mammary tumor virus envelope protein plays a role in virus-induced mammary tumors." *J Virol* **80**(18): 9000-8.
- Roth, J. A., D. Nguyen, et al. (1996). "Retrovirus-mediated wild-type p53 gene transfer to tumors of patients with lung cancer." *Nat Med* **2**(9): 985-91.
- Rouse, B. T., M. Rollinghoff, et al. (1972). "Anti-theta serum-induced suppression of the cellular transfer of tumour-specific immunity to a syngeneic plasma cell tumour." *Nat New Biol* **238**(82): 116-7.
- Rowe, M., R. Khanna, et al. (1995). "Restoration of endogenous antigen processing in Burkitt's lymphoma cells by Epstein-Barr virus latent membrane protein-1: coordinate up-regulation of peptide transporters and HLA-class I antigen expression." *Eur J Immunol* **25**(5): 1374-84.
- Rudin, M. and R. Weissleder (2003). "Molecular imaging in drug discovery and development." *Nat Rev Drug Discov* **2**(2): 123-31.
- Ruscetti, S. K., N. J. Janesch, et al. (1990). "Friend spleen focus-forming virus induces factor independence in an erythropoietin-dependent erythroleukemia cell line." *J Virol* **64**(3): 1057-62.
- Rusch, V., D. Klimstra, et al. (1997). "Overexpression of the epidermal growth factor receptor and its ligand transforming growth factor alpha is frequent in resectable non-small cell lung cancer but does not predict tumor progression." *Clin Cancer Res* **3**(4): 515-22.
- Salvatori, D., L. Gonzalez, et al. (2004). "Successful induction of ovine pulmonary adenocarcinoma in lambs of different ages and detection of viraemia during the preclinical period." *J Gen Virol* **85**(Pt 11): 3319-24.
- Sandler, A. B., J. Nemunaitis, et al. (2000). "Phase III trial of gemcitabine plus cisplatin versus cisplatin alone in patients with locally advanced or metastatic non-small-cell lung cancer." *J Clin Oncol* **18**(1): 122-30.

- Sato, E., S. H. Olson, et al. (2005). "Intraepithelial CD8+ tumor-infiltrating lymphocytes and a high CD8+/regulatory T cell ratio are associated with favorable prognosis in ovarian cancer." *Proc Natl Acad Sci U S A* **102**(51): 18538-43.
- Scagliotti, G. V., G. Selvaggi, et al. (2004). "The biology of epidermal growth factor receptor in lung cancer." *Clin Cancer Res* **10**(12 Pt 2): 4227s-4232s.
- Schaefer-Prokop, C. and M. Prokop (2002). "New imaging techniques in the treatment guidelines for lung cancer." *Eur Respir J Suppl* **35**: 71s-83s.
- Schiller, J. H., D. Harrington, et al. (2002). "Comparison of four chemotherapy regimens for advanced non-small-cell lung cancer." *N Engl J Med* **346**(2): 92-8.
- Schumacher, K., W. Haensch, et al. (2001). "Prognostic significance of activated CD8(+) T cell infiltrations within esophageal carcinomas." *Cancer Res* **61**(10): 3932-6.
- Schuster, D. P. (1998). "The evaluation of lung function with PET." *Semin Nucl Med* **28**(4): 341-51.
- Sedlacek, H. H. (2000). "Kinase inhibitors in cancer therapy: a look ahead." *Drugs* **59**(3): 435-76.
- Sekido, Y., K. M. Fong, et al. (1998). "Progress in understanding the molecular pathogenesis of human lung cancer." *Biochim Biophys Acta* **1378**(1): F21-59.
- Selvaggi, G., S. Novello, et al. (2004). "Epidermal growth factor receptor overexpression correlates with a poor prognosis in completely resected non-small-cell lung cancer." *Ann Oncol* **15**(1): 28-32.
- Sharp, J. and K. Angus (1990). Sheep pulmonary adenomatosis: studies on its etiology. Maedi-visna and related diseases  
G. Pétursson and R. Hoff-Jørgensen. Boston, Kluwer Academic Publishers: 177-185.
- Sharp, J. M. (1987). "Sheep pulmonary adenomatosis: a contagious tumour and its cause." *Cancer Surv* **6**(1): 73-83.
- Sharp, J. M., K. W. Angus, et al. (1983). "Rapid transmission of sheep pulmonary adenomatosis (jaagsiekte) in young lambs. Brief report." *Arch Virol* **78**(1-2): 89-95.
- Sharp, J. M. and J. C. DeMartini (2003). "Natural history of JSRV in sheep." *Curr Top Microbiol Immunol* **275**: 55-79.

- Sharp, J. M. and A. J. Herring (1983). "Sheep pulmonary adenomatosis: demonstration of a protein which cross-reacts with the major core proteins of Mason-Pfizer monkey virus and mouse mammary tumour virus." *J Gen Virol* **64 (Pt 10)**: 2323-7.
- Shepherd, F. A., J. Pereira, et al. (2004). A randomized placebo-controlled trial of erlotinib in patients with advanced non-small cell lung cancer (NSCLC) following failure of 1st line or 2nd line chemotherapy. A National Cancer Institute of Canada Clinical Trials Group (NCIC CTG) trial. *J Clin Oncol* (Meeting Abstracts).
- Shigematsu, H., L. Lin, et al. (2005). "Clinical and biological features associated with epidermal growth factor receptor gene mutations in lung cancers." *J Natl Cancer Inst* **97(5)**: 339-46.
- Shing, Y., G. Christofori, et al. (1993). "Betacellulin: a mitogen from pancreatic beta cell tumors." *Science* **259(5101)**: 1604-7.
- Shoyab, M., V. L. McDonald, et al. (1988). "Amphiregulin: a bifunctional growth-modulating glycoprotein produced by the phorbol 12-myristate 13-acetate-treated human breast adenocarcinoma cell line MCF-7." *Proc Natl Acad Sci U S A* **85(17)**: 6528-32.
- Shure, D. and P. F. Fedullo (1983). "Transbronchial needle aspiration of peripheral masses." *Am Rev Respir Dis* **128(6)**: 1090-2.
- Sigurdsson, B. (1958). "Adenomatosis of sheep's lungs; experimental transmission." *Arch Gesamte Virusforsch* **8(1)**: 51-8.
- Sills, R. C., G. A. Boorman, et al. (1999). "Mutations in ras genes in experimental tumours of rodents." *IARC Sci Publ(146)*: 55-86.
- Simon, G., R. J. Ginsberg, et al. (2001). "Small-cell lung cancer." *Chest Surg Clin N Am* **11(1)**: 165-88, ix.
- Sirotnak, F. M., M. F. Zakowski, et al. (2000). "Efficacy of cytotoxic agents against human tumor xenografts is markedly enhanced by coadministration of ZD1839 (Iressa), an inhibitor of EGFR tyrosine kinase." *Clin Cancer Res* **6(12)**: 4885-92.
- Sjogren, H. O., I. Hellstrom, et al. (1961). "Resistance of polyoma virus immunized mice to transplantation of established polyoma tumors." *Experimental Cell Research* **23(1)**: 204-208.
- Slingluff, C. L., Jr., D. F. Hunt, et al. (1994). "Direct analysis of tumor-associated peptide antigens." *Curr Opin Immunol* **6(5)**: 733-40.

- Snyder, S. P., J. C. DeMartini, et al. (1983). "Coexistence of pulmonary adenomatosis and progressive pneumonia in sheep in the central sierra of Peru." *Am J Vet Res* **44**(7): 1334-8.
- Songyang, Z., S. E. Shoelson, et al. (1993). "SH2 domains recognize specific phosphopeptide sequences." *Cell* **72**(5): 767-78.
- Sordella, R., D. W. Bell, et al. (2004). "Gefitinib-sensitizing EGFR mutations in lung cancer activate anti-apoptotic pathways." *Science* **305**(5687): 1163-7.
- Sorensen, A. B., M. Duch, et al. (1996). "Sequence tags of provirus integration sites in DNAs of tumors induced by the murine retrovirus SL3-3." *J Virol* **70**(6): 4063-70.
- Spencer, T. E., M. Mura, et al. (2003). "Receptor usage and fetal expression of ovine endogenous betaretroviruses: implications for coevolution of endogenous and exogenous retroviruses." *J Virol* **77**(1): 749-53.
- Steinman, R. A., B. Hoffman, et al. (1994). "Induction of p21 (WAF-1/CIP1) during differentiation." *Oncogene* **9**(11): 3389-96.
- Stevenson, R. G., A. J. Rehmtulla, et al. (1980). "Pulmonary adenomatosis (jaagsiekte) in sheep in Canada." *Can Vet J* **21**(9): 267-8.
- Stinson, J. C., A. Leibovitz, et al. (1972). "Filamentous particles in human alveolar cell carcinomas: electron microscopy studies of six cases (preliminary report)." *J Natl Cancer Inst* **49**(6): 1483-93.
- Strobl, B., C. Wechselberger, et al. (1998). "Structural organization and chromosomal localization of Hyal2, a gene encoding a lysosomal hyaluronidase." *Genomics* **53**(2): 214-9.
- Suau, F., V. Cottin, et al. (2006). "Telomerase activation in a model of lung adenocarcinoma." *Eur Respir J* **27**(6): 1175-82.
- Summers, C., P. Dewar, et al. (2005). "Jaagsiekte sheep retrovirus-specific immune responses induced by vaccination: A comparison of immunisation strategies." *Vaccine*.
- Summers, C., W. Neill, et al. (2002). "Systemic immune responses following infection with Jaagsiekte sheep retrovirus and in the terminal stages of ovine pulmonary adenocarcinoma." *J Gen Virol* **83**(Pt 7): 1753-7.
- Summers, C., M. Norval, et al. (2005). "An influx of macrophages is the predominant local immune response in ovine pulmonary adenocarcinoma." *Vet Immunol Immunopathol* **106**(3-4): 285-94.

- Suzuki, M., H. Shigematsu, et al. (2005). "Epidermal growth factor receptor expression status in lung cancer correlates with its mutation." *Hum Pathol* **36**(10): 1127-34.
- Swann, J. B. and M. J. Smyth (2007). "Immune surveillance of tumors." *J Clin Invest* **117**(5): 1137-46.
- Takahashi, T., M. M. Nau, et al. (1989). "p53: a frequent target for genetic abnormalities in lung cancer." *Science* **246**(4929): 491-4.
- Tanaka, Y., M. J. Tevethia, et al. (1988). "Clustering of antigenic sites recognized by cytotoxic T lymphocyte clones in the amino terminal half of SV40 T antigen." *Virology* **162**(2): 427-36.
- Terasaki, H., T. Niki, et al. (2003). "Lung adenocarcinoma with mixed bronchioloalveolar and invasive components: clinicopathological features, subclassification by extent of invasive foci, and immunohistochemical characterization." *Am J Surg Pathol* **27**(7): 937-51.
- Thormar, H. (2005). "Maedi-visna virus and its relationship to human immunodeficiency virus." *AIDS Rev* **7**(4): 233-45.
- Tokumo, M., S. Toyooka, et al. (2005). "The relationship between epidermal growth factor receptor mutations and clinicopathologic features in non-small cell lung cancers." *Clin Cancer Res* **11**(3): 1167-73.
- Toyoda, H., T. Komurasaki, et al. (1995). "Molecular cloning of mouse epiregulin, a novel epidermal growth factor-related protein, expressed in the early stage of development." *FEBS Lett* **377**(3): 403-7.
- Tracy, S., T. Mukohara, et al. (2004). "Gefitinib induces apoptosis in the EGFR L858R non-small-cell lung cancer cell line H3255." *Cancer Res* **64**(20): 7241-4.
- Travis, W., T. Colby, et al. (1999). World Health Organization histological classification of tumours: histological typing of lung and pleural tumours, Springer-Verlag.
- Travis, W. D., K. Garg, et al. (2005). "Evolving concepts in the pathology and computed tomography imaging of lung adenocarcinoma and bronchioloalveolar carcinoma." *J Clin Oncol* **23**(14): 3279-87.
- Travis, W. D., K. Garg, et al. (2006). "Bronchioloalveolar carcinoma and lung adenocarcinoma: the clinical importance and research relevance of the 2004 World Health Organization pathologic criteria." *J Thorac Oncol* **1**(9 Suppl): S13-9.

- Trigaux, J. P., P. A. Gevenois, et al. (1996). "Bronchioloalveolar carcinoma: computed tomography findings." *Eur Respir J* **9**(1): 11-6.
- Trusko, S. P., E. K. Hoffman, et al. (1989). "Transcriptional activation of cKi-ras proto-oncogene resulting from retroviral promoter insertion." *Nucleic Acids Res* **17**(22): 9259-65.
- Tuddenham, W. J. (1984). "Glossary of terms for thoracic radiology: recommendations of the Nomenclature Committee of the Fleischner Society." *AJR Am J Roentgenol* **143**(3): 509-17.
- Tustin, R. (1969). "Ovine jaagsiekte." *J S Afr Vet Med Assoc* **40**: 3-23.
- Unger, T., M. M. Nau, et al. (1992). "p53: a transdominant regulator of transcription whose function is ablated by mutations occurring in human cancer." *Embo J* **11**(4): 1383-90.
- Upham, J. W., P. T. Lee, et al. (2002). "Development of interleukin-12-producing capacity throughout childhood." *Infect Immun* **70**(12): 6583-8.
- Uyttenhove, C., J. Maryanski, et al. (1983). "Escape of mouse mastocytoma P815 after nearly complete rejection is due to antigen-loss variants rather than immunosuppression." *J Exp Med* **157**(3): 1040-52.
- Varmus, H. E. (1984). "The molecular genetics of cellular oncogenes." *Annu Rev Genet* **18**: 553-612.
- Verwoerd, D. W. (1990). Jaagsiekte (ovine pulmonary adenocarcinoma) virus. Virus Infections of Ruminants. S. Dento and B. Mosein, Elsevier: 453-462.
- Verwoerd, D. W., E. M. De Villiers, et al. (1980). "Aetiology of jaagsiekte: experimental transmission to lambs by means of cultured cells and cell homogenates." *Onderstepoort J Vet Res* **47**(1): 13-8.
- Verwoerd, D. W., R. C. Tustin, et al. (1985). Jaagsiekte: an infectious pulmonary adenomatosis of sheep. Comparative pathobiology of viral diseases. R. G. Olsen, S. Krakowaka and J. R. Blackslee. Boca Raton, CRC Press: 53-76.
- Volm, M., W. Rittgen, et al. (1998). "Prognostic value of ERBB-1, VEGF, cyclin A, FOS, JUN and MYC in patients with squamous cell lung carcinomas." *Br J Cancer* **77**(4): 663-9.
- Wakamatsu, N., T. R. Devereux, et al. (2007). "Overview of the molecular carcinogenesis of mouse lung tumor models of human lung cancer." *Toxicol Pathol* **35**(1): 75-80.
- Wandera, J. G. (1968). "Experimental transmission of sheep pulmonary adenomatosis (Jaagsiekte)." *Vet Rec* **83**(19): 478-82.

- Weintraub, L. R. (1969). "Lymphosarcoma." *Jama* **210**(8): 1590-1.
- Weisbrod, G. L., D. Chamberlain, et al. (1995). "Cystic change (pseudocavitation) associated with bronchioloalveolar carcinoma: a report of four patients." *J Thorac Imaging* **10**(2): 106-11.
- Weiss, R. A. and C. S. Taylor (1995). "Retrovirus receptors." *Cell* **82**(4): 531-3.
- Wingo, P. A., L. A. Ries, et al. (1999). "Annual report to the nation on the status of cancer, 1973-1996, with a special section on lung cancer and tobacco smoking." *J Natl Cancer Inst* **91**(8): 675-90.
- Wolf, D. and V. Rotter (1984). "Inactivation of p53 gene expression by an insertion of Moloney murine leukemia virus-like DNA sequences." *Mol Cell Biol* **4**(7): 1402-10.
- Wolff, L. and S. Ruscetti (1988). "The spleen focus-forming virus (SFFV) envelope gene, when introduced into mice in the absence of other SFFV genes, induces acute erythroleukemia." *J Virol* **62**(6): 2158-63.
- Wong, J. S., G. L. Weisbrod, et al. (1994). "Bronchioloalveolar carcinoma and the air bronchogram sign: a new pathologic explanation." *J Thorac Imaging* **9**(3): 141-4.
- Wootton, S. K., C. L. Halbert, et al. (2005). "Sheep retrovirus structural protein induces lung tumours." *Nature* **434**(7035): 904-7.
- Wootton, S. K., M. J. Metzger, et al. (2006). "Lung cancer induced in mice by the envelope protein of jaagsiekte sheep retrovirus (JSRV) closely resembles lung cancer in sheep infected with JSRV." *Retrovirology* **3**: 94.
- Wozniak, A. J., J. J. Crowley, et al. (1998). "Randomized trial comparing cisplatin with cisplatin plus vinorelbine in the treatment of advanced non-small-cell lung cancer: a Southwest Oncology Group study." *J Clin Oncol* **16**(7): 2459-65.
- Yarden, Y. and M. X. Sliwkowski (2001). "Untangling the ErbB signalling network." *Nat Rev Mol Cell Biol* **2**(2): 127-37.
- Yatabe, Y., T. Kosaka, et al. (2005). "EGFR mutation is specific for terminal respiratory unit type adenocarcinoma." *Am J Surg Pathol* **29**(5): 633-9.
- Yatabe, Y. and T. Mitsudomi (2007). "Epidermal growth factor receptor mutations in lung cancers." *Pathol Int* **57**(5): 233-44.
- Yoon, H. E., K. Fukuhara, et al. (2005). "Pulmonary nodules 10 mm or less in diameter with ground-glass opacity component detected by high-resolution

computed tomography have a high possibility of malignancy." *Jpn J Thorac Cardiovasc Surg* **53**(1): 22-8.

- Yoon, J. H., L. E. Smith, et al. (2001). "Methylated CpG dinucleotides are the preferential targets for G-to-T transversion mutations induced by benzo[a]pyrene diol epoxide in mammalian cells: similarities with the p53 mutation spectrum in smoking-associated lung cancers." *Cancer Res* **61**(19): 7110-7.
- York, D. F., R. Vigne, et al. (1992). "Nucleotide sequence of the jaagsiekte retrovirus, an exogenous and endogenous type D and B retrovirus of sheep and goats." *J Virol* **66**(8): 4930-9.
- You, M., Y. Wang, et al. (1992). "Parental bias of Ki-ras oncogenes detected in lung tumors from mouse hybrids." *Proc Natl Acad Sci U S A* **89**(13): 5804-8.
- Yousem, S. A., S. D. Finkelstein, et al. (2001). "Absence of jaagsiekte sheep retrovirus DNA and RNA in bronchioloalveolar and conventional human pulmonary adenocarcinoma by PCR and RT-PCR analysis." *Hum Pathol* **32**(10): 1039-42.
- Zavala, G., C. Pretto, et al. (2003). "Relevance of Akt phosphorylation in cell transformation induced by Jaagsiekte sheep retrovirus." *Virology* **312**(1): 95-105.
- Zhang, L., J. R. Conejo-Garcia, et al. (2003). "Intratumoral T cells, recurrence, and survival in epithelial ovarian cancer." *N Engl J Med* **348**(3): 203-13.
- Zhang, W. W., X. Fang, et al. (1994). "High-efficiency gene transfer and high-level expression of wild-type p53 in human lung cancer cells mediated by recombinant adenovirus." *Cancer Gene Ther* **1**(1): 5-13.
- Zhao, B., S. Magdaleno, et al. (2000). "Transgenic mouse models for lung cancer." *Exp Lung Res* **26**(8): 567-79.
- Zitvogel, L., A. Tesniere, et al. (2006). "Cancer despite immunosurveillance: immunoselection and immunosubversion." *Nat Rev Immunol* **6**(10): 715-27.
- Zwirewich, C. V., R. R. Miller, et al. (1990). "Multicentric adenocarcinoma of the lung: CT-pathologic correlation." *Radiology* **176**(1): 185-90.